

Hege Bergesen Husebø

Comparison of Long-Range Atmospheric Transported Pollutants in Snow and Moss Samples from Svalbard

Master's thesis in Environmental Toxicology and Chemistry

Supervisor: Øyvind Mikkelsen

July 2022

Hege Bergesen Husebø

Comparison of Long-Range Atmospheric Transported Pollutants in Snow and Moss Samples from Svalbard

Master's thesis in Environmental Toxicology and Chemistry

Supervisor: Øyvind Mikkelsen

July 2022

Norwegian University of Science and Technology

Faculty of Natural Sciences

Department of Chemistry



Norwegian University of
Science and Technology

Abstract

As a part of the Arctic, Svalbard is a remote area with few local sources emitting pollutants to the environment. Despite this, higher concentrations of pollutants than what would be expected are observed here due to long-range transport. Pollutants that are released to the atmosphere can be transported by the wind and end up in the Arctic. It is thus of interest to investigate the extent of pollutants found here. Analyzing moss and snow samples are two ways to study the atmospheric pollution, as both media take up atmospheric compounds. In this study, moss (*Hylocomium Splendens*) from Ny-Ålesund, Svalbard, is collected and analyzed for polychlorinated biphenyls, polycyclic aromatic hydrocarbons, and trace elements (with focus on the long-range atmospheric transport related elements V, Cr, Co, Ni, Cu, Zn, As, Se, Mo, Ag, Cd, In, Sn, Sb, W, Hg, Tl, Pb, and Bi). The results from different sampling locations are compared with each other, as well as the extent of trace elements in moss are compared to the extent of trace elements found in snow samples collected in proximity of Ny-Ålesund from 2017. This can provide interesting information about the potential long-range atmospheric transport of pollutants to Ny-Ålesund, as well as snow and moss' ability to study atmospheric pollution.

With the chosen method of analysis none of the PCBs are observed, but 11 out of the 16 PAHs are found. All detected PAHs and nine of the trace elements show highest concentrations in moss at the sampling location closest to settlement (Storvatnet), and influence of local sources can not be ruled out. Concentrations of PAHs are similar between the sampling locations Stuphallet and Austre Brøggerbre, but this is only the case for some of the trace elements (V, Cr, As, Mo, In, Tl, Pb, and Bi). Pearson's correlation coefficients and PCA plots suggest that most of the trace elements in moss samples are mainly influenced by local anthropogenic and geogenic sources. Mercury, Sb, and W are suggested to have a larger impact from marine environment (Hg) and atmospheric transport (Sb and W). Cadmium is present in similar concentration for all sampling sites (both in snow and in moss), indicating long-range transport of this element.

The results from this study indicate that the snow samples are more influenced by sea spray compared to moss samples. Furthermore, as several elements (V, Cr, As, Mo, Tl, and Pb) have their highest concentration at the sampling location closest to potential point sources for both moss and snow, it is assumed that local sources in Ny-Ålesund influence both these sampling media. Snow samples show a better correlation with moss samples that are suggested to be mainly influenced by local anthropogenic and geogenic sources. Thus, snow collected in this thesis seems to be less influenced by long-range atmospheric transport.

The results obtained in this study show how important the choice of sampling sites is when studying long-range atmospheric pollution. To better investigate the correlation between snow and moss samples regarding atmospheric pollution studying, it is recommended to compare samples from a location more remote.

Sammendrag

Som en del av Arktis er Svalbard et fjerntliggende område med få lokale kilder som slipper ut forurensninger til miljøet. Til tross for dette er det observert høyere konsentrasjoner av forurensninger enn hva som er forventet grunnet langtransport. Forurensninger som er sluppet ut i atmosfæren kan transporteres av vinden og ende opp i Arktis, og det er derfor av interesse å undersøke nivået av forurensninger funnet her. Analysing av mose- og snøprøver er to måter å undersøke atmosfæriske forurensninger ettersom begge mediene tar opp atmosfæriske komponenter. I denne studien er mose (*Hylocomium Splendens*) fra Ny-Ålesund, Svalbard, samlet og analysert for polyklorerte bifenyler, polysykliske aromatiske hydrokarboner, og sporelementer (med fokus på de atmosfæriske langtransportrelaterte elementene V, Cr, Co, Ni, Cu, Zn, As, Se, Mo, Ag, Cd, In, Sn, Sb, W, Hg, Tl, Pb og Bi). Resultatene fra ulike prøvelokasjoner er sammenliknet med hverandre, i tillegg er nivået av sporelementer i mose sammenliknet med nivået av sporelementer funnet i snøprøver samlet i nærheten av Ny-Ålesund i 2017. Dette kan gi interessant informasjon om den potensielle atmosfæriske langtransporten av forurensninger til Ny-Ålesund, samt snø og mose sin evne til å undersøke atmosfæriske forurensninger.

Med den valgte analysemetoden er ingen av PCB-ene observert, men 11 av 16 PAH-er er funnet. Alle detekterte PAH-er og ni av sporelementene viser høyest konsentrasjon i mose ved prøvelokasjonen nærest bebyggelse (Storvatnet), og påvirkning av lokale kilder kan ikke utelukkes. Konsentrasjoner av PAH-er er liknende ved Stuphallet og Austre Brøggerbre, men dette er kun tilfellet for noen av sporelementene (V, Cr, As, Mo, In, Tl, Pb og Bi). Pearsons korrelasjonskoeffisienter og PCA-plott foreslår at de fleste sporelementene i moseprøver er hovedsakelig påvirket av lokale antropogene og geogene kilder. Kvikksølv, Sb og W er foreslått å ha en større påvirkning fra marint miljø (Hg) og atmosfæriske transport (Sb og W). Kadmium er til stede i liknende konsentrasjoner ved alle prøvelokasjoner (både i snø og mose), noe som indikerer langtransport av dette elementet.

Resultatene fra denne studien indikerer at snøprøver er mer påvirket av sjøsprøyt sammenliknet med moseprøver. Ettersom flere av elementene (V, Cr, As, Mo, Tl og Pb) har høyest konsentrasjon ved prøvelokasjonen nærest potensielle punktkilder i både mose og snø, er det antatt at lokale kilder i Ny-Ålesund påvirker begge prøvemediene. Snøprøver viser en bedre korrelasjon med moseprøver som er foreslått å hovedsakelig være påvirket av lokale antropogene og geogene kilder. Derfor virker det som at snøprøvene i denne studien er mindre påvirket av atmosfæriske langtransport.

Resultatene oppnådd i denne studien viser hvor viktig valg av prøvelokasjon er når man studerer atmosfæriske langtransporterte forurensninger. Det er anbefalt å sammenlikne prøver fra mer avsidesliggende lokasjoner for å bedre kunne undersøke korrelasjonen mellom snø- og moseprøver i sammenheng med atmosfæriske forurensningsstudier.

Acknowledgements

First and foremost, I want to show appreciation for my supervisor, Øyvind Mikkelsen, for giving me the opportunity to perform this educational study. I want to thank him for the guidance and support during the project.

Furthermore, I want to thank Susana Villa Gonzalez, Anica Simic, Kyyas Seyitmuhammedov, Shannen Thora Lea Sait, and Sylvia Weging for the guidance through the laboratory work.

I want to thank Sara Johnson and Natalia Vylegzhanina for collaboration during fieldwork.

A special thanks to Mathilde Syvertsen for the collaboration during laboratory work, and discussion of results. I appreciate all the support I have received during the master project.

I would also want to show particular appreciation to Kyrre Ryan-Øye for proof-reading and giving suggestions to my thesis, and for the support.

Lastly, a general thanks to friends and family for mental and physical support.

Table of Contents

Abstract	i
Sammendrag	ii
Acknowledgement	iii
Table of Contents	vii
List of Tables	ix
List of Figures	xii
Abbreviations	xiii
1 Introduction	1
2 Background	3
2.1 Long-range transport of pollutants	3
2.1.1 Grasshopper effect and global distillation	5
2.2 Pollutants in the environment	6
2.2.1 Trace metals as inorganic pollutants	6
2.2.2 Persistent organic pollutants	9
2.3 Moss as a biomonitor for atmospheric pollution	14
2.3.1 Heavy metals in moss	15
2.3.2 <i>Hylocomium Splendens</i> for air pollution monitoring	16
2.3.3 Disadvantages with the moss method	17
2.4 The use of snow for monitoring air pollution	17
2.5 Analytical Technique	18
2.5.1 Sampling of moss	18
2.5.2 Sample preparation prior to analysis	18
2.5.3 Analysis techniques	20

2.6	Quality control and quality assurance	23
2.6.1	Limit of detection and limit of quantitation	24
2.6.2	Recovery of analytes	24
2.6.3	Quantification of analytes	25
2.7	Statistical methods	25
2.7.1	Mean	25
2.7.2	Standard deviation	26
2.7.3	Statistical test	26
2.7.4	Principal component analysis	26
3	Methods and materials	29
3.1	Study area	29
3.1.1	Description of sampling sites	30
3.2	Moss sampling	33
3.3	Preparation of moss samples prior to analysis	33
3.3.1	Separation and drying	33
3.3.2	Milling	34
3.3.3	Digestion of samples prior to inorganic analysis	34
3.3.4	Extraction and Concentration prior to organic analysis	34
3.4	Analysis of moss samples	36
3.4.1	ICP-MS for elemental quantification	36
3.4.2	GC-MS for POPs quantification	36
3.5	Data treatment	38
4	Results	39
4.1	POPs in moss samples	39
4.1.1	PCBs	39
4.1.2	PAHs	39
4.2	Concentrations of trace metals	41
4.2.1	Concentrations of trace elements in moss	41
4.2.2	Concentrations of trace elements in snow	43
5	Discussion	47
5.1	Persistent organic pollutants in moss samples	47
5.1.1	PCBs	47
5.1.2	PAHs	48
5.2	Trace elements	49
5.2.1	Trace elements in moss	49
5.2.2	Trace elements in moss samples compared to snow samples	52
5.3	Principal component analysis	55
5.3.1	PCA for moss samples	56
5.3.2	PCA for moss and snow samples	60
5.4	Validation of the method	64
5.5	Limitations regarding study design	65
6	Conclusion	67

Bibliography	69
Appendix	79
6.1 Chemicals and materials	81
6.2 Sample locations	83
6.3 Calibration curves for PAHs	84
6.4 PAH concentrations	90
6.4.1 PAH concentrations corrected for recoveries	90
6.4.2 LOD and LOQ for POPs	92
6.5 Box plots	94
6.6 Bar charts	97
6.7 Correlation matrix	102
6.7.1 Correlation with Sc	103
6.8 Additional PCA plots	104

List of Tables

2.1	Concentration of elements in geological (lithogenic) sources	7
2.2	Properties and chemical structure of PCBs	11
2.3	Properties and chemical structure of PAHs	13
2.3	Continued.	14
3.1	ASE instrument setup	35
3.2	System parameters for ICP-MS	36
3.3	System details and parameters for GC-MS	37
3.4	GC-MS temperature program	37
4.1	Concentrations of detected PAHs	40
4.2	Mean concentration and standard deviation of elements in moss samples .	42
4.3	p-values from Mann-Whitney U test performed on moss data	43
4.4	Mean concentrations and standard deviation of elements in snow samples	45
4.5	p-values from Mann-Whitney U test performed on snow data	46
5.1	Mean concentrations of PAHs in moss from Ny-Ålesund in a previous study.	49
5.2	Mean concentrations of elements in previous studies	51
6.1	Chemicals and materials used in the study	81
6.1	Continued.	82
6.2	Coordinates of the moss sampling locations	83
6.3	Coordinates for snow sampling locations	83
6.4	PAH concentrations corrected for absolute and relative recoveries	91
6.5	Calculated LOD and LOQ	92
6.6	The elements' correlation with Sc	103

List of Figures

2.1	The three steps of long-range atmospheric transport.	4
2.2	Atmospheric transport of pollutants around the globe	6
2.3	Fate of Hg	8
2.4	General structural formula of PCB	9
2.5	<i>Hylocomium Splendens</i>	16
2.6	Schematic presentation of accelerated solvent extractor (ASE) system . .	19
2.7	Schematic presentation of ICP-MS system	21
2.8	Schematic presentation of GC-MS system	23
3.1	Map of Svalbard	29
3.2	Map showing locations for moss sampling	30
3.3	Sample location Stuphallet	31
3.4	Sampling sites at Storvatnet	32
3.5	Sample location Storvatnet	32
3.6	Sample location Austre Brøggerbre	33
3.7	ASE cell loading	35
4.1	Total concentration of PAHs at different locations	41
4.2	Map of snow sampling locations	44
4.3	Sampling sites for snow collections at Austre Brøggerbre and Storvatnet .	44
5.1	Relative distribution of the elements in snow and moss	53
5.2	Relative distribution of selections of elements in snow and moss	54
5.3	PCA loading plot for moss samples	57
5.4	PCA score plot for moss samples	58
5.5	PCA loading plot for moss and snow samples	61
5.6	PCA score plot for moss and snow samples	62
6.1	Calibration curve for naphthalene	84
6.2	Calibration curve for FLU	84

6.3	Calibration curve for PHE	85
6.4	Calibration curve for ANT	85
6.5	Calibration curve for FLT	86
6.6	Calibration curve for PYR	86
6.7	Calibration curve for BaA	87
6.8	Calibration curve for CHR	87
6.9	Calibration curve for BbF	88
6.10	Calibration curve for BkF	88
6.11	Calibration curve for BgP	89
6.12	Boxplots of elements in moss samples	96
6.13	Relative distribution of elements in snow and moss samples from Austre Brøggerbre	97
6.14	Relative distribution of selections of elements in snow and moss samples from Austre Brøggerbre	98
6.15	Relative distribution of elements in snow and moss samples from Storvatnet	99
6.16	Relative distribution of selections of elements in snow and moss samples from Storvatnet	100
6.17	PCA loading plot for moss, snow, and soil samples	105
6.18	PCA score plot for moss, snow, and soil samples	106
6.19	PCA loading plot for moss and snow showing PC3 and PC4	107
6.20	PCA score plot for moss and snow showing PC3 and PC4	108
6.21	PCA loading plot for moss, snow, and soil showing PC3 and PC4	109
6.22	PCA score plot for moss, snow, and soil showing PC3 and PC4	110

Abbreviations

ASE	=	Accelerated solvent extraction
CEC	=	Cation-exchange capacity
CRM	=	Certified reference material
ES	=	External standard
GC	=	Gas chromatography
GC-MS	=	Gas chromatography-mass spectrometry
ICP-MS	=	Inductively coupled plasma mass spectrometry
IS	=	Internal standard
LOD	=	Limit of detection
LOQ	=	Limit of quantification
LRAT	=	Long range atmospheric transport
LRT	=	Long range transport
MM	=	Matrix match
OM	=	Organic matter
PAH	=	Polycyclic aromatic hydrocarbons
PC	=	Principal component
PCA	=	Principal component analysis
PCB	=	Polychlorinated biphenyls
POP	=	Persistent organic pollutants
QA	=	Quality assurance
QC	=	Quality control
R_{abs}	=	Absolute recovery
R_{rel}	=	Relative recovery
RR	=	Relative response
SD	=	Standard deviation
SIM	=	Selected ion monitoring
SP	=	Spike sample

Chapter 1

Introduction

Although natural events like volcanic eruptions have caused air pollution as long as the Earth has existed, the extent of air pollution is increased due to anthropogenic emissions such as burning of fossil fuels and release of industrial waste [1]. If the properties of the compounds allow it, the pollutants can undergo long-range transport and end up far away from their point of release. Persistent and semi-volatile substances that evaporates at ambient temperature in industrialized areas can travel with the atmosphere and reach areas of higher latitudes due to the temperature gradient. Persistent and water soluble substances can be transported via the ocean, and also animals are potential route of transport. Because of this, Arctic – that is considered remote with few local sources – has experienced elevated concentrations of pollutants [2]. This is of great concern as some of the pollutants can accumulate in living organisms and biomagnify in the food web, and thus cause harm to the ecosystem [3].

Both organic and inorganic pollutants have the potential to be transported over large areas. Polychlorinated biphenyls (PCBs) and polycyclic aromatic hydrocarbons (PAHs) are examples of persistent organic pollutants (POPs). These compounds are considered to be of great concern as they poses a severe threat to the environment. Depending on their characteristics, POPs can travel large distances with air (if they are stable and volatile), and eventually end up in the Arctic [4]. Trace elements are example of inorganic pollutants. Most metals released to the atmosphere are associated with particulate matter/aerosols, and the potential of transport is dependent on the properties of the particles [5]. Some trace elements can however also be released in gas phase, such as Hg. Elements like mercury can, in the same way as POPs, travel large distances with the air and eventually end up in the Arctic [6]. Although some of the trace elements are necessary for living organisms, elevated concentrations can cause severe damage [7]. There are several ways of studying air pollution. In addition to directly analyzing air samples, collecting precipitation with subsequent analysis can also be performed. Due to snow's larger surface and slower deposition rate, snow sampling is considered a better method than collecting rain water [8].

Snow take up air pollution, and the pollutants found in the snow pack is considered to reflect the pollutants in winter air [9]. The use of bioindicators is another way of studying pollution. Moss has received special attention and is considered a sufficient biomonitoring method for air pollution studies. The main reason for this is that moss does not have a developed root system, and instead gets its nutrients from the surrounding air. Thus, moss does also take up atmospheric pollutants [10].

The objectives of this study are to compare levels of pollutants in moss sampled from different sample locations in proximity of Ny-Ålesund, as well as comparing the pollutants found in moss with pollutants found in snow. It is hypothesized that that the pollutants that are found in snow samples will also be observed in moss samples. Further, it is expected that the moss sampled closer to settlement will have higher concentrations of pollutants compared to the moss sampled further away.

Background

2.1 Long-range transport of pollutants

Some pollutants have the tendency to travel thousands of kilometers from the emission source and can potentially end up in the Arctic. Pollutants can travel to the Arctic via various routes, such as the atmosphere, water currents, and sea-ice drift. The compound's properties – volatility, water solubility, and its tendency to adsorb to particles – together with geographic location and weather condition decide the pathway. Out of the possible routes of transport, atmospheric transport is considered the most important for most volatile compounds [2].

Long-range atmospheric transport can be divided into three steps, as shown in figure 2.1. In the first step, the compound is released to the atmosphere in sufficient amounts, either from primary sources or by reemitting from a medium in which it has been deposited. When the compound is released to the atmosphere, it can in the second step be transported over large distances and eventually reach remote areas. For this step to occur, the chemical must be sufficiently stable in order to be dispersed by wind currents. The level of persistence determines the transport distance. In the last step, the compound will deposit in the remote area if it has properties to do so, or be taken up by e.g., moss. When deposited, it can impact the local environment [11].

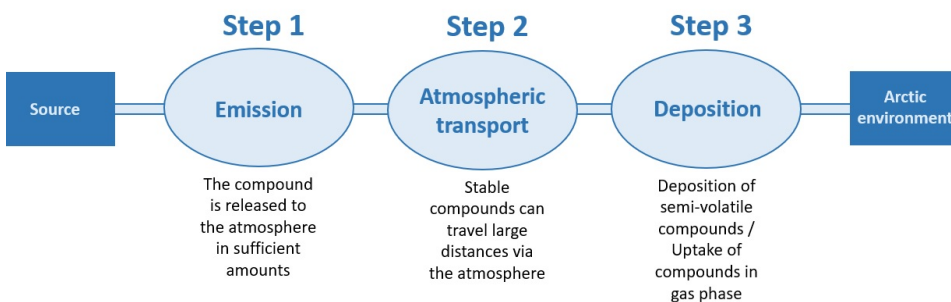


Figure 2.1: The three steps of long-range atmospheric transport. Figure adapted from Wania [11].

The fate of heavy metals emitted to the atmosphere is affected by their physical and chemical form. Heavy metals are most commonly emitted to the atmosphere as aerosols, and their potential to travel via the atmosphere is dependent on the particle size and the metal solubility. Larger particles have a tendency to deposit near the emission source, while smaller particles can travel farther. Some heavy metals, such as Hg and Se, can also be emitted in gaseous phase. Gaseous metal form is more prone to long-range atmospheric transport, and these metals can be globally distributed [5].

The characteristics of different persistent organic pollutants (POPs) cause them to migrate at varying velocities, and they are therefore deposited at different latitudinal regions during their transport towards the Arctic. Although a mixture of several POPs is released from the source, the distribution of the compounds will change over a latitudinal range due to the different characteristics of the compounds. The most volatile POPs have a potential to persist in the atmosphere and travel far, while less volatile POPs will partition in different media such as water bodies, snowpack, vegetation cover, etc. [4].

In tropical and subtropical regions, the warm temperature facilitates evaporation of POPs from Earth's surface. Vice versa, in colder regions such as the Arctic, cool temperatures facilitate adsorption of POPs to atmospheric particulates which further deposit to water or land surfaces [4].

There are two particularly important properties of POPs that affect their potential to undergo long-range atmospheric transport: vapor pressure and octanol-air partition coefficient, K_{OA} . A compound's vapor pressure describes the compound's potential to evaporate or sublime, so that a volatile compound will have high vapor pressure. K_{OA} is the compound's partition ratio between octanol and air at equilibrium. It is suggested that K_{OA} is best for evaluating the compound's partitioning between the atmosphere and the terrestrial compartment, and K_{OA} also indicates the terrestrial surface's ability to preserve the chemical [4]. The water solubility of POPs is also important for the overall transport of these compounds, and is expressed in terms of the air-water partitioning coefficient, K_{AW} . It has been postulated that persistent organic pollutants that are either relatively volatile ($\log K_{OA}$ less than 9) and water soluble ($\log K_{AW}$ between -0.5 and 4) or semi-volatile ($\log K_{OA}$ between 6.5 and 10) and relatively hydrophobic ($\log K_{AW}$ above -3) are most prone to reach and accumulate in Arctic environment. The most volatile compounds can however also

reach the Arctic, but is less likely to deposit to the surface. Non-volatile chemicals are, on the other hand, usually permanently deposited with atmospheric particles and therefore less likely to travel far [11].

Pollutants can be temporarily retained in different chemical reservoirs, such as soil, before being reemitted to the atmosphere. Thus, areas can keep releasing contaminants although the primary emission source has ceased to release contaminants. Because of this, the concentrations of pollutants in remote areas can continue to increase [4].

2.1.1 Grasshopper effect and global distillation

The two most known models for long-range atmospheric transport are the “grasshopper effect” and the “global distillation” processes (see figure 2.2). Global distillation (sometimes called “global fractionation”) is the term used for the phenomenon in which pollutants with different properties deposit at various latitudes due to ambient temperature differences. The vapor pressure is a key property in this process [2, 12].

POPs that are emitted to the atmosphere can, as already stated, deposit to Earth’s surface and in turn volatilize again. The grasshopper effect is the process in which this scenario is repeated. Instead of undergoing one single emission-deposition event, molecules can experience several “hops” from lower to higher latitudes in line with changes in ambient temperature. The POPs are distributed on a latitudinal range as individual pollutants undergo different levels of “hopping”. When depositing, an amount of the substance will be permanently removed, for instance by burial or degradation, whilst the other part can volatilize back to the atmosphere and continue to travel. This process is largely dependent on both the K_{OA} and K_{OW} in addition to the vapor pressure [4, 13].

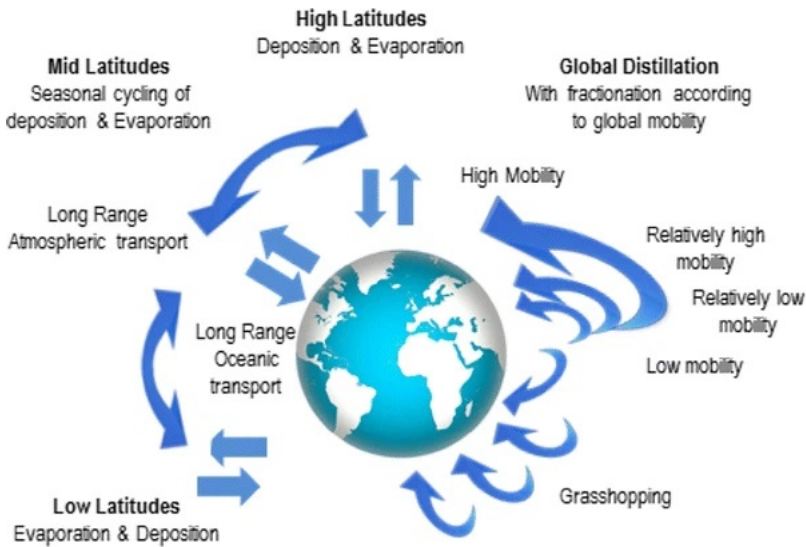


Figure 2.2: Atmospheric transport of pollutants around the globe [14].

2.2 Pollutants in the environment

Pollutants are substances that disturb the natural ecosystem dynamics and cause harm to living organisms. They are either synthetically produced or naturally occurring with enhanced levels due to human activities [15]. This study focuses on persistent organic pollutants (POPs) and trace metals as pollutants.

2.2.1 Trace metals as inorganic pollutants

“Trace metals” include (heavy) metals, metalloids and organometals that have a similar biogeochemical behavior, and that have a potential to be toxic to biota [15]. Trace metals can be divided into “essential metals” (micronutrients) or “non-essential metals”. Essential metals are required in certain amounts by living organisms, because they play a role in vital metabolic pathways. Copper, Zn, Fe, Mo, and Co are examples of essential metals since these elements participate in several physiological processes. However, these elements will become toxic in concentrations above a given threshold. Non-essential metals are not required for living organisms. For instance, no biological significance has been found for metals such as Hg, Cd, Cr, Ni, and Pb [7]. The toxicity threshold varies between different trace metals, and the toxic effects differs for dissimilar organisms. The approximate order for toxicity of a selection of trace metals (inorganic form) is $Hg > Ag > Cu > Cd > Zn > Ni > Pb > Cr > Sn$ [7, 15]. Toxic metals can execute oxidative damage on cells in living organisms, which can result in impairment of neurological, immune, endocrine, digestive, respiratory, and detoxification functions of the body [16].

Trace metals occur naturally in the Earth’s crust, and are released to the environment via natural sources such as soil erosion and weathering. Various elements found in different

geogenic sources are shown in table 2.1. Nevertheless, the biochemical and geochemical cycles of trace metals are altered due to human activities. The major anthropogenic sources of heavy metals are manufacturing industries and construction, electricity and heat production, road transportation (from brake wear, petrol, tires), petroleum refining, and phosphate fertilizers in agricultural areas [17, 16].

Table 2.1: Concentration (mg kg^{-1}) of various elements in a selection of geological (lithogenic) sources. Table adapted from Alloway [18].

	Concentration (mg kg^{-1})				
	Upper crust	Sandstone	Shales	Limestones	Coal
Ag	0.07	0.25	0.07	0.12	-
As	2	0.5	13	1.5	10
Ba	668	300	550	90	250
Cd	0.1	<0.04	0.25	0.1	1
Co	12	0.3	20	0.1	10
Cr	35	35	100	5	20
Cu	14	2	45	6	20
Mn	527	100	850	15	40
Mo	1.4	0.3	2	0.3	3
Ni	19	2	70	5	20
Pb	17	10	22	5	20
Sb	0.3	0.05	1	0.15	2
Sn	2.5	0.6	5	0.3	8
U	2.5	1.3	3.2	1	2
V	53	20	130	15	40
Zn	52	20	100	40	50

Volatile heavy metals and metals that bind to airborne particles (particulates) can travel large distances via the atmosphere, and are often deposited thousands of miles from the original source [16]. Because of their characteristics – being non-biodegradable and ubiquitous – heavy metals are persistent in the environment, and have a tendency to biomagnify in the food web [7].

Mercury is one of the trace metals that is considered non-essential. Both natural and anthropogenic sources are responsible for the emission of mercury to the environment. Natural sources include wildfires and volcanoes, evasion from different surfaces (soil, water bodies, vegetation), and outgassing of the Earth's mantle. Examples of anthropogenic sources are coal combustion, waste incineration, metal smelting, and refining and manufacturing [6].

There are three predominant species of mercury: elemental mercury (Hg^0), Hg(II) species in gas phase, and mercury in particulate form (Hg(p)). In the air, mercury ($\log P_L = -0.58$ Pa [19]) exists mainly in gaseous form which makes the element unique compared to other metals that usually are present in solid phase related to airborne particulate matter [6].

Mercury vapor that is released to the atmosphere can be distributed over large areas due to the long atmospheric residence time of one year. The long residence time can be explained by mercury's ability to exist in gaseous form and the fact that it is relatively resistant to chemical reactions with several components in air, as well as not being particularly soluble in pure water. The residence time of other metals are decided by the residence time of the associated airborne particulate matter, which usually is a lot less (few days or weeks). Mercury that has been deposited can reemit to the atmosphere, and the wide dispersion of mercury is a result of its potential to participate in repeated air-surface exchange processes [6, 20].

Mercury released to the atmosphere can undergo different physical, chemical or photochemical processes [6]. Elemental mercury can for instance dry deposit onto land or ocean surfaces, or oxidize to Hg(II). Hg(II) in the atmosphere can deposit through wet and dry deposition, and Hg(II) in the ocean can undergo sedimentation or participate in biological processes resulting in methylated mercury. These transitions can also occur the other way around [20, 21], and are summarized in 2.3 together with other processes. The fate of mercury in the environment depends on the compounds own characteristics (physical and chemical), as well as the surrounding environmental conditions [6].

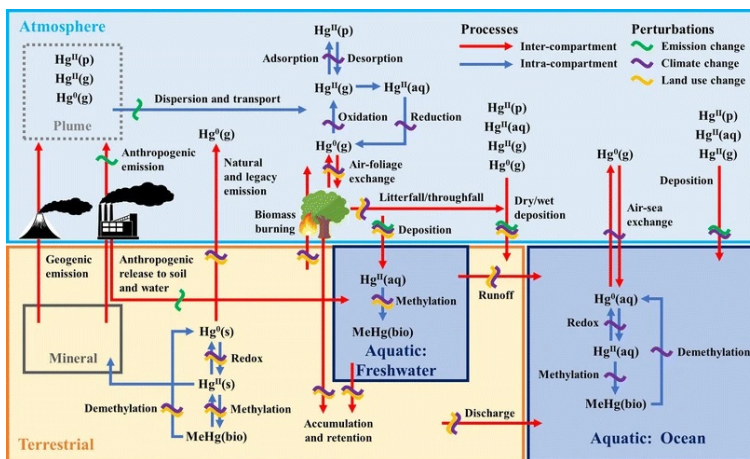


Figure 2.3: A schematic overview of the fate of Hg. The influence of changes in emission, climate, and land are also included [22]

The methylated mercury species are the major reason for concern due to their ability to biomagnify in aquatic food web. Methylated mercury serves as a neurotoxin and has the ability to cross the blood-brain barrier which is supposed to hinder toxins to enter the blood stream [6].

2.2.2 Persistent organic pollutants

Persistent organic pollutants (POPs) are a class of stable organic substances that have toxic characteristics and have a tendency to bioaccumulate, as well as their properties make them suited to undergo long-range atmospheric transport. This, combined with their low degradability, leads to accumulation of POPs over the globe, even in remote areas like the Arctic. Some of the substances have natural origin (e.g., PAHs), however, the pollutants are mainly released from anthropogenic sources, such as waste incineration, industry, and burning of fossil fuel [3].

POPs are able to cause harmful effects on human health and environment [3]. Since these pollutants usually are hydrophobic and lipophilic (i.e., repel water and bind to fat), POPs are often stored in adipose tissues in organisms. Because of slow metabolism in biota, POPs have a tendency to bioaccumulate in food chains, and will therefore be of special concern for top predator species [23]. The toxic effects of POPs are a concern for animal reproduction, development, and immunological function [3].

This study focuses on two types of POPs; polychlorinated biphenyls and polycyclic aromatic hydrocarbons.

Polychlorinated biphenyl

Polychlorinated biphenyls (PCBs) are organic compounds made up of 1-10 chlorine atoms attached to a biphenyl nucleus. This gives the general chemical formula $C_{12}H_{10-n}Cl_n$ with belonging molecular structure shown in figure 2.4 [24]. There is a total of 209 different PCBs, where the degree of chlorination and the substitution position varies [23].

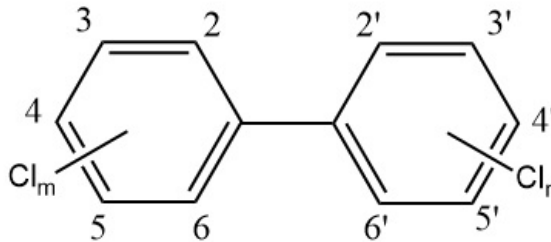


Figure 2.4: General structural formula of PCB, adapted from Borja et al. [24].

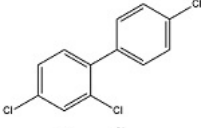
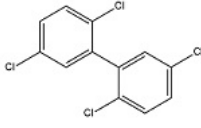
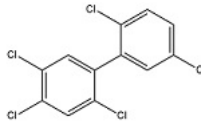
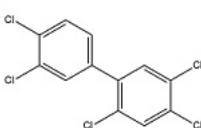
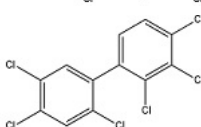
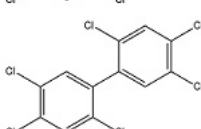
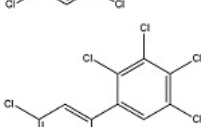
The degree of chlorination affects the properties of the PCB congener. Although PCBs primarily exist in vapor phase, the increase in chlorination degree will increase the tendency to adsorb on particulates. Furthermore, increasing chlorination also yields increasing persistence and decreasing water solubility [25, 24]. This can be seen in table 2.2 where the partition coefficients between octanol and water (K_{OW}), between octanol and air (K_{OA}), as well as the vapor pressures (P_L) are given for a selection of PCBs. An increase in chlorination is generally accompanied with increase in K_{OW} and K_{OA} , and a decrease in P_L .

Between 1930s and 1970s, PCBs were extensively used in industrial applications. PCBs' physical and chemical characteristics gave them desirable properties such as thermal and chemical stability, non-flammability, high dielectric constant and low acute toxicity. The compounds were for instance used as oil in transformers, dielectrics in capacitors, hydraulic fluids, and was even used in pesticides, inks, and surface coatings to mention some usages. The use of PCBs was banned in the 1970s due to the concern for the impact of PCBs and their persistence in the environment. However, natural soil and aquatic biota are not able to significantly degrade these compounds, and PCBs can therefore remain in soils and water bodies for several years [24].

The health effects of PCBs are related to route of exposure, age, sex, and where the PCB is concentrated in the body. PCBs are considered carcinogenic and can have a reducing effect on the reproductive capacity for animal species. There have been shown acute effects related to PCB exposure, such as skin disease, liver damage and damage to the central nervous system. PCBs also impact the productivity of phytoplankton, which is critical, as phytoplankton is important for oxygen production and as an important food source for sea organisms [24].

Out of the 209 PCBs that exist, this study focuses on 7 PCBs, whose properties and chemical structures are listed in table 2.2.

Table 2.2: Logarithmic values of the partitioning coefficient between octanol and water (K_{OW}), partitioning coefficient between octanol and air (K_{OA}), and vapor pressure of subcooled liquid (P_L) of seven PCBs together with chemical structure [26].

	$\text{Log } K_{OW}$	$\text{Log } K_{OA}$	$\text{Log } P_L$ (Pa)	Chemical structure
PCB-28	5.66	7.85	-1.57	
PCB-52	5.91	8.22	-1.92	
PCB-101	6.33	8.73	-2.61	
PCB-118	6.69	9.36	-3.00	
PCB-138	7.22	9.66	-3.25	
PCB-153	6.87	9.44	-3.22	
PCB-180	7.16	10.16	-3.97	

Polycyclic aromatic hydrocarbons

Polycyclic aromatic hydrocarbons (PAHs) consist of carbon and hydrogen atoms, arranged in two or more condensed aromatic rings [3]. These rings can be bonded in linear, cluster, or angular arrangements [27]. PAHs are mobile in the environment due to their physico-chemical properties. Physical properties depend on molecular weight and structure of the PAH. Increasing molecular weight will for instance decrease the vapor pressure, and the solubility in water decreases with increasing amount of aromatic rings [28]. This can be seen from the values given for a selection of PAHs in table 2.3, where larger molecules generally have higher octanol-water and octanol-air coefficients, and lower vapor pres-

tures.

PAHs in the atmosphere can be present in two different phases. They can appear either in vapor phase, or sorbed onto particulate matter (solid phase), according to the vapor pressure of the individual compound. PAHs with high vapor pressure tends to be in vapor phase, whereas PAHs with lower vapor pressure usually exist sorbed to particulate matter [27].

Like mercury, PAHs can be emitted from natural sources such as volcanoes and forest fires. However, the major sources of PAHs to the atmosphere stem from the anthroposphere in the form of fossil fuel combustion (e.g., traffic, and electricity production), and aluminum and coke production [3].

In the same way as PCBs and several other POPs, PAHs are lipophilic and have potential to bioaccumulate. PAHs are of great concern as some of the compounds cause carcinogenic, mutagenic, and teratogenic effects [28].

Most studies (and regulations) focus on 14-20 individual PAH compounds, although there exist many more [27]. In this research the 16 PAHs listed with properties and molecular structure in table 2.3 have been studied. These PAHs are established as the priority PAHs by the U.S. Environmental Protection Agency (EPA) [15].

Table 2.3: Logarithmic values of the partitioning coefficient between octanol and water (K_{OW}), partitioning coefficient between octanol and air (K_{OA}), and vapor pressure of subcooled liquid (P_L) of 16 U.S. EPA priority PAHs, together with chemical structure [29].

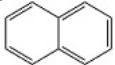
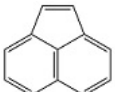
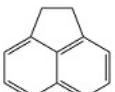
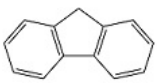
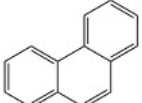
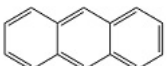
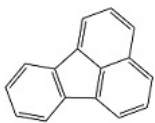
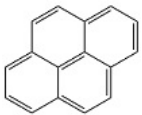
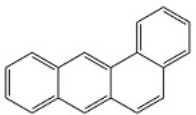
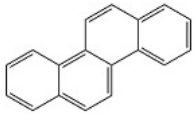
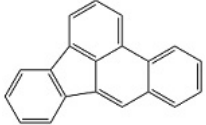
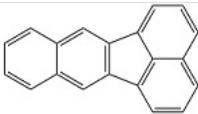
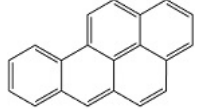

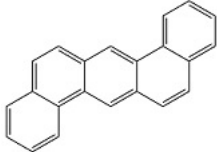
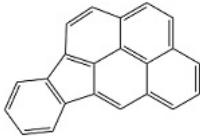
	Log K_{OW}	Log K_{OA}	Log P_L (Pa)	Chemical structure
Naphthalene (NAP)	3.30	5.90	0.51	
Acenaphthylene (ACY)	3.60	8.55	-0.69	
Acenaphthene (ACE)	3.60	7.47	-0.51	
Fluorene (FLU)	4.20	7.77	-0.87	
Phenanthrene (PHE)	4.50	8.55	-1.62	
Anthracene (ANT)	4.50	8.55	-1.76	
Fluoranthene (FLT)	5.00	10.11	-2.73	
Pyrene (PYR)	5.00	10.11	-2.95	
Benzo(a)anthracene (BaA)	5.70	11.20	-4.06	
Chrysene (CHR)	5.70	11.20	-3.99	
Benzo(b)fluoranthene (BbF)	6.10	12.76	-5.16	

Table 2.3: Continued.

	Log K_{OW}	Log K_{OA}	Log P_L	Chemical structure
Benzo(k)fluoranthene (BkF)	5.30	11.98	-5.41	
Benzo(a)pyrene (BaP)	6.10	12.76	-5.56	
Benzo(ghi)perylene (BgP)	6.60	14.33	-6.64	
Dibenzo(a,h)anthracene (DbA)	6.80	13.85	-7.17	
Indeno(1,2,3-cd)pyrene (InP)	6.60	12.76	-6.53	

2.3 Moss as a biomonitor for atmospheric pollution

Moss can serve as a bioindicator for atmospheric pollution, and has been used for biomonitoring in several studies [30, 31, 32, 33, 34]. A bioindicator is an organism (e.g., plants, animals, microbes) that can reveal pollution in the environment by reacting on pollutants, either by showing specific symptoms or morphological changes, or by showing appearance or disappearance in the ecosystem. There are two categories of mosses used as pollution-indicator; mosses can either show pollution due to visible harm on the species, or by absorbing and retaining pollutants without it causing negative effects on the moss [7]. Steinnes et al. [34] have used moss as a bioindicator in his nationwide air pollution studies in Norway since 1977.

Two ways of using moss for analyzing air pollution are by collecting naturally growing moss in the area of interest or by exposing so-called moss bags. In the latter method, moss is collected in an area considered clean, before it is washed and put into nylon mesh bags, which are subsequently distributed in the research area. This technique allows known exposure time [35].

There are several reasons why moss is suitable as an air pollution monitor. Firstly, moss

does not have a developed root system, and most of the species' nutrient uptake is therefore dependent on the surrounding air. Some acrocarpous mosses may receive nutrients from the substrate, but the nutrient uptake for feathermosses are mainly, if not only, from wet and dry deposition of particles and soluble salts [36]. The root-like filaments of mosses do not participate in nutrient uptake, but serve mainly as attachment to the substrate (i.e., soil, rock, sand) [7]. Several mosses do also have leaves that consist of only one cell layer and a cuticle that is weakly developed, which makes it easy for water, gaseous pollutants, and metal ions to penetrate into the moss [10, 7], and accumulate in the moss tissue [7]. Other characteristics of mosses that make them suitable are the large surface to weight ratio, the slow growth rate, and the habit of growing in groups. Additionally, there are minimal variation in the morphology during the lifetime of mosses, and mosses are able to survive in highly polluted environment [10]. Using moss samples for studying air pollution is easier and cheaper than conducting precipitation analysis. Moss sampling does not require any expensive tools [36], while precipitation analysis, on the other hand, require distribution of precipitation collectors with subsequent sample collection and analysis [10].

Various factors affect the uptake mechanism of pollutants by moss. The structure of the moss and morphology of their shoot will for instance decide the retention of pollutants. Also the physical and chemical properties of the pollutant, such as molecular weight, aqueous solubility and vapor pressure, will affect the uptake. Furthermore, climate and environmental condition affect the uptake for instance due to the quantity of precipitation, or the incident where elements on the moss surface can be eliminated by wind. For heavy metals, acidic conditions will facilitate metal ion desorption because of increased concentration of protons. In relation to this, the affinity of metals to functional groups on the cell wall will play an important role for the uptake [3, 7].

2.3.1 Heavy metals in moss

Although the mechanism of POPs uptake in moss remains uncertain [29], there have been postulated different mechanisms for uptake of heavy metals in moss. The metal can be transported inside the cytoplasm through intracellular uptake. This occurs either through diffusion or membrane channels and transport proteins, or through leaf and rhizoids along with water and micronutrients. Metals can also undergo extracellular uptake where they attach the cell wall either by ion-exchange or chelation. Lastly, heavy metals in dry deposition can be deposited on the cell surface, and can in turn reach cytoplasm via the mechanisms of intracellular uptake [7]. The heavy metals that are taken up by moss are thus not evenly distributed within the plant, but can either occur in liquids surrounding cells, be bounded to the cell wall, or occur within the cell itself [37].

The cation-exchange capacity (CEC) of the moss' cell wall has been considered the most probable mechanism for the accumulation of heavy metals [7]. CEC is defined as "the maximal number of cations exchanged with anions at the cell wall per gram of tissue dry weight" [38]. The cell wall contains polygalacturonic acid and hold several functional groups such as phosphodiester, amine, and sulfhydryl. Depending on the pH and the affinity of the element to the given functional group, metal ions can replace hydrogen atoms (or already present metal ions) and bind to anionic sites (e.g., carboxyl and phosphoryl groups) on the cell wall [7].

Several factors affect the ion exchange in mosses. The amount of available exchange sites is important, since no more metal ions can be bound to the cell wall than there are cation exchange sites present. Furthermore, the type of these sites, as well as the composition of the pollutants, affect the ion exchange. The cell's age and the growing condition do also play a role. Additionally, environmental factors, such as temperature, pH and precipitation, affect the exchange process [39].

2.3.2 *Hylocomium Splendens* for air pollution monitoring

According to Mahapatra et al. [7], there are three criteria that should be fulfilled when selecting the moss type in such studies. Firstly, the moss type should be widely distributed. Secondly, the structural and physiological characteristics should provide efficient pollutant uptake. Lastly, there should already be existing information about the habitat and morphology of the species [7].

Several researches have used the moss species *Hylocomium Splendens* for studying atmospheric pollution [40, 41, 17]. The reasons for why *Hylocomium Splendens* is extensively used for these kind of surveys are that this moss is widespread and has a circumpolar distribution, which makes it feasible for studying over large areas. Furthermore, because of its composition with a sympodial chain of annual shoots [42], the annual growth increments are identifiable. This characteristic makes the species suitable for studying the contamination in relation to age [43]. *Hylocomium Splendens* is also easy to distinguish from other moss species [41]. The growth rate of *Hylocomium Splendens* is usually more or less constant. However, the rate is significantly lower in arctic regions [41].



Figure 2.5: The moss species *Hylocomium Splendens*.

2.3.3 Disadvantages with the moss method

Although moss is widely used as a biomonitor for air pollution, there are a couple of disadvantages regarding the technique. Leakage can occur for some trace metals which exhibit a lower affinity for the ligands in the moss tissue, such as Zn and Cd. For the same reason, the sorption is not necessarily complete for these elements, and the concentration measured in the moss in such cases will not correspond to the concentration in the atmosphere. Other disadvantages are related to the sampling site. Carpet forming feather mosses, which are the most suitable species for these studies, can be difficult to find in urban locations which make this method hard to perform in such areas. Furthermore, if the sampling is conducted in forest areas, leaching from tree canopy can impact the levels of elements found in the moss [36]. Problems can also occur for moss sampling in areas affected by marine environment, due to competition from sea-salt cations [41]. Moss is neither a sufficient monitoring device if the exposure time is less than a year [36].

2.4 The use of snow for monitoring air pollution

Snow can be used for monitoring air pollution in cold climate regions [44, 45, 46]. It is an efficient and economic alternative as it, in the same way as moss sampling, is cheaper and easier than air sampling [8]. Snow's high ability to absorb and store pollution (heavy metals, salt, and organic substances) makes it suitable for studies on migration of atmospheric pollution [47, 8]. Snow can take up natural and anthropogenic components from the atmosphere, organic as well as inorganic components. Both solid particles and solutes can accumulate in snow [9], and it retains most of the pollutants, even compounds that are not very stable [48].

Snow that deposits is persistent on the substrate, and the snowpack can therefore serve as an "archive" of particles that have precipitated during the winter season [9, 44]. When land and water surfaces are covered in snow or ice in the winter, there is a minimal input of mineral compounds from surrounding areas. Because of this, the major affects on the snow's chemical composition in remote areas stem from long-range atmospheric transport of anthropogenic particles [44]. Dry deposition and gas absorption can also contribute to the total pollution content in the snow cover [8].

Snow sampling is perhaps better and easier than sampling rain water for atmospheric pollution studies. This is because snow accumulates more pollutants than rain water due to the larger surface area of snow flakes. Additionally, snow flakes fall at a slower velocity compared to raindrops, and therefore collect more pollutants than rain [8]. Because of this, snowpack contains two or three orders more pollutants compared to other atmospheric precipitation [47], which makes pollutants easier to detect in this sample media. Meteorological data can further be used to define the deposition time [8].

Although snow efficiently collects pollutants from the air, pollutants in snow can, however, be transformed and transferred to the hydrosphere, the lithosphere, and the biosphere, as well as they can be transferred back to the atmosphere. This happens in processes such as melting, refreezing, evaporation, and sublimation [49]. Melting and wind erosion can result in redistribution of elements found in the upper part of the snow cover [50].

2.5 Analytical Technique

2.5.1 Sampling of moss

There are several principles that should be followed when sampling moss for monitoring atmospheric deposition of pollutants. To avoid influence from tree canopy leakage, moss should be samples minimum three meters away from the nearest tree canopy. Furthermore, areas with running water should be avoided. Moss covered in sand should not be collected, and in cases of coarse contamination this should be removed carefully. There should be at least 300 meters from main roads, villages, and industries, and 100 meters from smaller roads and houses to the sampling sites. For comparison studies, the sampling should be performed at the same sampling points as previous moss studies. Minimum three samples per site should be collected in order to determine variability [51]. However, 30 samples are preferred to ensure statistical certainty [52]. Paper or plastic bags can be used for storing moss meant for metal analysis, while pre-heated glass jars are recommended for moss meant for POP analysis. The storage containers should be tightly closed in order to avoid contamination during transport [51].

2.5.2 Sample preparation prior to analysis

Digestion of samples for inorganic analysis

Most instrumental analyze methods require the sample to be in liquid form. Digestion can be performed to accomplish this for solid samples. In order to achieve accurate analysis of the sample, the digestion have to decompose the sample matrix in a way that ensures the analytes to be completely released and solubilized [53]. Not all analytes are always entirely released, thus, reference material or standards should be included with the samples to state the recovery (see 2.6.2).

In microwave-assisted digestion, the solid sample is dissolved in strong acid (e.g., HNO_3) and placed in a microwave cavity where the solution absorbs microwave energy directly. The direct absorption of microwave energy facilitates fast and uniform heating of the sample. The use of closed vessels will additionally ensure contamination avoidance [54].

Extraction of samples for organic analysis

Accelerated solvent extraction (ASE) is an extraction method used for solid and semi-solid samples. In this method, a container with the sample is filled with extraction fluid, which extracts the sample under increased temperature and pressure. The high pressure allows the temperature to be above the boiling point of the organic solvent in use. There are several reasons for using liquid solvents at higher temperatures and pressures. Firstly, higher temperatures enhances the solvents' capacity to solubilize analytes. The solubility of water in organic solvents will also increase with higher temperature, which allows analytes contained in water-sealed pores to be more available. This increases the efficiency of the extraction. Another advantage with higher temperature is that this will weaken the interaction between the solute and the matrix, since the activation energy that is needed to desorb the analytes is decreased due to thermal energy. Furthermore, enhanced tempera-

ture will decrease the viscosity of the solvent and also decrease the surface tension of the solvent, solutes and matrices. This will contribute to better extraction due to the resulting interaction between the solvent and the matrix. In addition to allowing high temperatures, the high pressure will assure the solvent to pass through matrix pores where analytes are trapped, and therefore enhance the efficiency of the extraction. Also, air bubbles will solubilize due to the higher pressure of the flow, resulting in a faster contact between solvent and sample matrix [55]. A schematic presentation of the ASE system is shown in 2.6.

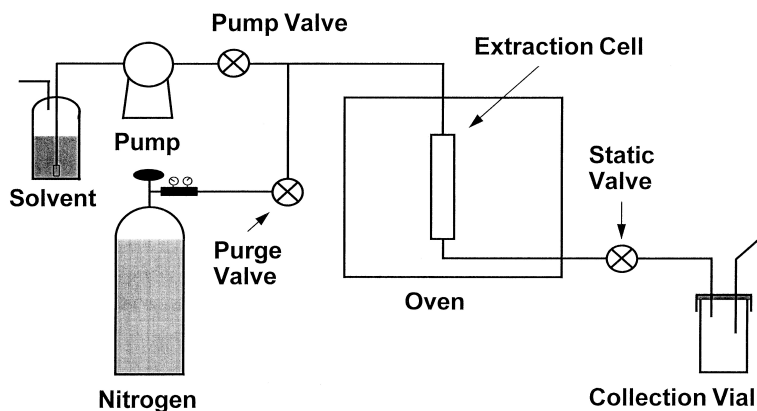


Figure 2.6: Schematic presentation of accelerated solvent extractor (ASE) system. Reprinted with permission from Richter et al. [55]. Copyright 2022 American Chemical Society.

In preparation for ASE, the solid sample should be dried, homogenized, and sieved. If sample particles are surrounded by a thin water film, nonpolar solvent will not get in contact with the analytes bound to the matrix. In such cases where the sample is not completely dried, a drying agent (e.g., diatomaceous earth) should be mixed with the sample. An alternative is to use a mixture of a polar and nonpolar solvent (e.g., acetone/dichloromethane) [56].

ASE gives the possibility for in-cell clean-up. Copper can be added to the extraction cell to remove sulfur [56], and aluminum oxide (Al_2O_3) can be added to remove lipids [57].

Both temperature, pressure, and choice of solvent affect the extraction. Regarding solvents, toluene, n-hexane, dichloromethane, as well as mixtures of these solvents are particularly suitable for the extraction of lipophilic compounds. For plant samples, n-hexane (and toluene) have shown to yield the good results for extraction of POPs [58]. Acetone-dichloromethane (1:1, v/v) and acetone-hexane (1:1, v/v) have also been suggested for extraction of PAHs and PCBs [59].

As is the case for digestion, accelerated solvent extraction may not completely isolate the analytes of interest from the sample matrix. The degree of extraction is therefore important to monitor, and standards or reference material should be included to enable

recovery calculations (see 2.6.2) [60].

2.5.3 Analysis techniques

ICP-MS for inorganic analysis

Inductively coupled plasma mass spectrometry (ICP-MS) is a technique used in analytical chemistry to measure elements at trace levels. There are several benefits with the ICP-MS system, for instance its capability to measure multiple elements during one sequence. Other advantages are simple sample preparation and the short time required for the analysis, as well as the detection limits are extremely low (parts per trillion range) [61, 62]. The plasma is suited as an element ionizer for all types of samples and matrices due to the ion density and the high temperature (approximately 5000 - 1000 K [63]). Since all bonds in the compounds are broken in the plasma, the data that are obtained from ICP-MS will represent the total content of the different elements present in the sample, regardless of the species containing the element [64].

The ICP-MS system consists of six main compartments, namely the sample introduction system, inductively coupled plasma, interface, ion optics, mass analyzer, and detector, as shown in figure 2.7 [61]. When the sample, usually a liquid, is introduced to the ICP-MS instrument, it is first sent in to the nebulizer where it is converted into an aerosol with the help of argon gas. A spray chamber then separates fine droplets from larger droplets in the aerosol, and these fine droplets are transported through a sample injector and into the plasma torch. The sample droplets are ionized in the plasma, and the ions are directed towards the mass spectrometer passing the interface. The interface allows the ions to be efficiently transported to the ion optics which guide the ions to the mass separation device, while hindering photons, particulates, and neutral species to reach the detector. The mass spectrometer separates the ions based on their mass-to-charge (m/z) ratio, and filters out non-analytes and interfering ions. An ion detector lastly converts the ions into electrical signals. ICP-MS calibration standards are used to convert the processed electrical signals into analyte concentrations [62].

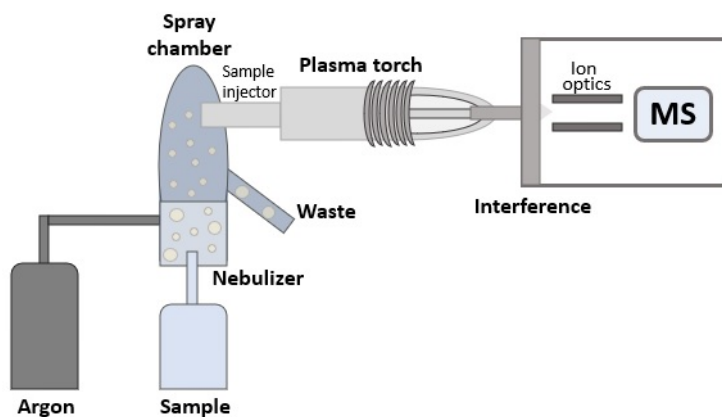


Figure 2.7: A schematic overview of the ICP-MS system. Adapted from [62].

Interferences

Although ICP-MS is a well-established technique, interferences causing errors can occur during analysis. Interferences can either be a consequence of ions that share m/z ratio with the compound of interest, denoted as spectroscopic interferences, or the interference can be non-spectroscopic where the sample matrix or instrument give rise to the problem [61].

In the occasion where isobaric elements are present in the system, that is, isotopes of different elements but with equal masses, the measurement of the specific isotope of these elements will interfere with each other. Another type of spectroscopic interference can happen for some elements that can form double charged ions, such as gadolinium (Gd). These ions can interfere with ions of double mass as ICP-MS separates ions based on the m/z ratio. Furthermore, polyatomic ions with the same m/z ratio as the analyte of interest can be formed in the plasma from e.g., sample matrix or argon gas, and can interfere with the analyte. Lastly for the spectroscopic effects is the so-called tailing interference, where elements with adjacent mass may overlap with the analyte [61].

The sample matrix can give rise to interferences termed matrix effects. These effects can result in both increased and decreased analyte signal depending on the mechanisms that take place. Matrix effects can occur as the sample is introduced to the system if physical and chemical properties are altered resulting in a change in the characteristics of the sample aerosol. Property changes can enhance the extent of sample delivered and therefore cause increased signal. However, overloading can decrease the signal due to the occurrence of a cooling effect in the plasma. Plasma effects can happen in the presence of elements that are easily ionized such as sodium, which decreases the signal, or carbon, which increases ionization of analyte and therefore the analyte signal. The matrix effect that is considered the most significant for ICP-MS is the space-charge effect. This effect occurs when positive ions are formed in the ion beam. When this happens, fewer ions reach the detector as the ion beam broadens due to the repel between positive ions. Impacts on the analyte signal due to instrument drift is another type of potential non-spectroscopic

interference. For instance can samples deposit in the colder part of the system, and this can over time result in a blockage of the inlet to the mass spectrometer [61].

Several strategies have been developed in order to minimize potential interferences. This can be done by avoiding reagents that can interfere with target analytes, using an analyte isotope that is interference-free (but with the awareness of the potential polyatomic or isotope interferences), optimizing the operating conditions of the instrument, and more. The most used strategy is to include a collision or reaction cell that reduces spectroscopic interferences through chemical reactions or by a reduction in the polyatomic ions' kinetic energy [61].

GC-MS for organic analysis

Chromatography is a separation technique that works by distributing the compounds in a mixture between two different phases, namely the stationary phase and the mobile phase. Different compounds have different affinities for the two phases, which facilitates separation. How easily a compound is retained is dependent on the chemical properties of the compound itself, and what stationary and mobile phases are used [65].

To express the difference between the time it takes for various compounds to elute, it is normal to use the retention time. The retention time is the time it takes for a sample to elute through the column and reach the detector after being injected into the system. Several compounds can have the same retention time, and the retention time for a specific compound varies in different systems [65].

The detected compounds are presented as peaks in a so-called chromatogram [66]. The relative amount of the compound present is described from the size of the peak, either by the height or the area. A calibration curve is used to determine the actual quantitation of a compound, see chapter 2.6.3 [65].

Gas chromatography is a technique that separates complex mixtures based on differences in vapor pressures and polarities. In gas chromatography, an inert gas is used as mobile phase, and the stationary phase is a solid often coated with a liquid. The sample is introduced to the system in the injector, and are carried through the column by the mobile phase/carrier gas [65].

As gas chromatography is only a technique for separation, it has to be coupled to a detector in order to provide analytical data. A detector, such as mass spectrometer (MS), gives an electronic signal proportional to the amount of analytes that elute [65].

Compounds are fragmented and ionized by the mass spectrometer using electron or chemical ionization sources. These ions will be sorted by their m/z ratio, and the m/z are then detected. Relative amounts of ions belonging to the different m/z ratios are presented in a mass spectrum, that is, a visual representation with x-axis representing the m/z ratio and the y-axis representing the abundance to the belonging ions [65].

A database with the spectrum to the target analytes can help confirming the identity to the analyte when using full-spectrum data [66].

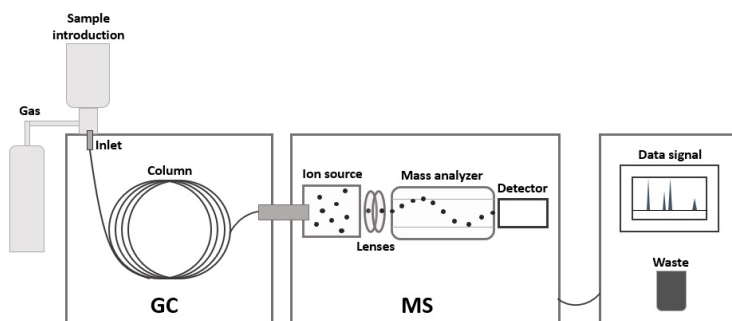


Figure 2.8: Schematic overview of GC-MS system. Adapted from Wewing [67], originally from [68].

Uncertainty can occur when identifying individual compounds with GC. Retention time and peak resolution are important for every chromatographic analysis and give the basis for quantitation and identification. The target analyte is identified by comparing the retention time in the sample with the retention time in a standard. Thus, if non-targets with the same retention time is present in the sample, this will give a false positive result. False negative results can occur if the target analyte are chemically interfering with other substances in the sample, causing the target analyte to elute at a different time. However, these potential errors can be reduced by choosing MS as the detector, since MS gives reliable identification as it takes the compound's m/z ratio into account when identifying the compound [69].

Although MS provides reliable identification, errors regarding quantitation can still occur. Compounds that coelute will affect quality of the peak resolution, thus making it more difficult to quantify. Clean-up of the sample is therefore important before running in order to remove potential interfering non-target compounds [69].

2.6 Quality control and quality assurance

Quality assurance (QA) and quality control (QC) should be implemented in order to ensure good laboratory practice. QA includes all measures (actions, procedures, checks, etc.) that the laboratory apply to assure quality (representativeness, accuracy, and reliability) of analytical results [70, 71]. These measures can for instance be using traceable methods, getting accreditation, and applying QC criteria. QC includes measures that ensure control of analytical data, and is important in all steps of the process; from sampling to data treatment [70].

Because of potential interferences, instrumental noise, and uncontrolled gain or loss of analyte, the measured concentration of an analyte can differ from the actual concentration in the sample, and therefore cause uncertainty regarding the analysis [72].

To be aware of potential contamination in the system or carryover of analyte between different samples, blanks should be utilized [66]. There are different types of blanks. A

field blank can be used to determine contamination or losses during sampling, where a clean sample of the given matrix is brought to the field and treated as other samples (same sample container, storage, etc.) [71]. A method blank is prepared in the same way as the samples, without containing the analytes, and are subjected to every step in the sample preparation and subsequently the analysis technique [66]. Reagent blanks can be used to determine analyte concentrations that do not originally stem from the sample but contribute to the overall concentration [71]. Such blank consists of the particular solvent and are run through the analysis step.

The use of certified reference material (CRM) and internal standards can be used to control variation in the analysis. CRM is a certified substance with established property values (e.g., concentration of a particular analyte), which can be used to calibrate instruments, evaluate quality of methods, or ensure traceability of results [73]. An internal standard is a substance with chemical characteristics similar to the compound of interest, but that elute at a different time to make sure the signal does not overlap with the signal of the target analyte [66]. This substance is added to the sample in a known amount, and can contain several compounds; one for each analyte that will be analyzed for. The internal standard can be used to correct for sample losses during sample preparation [66].

2.6.1 Limit of detection and limit of quantitation

Limit of detection (LOD) and limit of quantitation (LOQ) are important for validating the method. LOD is the lowest concentration of the analyte that can be reliably detected with the given analytical process, while LOQ is the lowest concentration of the analyte that can be quantified [72, 74].

There are several ways to calculate LOD and LOQ. One way is to use the signal-to-noise ratio ($\frac{S}{N}$). In this method, LOD and LOQ are defined as the lowest concentration with a signal-to-noise ratio of 3 and 10, respectively (equation 2.1 and 2.2) [75].

$$\text{LOD} = 3 \cdot \frac{S}{N} \quad (2.1)$$

$$\text{LOQ} = 10 \cdot \frac{S}{N} \quad (2.2)$$

2.6.2 Recovery of analytes

In most chemical analyses, the analytes of interest have to be transferred from the original matrix to a matrix that is suitable for the instrumental determination. However, these transfers are not always complete. Losses during the sample preparation can occur, which results in a lower measured concentration than what is present in the actual sample. This is controlled by performing recovery studies [76]. The recovery is the amount of analyte measured compared to the amount of analyte in the original samples [77].

Recoveries can be measured in different ways. One example is to use matrix reference materials that contain the analyte of interest in a known amount. The recovery is then

the ratio between the measured concentration and the actual concentration [76]. Another way of determining the recovery is by spiking with the analyte [76]. Absolute and relative recovery can be determined by comparing spiked (SP) samples, that is, samples spiked before extraction, with matrix match (MM) samples, that is, samples spiked after extraction. Potential contamination can be corrected for by subtracting the signal area of the method blanks (MB). Absolute recovery (%) can be calculated with the following equation (2.3),

$$R_{\text{abs}}(\%) = \frac{(\text{Area}_{\text{A;SP}} - \text{Area}_{\text{A;MB}})}{(\text{Area}_{\text{A;MM}} - \text{Area}_{\text{A;MB}})} \cdot 100\%, \quad (2.3)$$

where $\text{Area}_{\text{A;SP}}$, $\text{Area}_{\text{A;MB}}$, and $\text{Area}_{\text{A;MM}}$ refers to the area of the analyte signal in the spiked sample, method blank, and matrix match, respectively. Alternatively can the recovery relative to the internal standard response be calculated by 2.4:

$$R_{\text{rel}}(\%) = \frac{\left(\frac{\text{Area}_{\text{A;SP}}}{\text{Area}_{\text{IS;SP}}} - \frac{\text{Area}_{\text{A;MB}}}{\text{Area}_{\text{IS;MB}}}\right)}{\left(\frac{\text{Area}_{\text{A;MM}}}{\text{Area}_{\text{IS;MM}}} - \frac{\text{Area}_{\text{A;MB}}}{\text{Area}_{\text{IS;MB}}}\right)} \cdot 100\% \quad (2.4)$$

Here $\text{Area}_{\text{IS;SP}}$, $\text{Area}_{\text{IS;MB}}$, and $\text{Area}_{\text{IS;MM}}$ denotes the area of the internal standard signal in the spiked sample, method blank, and matrix match, respectively [78, 67].

2.6.3 Quantification of analytes

In order to quantify the compounds of interest, a calibration curve is made. This is done by preparing typically five or six calibration standards, that is, solutions containing the target analytes at different concentrations. The concentrations should be in the range where it is expected that the concentration in the unknown samples will be. It is normal to use the same matrix as the unknown samples. The internal standard method is recommended in GC/MS to achieve the most accurate quantification. This method is preferred as it accounts for errors regarding volume. In the internal standard method, a known amount of internal standard is added to each calibration solution [66, 77, 79]. The calibration curve is obtained by plotting the relative response ratio, given by equation 2.5, against the concentration of the analyte over the concentration of the internal standard ($\frac{C_{\text{A}}}{C_{\text{IS}}}$) [77].

$$RR = \frac{\text{Area}_{\text{A}}}{\text{Area}_{\text{IS}}} \quad (2.5)$$

Area_{A} and Area_{IS} denotes the area of the analyte and internal standard in the sample, respectively.

2.7 Statistical methods

2.7.1 Mean

The mean of a data set is the value found by adding all numbers in the data set and dividing by the amount of numbers, as shown in equation 2.6 [80].

$$\bar{X} = \frac{\sum_{i=1}^n X_i}{n} \quad (2.6)$$

Here n is the number of samples in the data set, and X_i denotes the value of number i .

2.7.2 Standard deviation

To determine the spread of the data set, the standard deviation (SD) is calculated. The standard deviation is the average distance from one point in the data set to the data set's mean, and is calculated as shown in equation 2.7 [80].

$$SD = \sqrt{\frac{\sum_{i=1}^n (X_i - \bar{X})^2}{(n - 1)}} \quad (2.7)$$

It is common to use $(n - 1)$ in the denominator when the data set is a subset of the total population, while n is used when the entire population is sampled [80].

The spread can also be described by the variance, which is the standard deviation squared [80].

2.7.3 Statistical test

The Mann-Whitney U test is a statistical test that compares two independent groups without requiring normal distribution. It is a so-called non-parametric test, and is necessary when the distribution is not symmetrical. One of the advantages of this test is that it can be used for small samples of subjects (five to 20). Small samples can be methodologically questionable, for instance since generalization is difficult, however, with the appropriate statistical test, they can be useful for drawing conclusions on the population [81].

The null hypothesis (H_0) of Mann-Whitney U test states that the two groups stem from the same population, while the alternative hypothesis (H_1) states that the group data distribution differs from one another. The null hypothesis is rejected if the test statistic is below the predetermined significance level [81].

2.7.4 Principal component analysis

Principal component analysis (PCA) can be used to identify patterns in the data set [80]. One of the advantages with PCA is that it keeps the trends and patterns in the high-dimensional data set while simplifying the complexity [82]. The data set is considered a matrix with n rows (objects, such as samples) and p columns (variables, such as elements). The variables are characterizing the various objects. If the data set is plotted in an orthogonal coordinate system with p dimensions, then each object is represented by a point. In PCA it is desired to find new variables composed from the original data set in such way that the variation is maximized. This new variable is called a principal component (PC), and can be found with the least squares fit, that is, finding the line in which the

sum of the squared distances between every point perpendicularly to the line is the smallest. The first principal component (PC1) will lay in the direction with largest variance, and PC2 will lay orthogonally onto PC1 in the direction of second largest variance, and so on [83].

These new variables are linear combinations of the unit vectors in the original coordinate system with p dimensions. The *loadings* are the coefficients of the linear combinations, in other words, the loadings describe the contribution of the original variables to each PC. In a loading plot, the PC_i axis denotes the coefficients for the variables determining PC_i . Two variables with similar loadings (i.e., are found together along an axis in the loading plot) will correlate positively, and variables that are found with opposite signs will correlate negatively [83].

Another useful plot is the score plot. *Scores* are the relative coordinate to the PC-origin when an object is perpendicularly projected onto PC_i . Each object will then get a set of coordinates (relative coordinates projected onto the different PCs), that are plotted in a score plot. Thus, the score plot shows the relation between different objects, and can be used to identify trends, groups, or outliers, etc. Together with the belonging loading plot, the score plot can give information about the variables in relation to the objects [83].

Methods and materials

3.1 Study area

Svalbard is an archipelago located from 74 °N to 81 °N, and between 10 °E and 35 °E. Since Svalbard is considered lacking local sources, it is popular for measuring background levels of pollutants [84].

Ny-Ålesund (78 °55' N, 11 °56' E) is located north-west on Svalbard's largest island, Spitsbergen, and is one of the world's northernmost human settlements. See figure 3.1 The area consists of both marine and terrestrial environments, with typical high-Arctic ecosystems. Both 'Arctic desert', lush tundra and grassland communities can be found here, thus, the vegetation is varied [85].



Figure 3.1: Map of Svalbard. Ny-Ålesund is pointed out in red. From Norwegian Polar Institute.

Between 1917 and 1963, Ny-Ålesund served as a mining settlement. The town is now exclusively run as a research facility [86], and has been designated as an international research base for natural sciences by the Norwegian government. In 1968, the Norwegian Polar Institute's research station was established here, which allowed continuous year-round observations. Several researches for long-range atmospheric pollution have been conducted here [87, 88, 89], and at the top of the Zeppelin mountain, an atmospheric chemistry station provides measurements of e.g., the composition of air, persistent organic pollutants, and mercury species in the atmosphere [85]. Although Ny-Ålesund is considered having few local pollution sources, there is still contamination potential due to the old landfill and dumpsites in Thiisbukta, the closed mining areas, and the fuel storage in the settlement, the airport, and the sewage outlet [86].

3.1.1 Description of sampling sites

Every sampling site was located on Brøggerhalvøya (the Brøgger peninsula) on Spitsbergen, in proximity of Ny-Ålesund. A map showing all sampling sites is given in figure 3.2. The sample location coordinates can be viewed in 6.2.

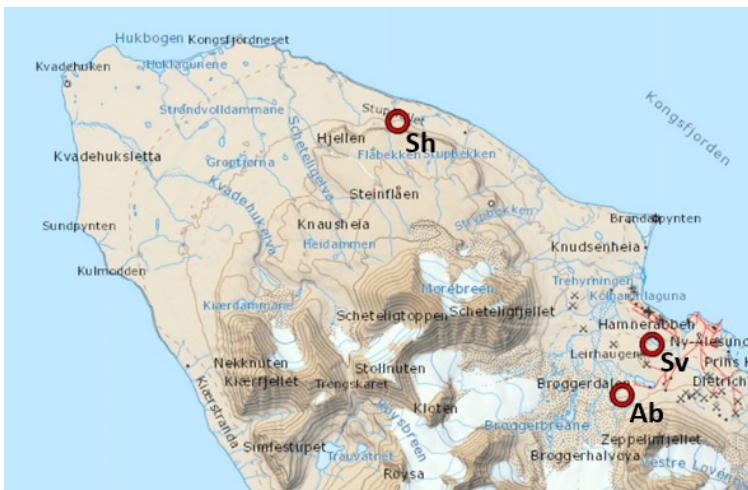


Figure 3.2: Map of locations for moss sampling. Sh, Sv, and Ab denote Stuphallet, Storvatnet, and Austre Brøggerbre, respectively. From Norwegian Polar Institute.

Stuphallet (78.96 °N, 11.63 °E)

The sample location at Stuphallet was furthest away from settlement. The sampling found place beneath a bird area, and the area was mostly covered in vegetation (see photo 3.3). The area where most of the sampling was conducted could resemble a small “valley” with rocks on each side that worked as a shelter for the wind. The sampling site was slightly elevated compared to the surrounding area. The moss was a bit moist due to light rainfall in advance of sampling. The growth size of the moss samples varied.



Figure 3.3: Sample location Stuphallet.

Storvatnet (78.92 °N, 11.88 °E)

The sample location near Storvatnet was close to the runway, as well as it was the location closest to the settlement of Ny-Ålesund (see 3.2). The sampling was more difficult to conduct in this area due to lack of vegetation and therefore the moss of interest. Sampling was done at three separate sites shown in figure 3.4 with individual coordinates (listed in 6.2). The area was more of an open landscape compared to the location at Stuphallet, as can be seen in photo 3.5. The moss collected here was moister than the moss collected at Stuphallet.

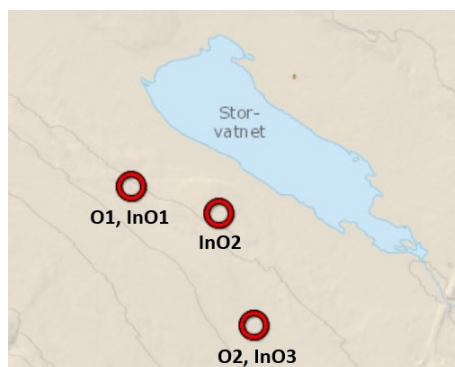


Figure 3.4: The three different sampling sites at Storvatnet. O_x and InO_x denotes sample x meant for organic and inorganic analysis, respectively. From Norwegian Polar Institute.



Figure 3.5: Sample location Storvatnet.

Austre Brøggerbre (78.91 °N, 11.85 °E)

The third sampling was conducted close to Austre Brøggerbre, at the foot of the Zeppelin mountain. This area was further away from settlement compared to the sampling sites at Storvatnet, but still closer than the sampling site at Stuphallet. The terrain was flat but contained a few bumps. This area had a bit more vegetation compared to Storvatnet, but not in the same extent as Stuphallet (see photo 3.6). The moss sampled here was smaller/shorter compared to the two other sampling sites.



Figure 3.6: Sample location Austre Brøggerbre.

3.2 Moss sampling

The collection of moss samples was performed in late summer, August 2021.

The moss type of interest was *Hylocomium Splendens*. The number of samples varied between 3 and 14 for inorganic analysis, and 2 and 7 for organic analysis. Each sample was approximately 10 x 20 cm.

The moss was picked by hand using nitrile gloves, and preferably from the exact same area. In cases where this was not possible (e.g., the “moss pile” was not large enough for one sample), moss in the same sample was collected within a radius of 10 meters. The samples were transferred to a paper bag (for inorganic analysis) or aluminum box (for organic analysis). After the fieldwork, the samples were left to dry. The lids on the aluminum boxes were opened to ensure air exchange.

3.3 Preparation of moss samples prior to analysis

Details about chemicals and materials used in the sample preparation steps can be viewed in 6.1.

3.3.1 Separation and drying

The paper bags were ripped opened and a plastic tweezer were used to pick out everything except the moss of interest. The remaining moss was transferred to a new paper bag. The moss collected for organic analysis was poured over aluminum foil and a metal tweezer was used for the separation in this case. The remaining moss was then transferred back to the aluminum box.

The samples were left on the working bench in room temperature (21 °C) to dry completely. The samples were considered dry when the sample weight did not change more than $\pm 10\%$ over three days.

3.3.2 Milling

Oscillating Mill MM400 (Retsch®) was used for milling the samples. The procedure explained in the instrument's manual was followed, running the samples in two minutes at a frequency of 30 Hz. By doing this, a grain size of $< 100 \mu\text{m}$ was obtained. Containers of 35 mL were used together with a ball of 20 mm in diameter [90]. Teflon containers and teflon ball were used for inorganic samples, while stainless steel container coated with zirconium oxide and zirconium oxide ball were used for organic samples. The milled samples were transferred back in paper bags and aluminum boxes (using a rubber policeman) for inorganic and organic analysis, respectively. Containers and balls were cleaned with soap and water between different sample runs, and dried using paper tissue. The outer parts of the instrument were also swiped over with a wet paper tissue between samples.

3.3.3 Digestion of samples prior to inorganic analysis

Approximately 250 mg of each sample meant for inorganic analysis was precisely measured out in separate 20 mL teflon vials. 3 mL 50% nitric acid (HNO_3 , v/v) was added carefully to each vial, before the samples were decomposed in a high-pressure microwave digestion reactor (UltraClave, Milestone GmbH, Leutkirch, Germany). After digestion, the samples were transferred to 50 mL centrifuge tubes. The teflon vial was rinsed with ultrapure water ($\sim 18.2 \text{ M}\Omega\cdot\text{cm}$) which was collected in the centrifuge tube. Ultrapure water was then added to reach a weight of 30.50 grams to achieve a final HNO_3 concentration of 0.6 M. The samples were lastly analyzed with ICP-MS system (see 3.4.1).

The teflon vials were cleaned before use by rinsing the vial and cap three times with ultrapure water. They were stored with a small amount of 65% HNO_3 and ultrapure water until usage. Before adding the samples to the vials, they were yet again rinsed three times with ultrapure water and air dried.

3.3.4 Extraction and Concentration prior to organic analysis

Before analyzing the milled moss for organic substances, extraction, solvent exchange and concentration were performed. These steps were done as described by Weging [67].

Accelerated solvent extractor (ASE) was used to extract the samples. This was performed using Dionex™ (Sunnyvale, CA, USA) ASE 150 accelerated solvent extractor, with instrument setup according to Weging [67] (table 3.1), and with dichloromethane as solvent. Copper, aluminum oxide and diatomaceous earth was included in the cell. Roughly 0.5 grams of moss sample was precisely weighed out and added to a beaker, before 50 μL F-PCB ($1 \mu\text{g mL}^{-1}$) and 50 μL F-PAH ($1 \mu\text{g mL}^{-1}$) internal standards dissolved in ethyl acetate were added.

Table 3.1: ASE instrument setup.

Parameter	Value
Oven temperature	100 °C
System pressure	1500 psi
Static time	5 min
Number of static cycles	3
Purge volume	60%
Nitrogen purge time	60 s
Total time per sample	24 min
Total solvent per sample	approx. 35 mL

Resins (roughly two grams of each) and sample were loaded in 22 mL stainless steel containers in the following order: two filters, copper, one filter, aluminum oxide, one filter, sample (including standards and diatomaceous earth). See figure 3.7. Ottawa sand was added to the cell to make it completely full. Diatomaceous earth and ottawa sand was activated in the oven for 4 hours at 400 °C before use. The outcome of the extraction was collected in 60 mL amber collection vials with parafilm covering the cap, and stored in the freezer at -20 °C while waiting for the solvent exchange step. A total of five method blanks were prepared, doing the exact same excluding sample material.

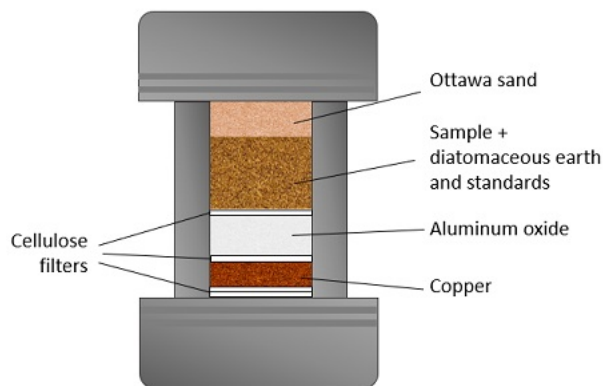


Figure 3.7: ASE cell loaded with filters, copper, aluminum oxide, sample mixture and ottawa sand. Adapted from Weging [67].

Solvent exchange and concentration were done with a Biotage TurboVap Classic LV evaporator (fra Sylvias). The collected extract from ASE was evaporated to approximately 2 mL in a water bath at 35 °C, under nitrogen gas with a pressure of 5 psi. Ethylacetate (10 mL) was added to the ASE collection vial along the walls to reduce sample loss, before the solution was filtered over in a 15 mL centrifuge tube. The sample solution was then concentrated to 1 mL and transferred to an amber vial. Amber vials were stored in the freezer at -20 °C until GC-MS running. Samples meant for matrix match were added internal and

external standards after the last concentration. One concentration blank, only consisting ethylacetate, was included in each round of samples ran.

3.4 Analysis of moss samples

3.4.1 ICP-MS for elemental quantification

The elemental composition of the samples was analyzed using 8800 Triple Quadrupole inductive coupled plasma mass spectrometry (ICP-MS) system (Agilent, USA) equipped with prepFAST M5 autosampler (ESI, USA). System parameters are listed in table 3.2.

Table 3.2: System parameters for ICP-MS.

General parameters	
RF Power	1550 W
Nebulizer Gas	0.80 L/min
Makeup Gas	0.40 L/min
Sample depth	8.0 mm
Ion lenses	x-lens
H₂ mode	
H ₂ gas flow	4.5 mL/min
He gas flow	1.0 mL/min
O₂ mode	
O ₂ gas flow	0.525 mL/min

For quality control, three samples with reference material were prepared in the exact same manner as described in 3.3.3, using Intercalibration sample, moss, *Pleurozium schreberi* (Finnish Forest Research Institute, Muhor Research Station). Additionally, six blanks were prepared in the same way excluding moss.

3.4.2 GC-MS for POPs quantification

The concentrations of PAHs and PCBs were determined using Agilent 7890A gas chromatograph with a GC Pal autosampler (CTC Analytics, Zwingen, CH). The chromatograph was coupled to an Agilent 5975 single quadrupole mass spectrometer. The column used was a Thermo Scientific™ TraceGOLD™ TG-5MS GC Column (5% diphenyl/95% dimethyl polysiloxane 30 m x 0.25 mm inner diameter with 0.5 µm film thickness). The carrier gas flow was kept at a rate of 1 mL per minute. A summary is given in table 3.3. Each sample had a total analysis time of 36.75 minutes. The temperature for the transfer line and injection port was 290 °C. The temperature program for the column is listed in table 3.4.

Table 3.3: System details and parameters used during GC-MS running.

System/Parameter	Type/Value
Instrument	Agilent 7890A gas chromatograph
Sample introduction system	GC Pal autosampler (CTC Analytics, Zwingen, CH)
Detector	Agilent 5975 single quadrupole mass spectrometer
Column	Thermo Scientific™ TraceGOLD™ TG-5MS GC Column (5% diphenyl/95% dimethyl polysiloxane, 30 m x 0.25 mm inner diameter x 0.5 µm film thickness)
Carrier gas	Helium
Carrier gas flow rate	1 mL per min
Injection method	Splitless
Injection volume	1 micro L
Injection port temperature	290
Mass detector mode	Selected ion monitoring (SIM)
Electron impact ionization (EI)	70 eV

Table 3.4: Temperature program for GC-MS.

Time interval	Temperature
0 - 2 min	Stable at 50 °C
2 - 12 min	Increasing by 25 °C per min
12 - 13 min	Stable at 250 °C
13 - 25 min	Increasing by 3 °C per min
25 - 28 min	Stable at 286 °C
28 - 30.75 min	Increasing by 8 °C per min
30.75 - 31.75 min	Stable at 308 °C
31.75 - 33.75 min	Increasing by 1 C per min
33.75 - 36.75 min	Stable at 310 °C

“Dutch seven PCB” standard and 16 U.S. EPA priority pollutant PAH mixture (see table 6.1) dissolved in ethyl acetate were used to prepare six calibration solutions of concentration 0.5 ng mL⁻¹, 5 ng mL⁻¹, 10 ng mL⁻¹, 30 ng mL⁻¹, 50 ng mL⁻¹, and 100 ng mL⁻¹, respectively. The calibration solutions also contained 50 ng mL⁻¹ internal standards (F-PAH and F-PCB).

To check for potential cross-contamination and carry-over, a reagent blank consisting of ethyl acetate was repeatedly analyzed.

Recoveries were calculated using equation 2.3 and 2.4. Three collective samples (sample batch with each original sample present) were spiked with a known amount of internal standards (50 ng mL⁻¹) and two different concentrations of external standards (50 ng mL⁻¹ and 100 ng mL⁻¹) before sample preparation (referred to as spiked samples). Two other collective samples were spiked with internal standard (50 ng mL⁻¹) and two different concentrations of external standards (50 ng mL⁻¹ and 100 ng mL⁻¹) post sample preparation

(referred to as matrix match).

3.5 Data treatment

ChemStation 2 and MassHunter Workstation Software Quantitative Analysis (Version B.08.00), ©Agilent Technologies, were used for processing GC/MS chromatograms.

Microsoft® Excel® for Microsoft 365 MSO (Version 2205 Build 16.0.15225.20278) 64-biters was used for data treatment.

RStudio Version 1.4.1103 was used to visually present the data in form of boxplots and (stacked) bar charts, to make calibration curves, and to run statistical tests.

PCA plots were made using Aspen Unscrambler version 12.1. The data were centered with arithmetic mean and divided by standard deviation.

ChemDraw 19.1 was used for drawing PAHs and PCBs. Microsoft® Excel® for Microsoft 365 MSO (Version 2206 Build 16.0.15330.20144) 64-biters was used to make schematic diagrams.

Chapter 4

Results

The results obtained by running GC-MS and ICP-MS for moss samples meant for organic and inorganic analysis, respectively, are presented here. Raw data for the analyses can be found in the supplementary files. The results from inorganic analysis of snow samples from 2017 are also included.

4.1 POPs in moss samples

4.1.1 PCBs

None of the seven PCBs analyzed for in the moss samples (PCB28, -52, -101, -118, -138, -153, -180) were found in any of the samples. Equation 2.1 and 2.2 were used to calculate limits of detection and quantification, and the results can be viewed in table 6.5 in 6.4.

4.1.2 PAHs

The moss samples were analyzed for 16 PAHs, where eleven PAHs (NAP, FLU, PHE, ANT, FLT, PYR, BaA, and CHR) showed concentrations above LOD. Calibration curves were made by plotting relative response against the concentration of analyte divided by concentration of internal standard, and can be viewed in 6.3. The concentration calculated from calibration curves are given in [table]. Equation 2.3 and 2.4 were used to calculate absolute and relative recovery percentage, and corrected concentrations are listed in table 6.4 in 6.4. The calculated limits of detection and quantitation can be viewed in table 6.5 in 6.4.

The highest concentration of each PAH was detected in one of the samples from Storvatnet (sample denoted Sv2), and was more than twice as large in this sample compared to other samples for most of the compounds. Further, NAP, PHE, and FLT were found in

quantifiable quantities at all sampling sites. ANT, BaA, CHR, BbF, BkF, and BgP were only found in the location close to Storvatnet.

Table 4.1: Concentrations (ng g^{-1}) of PAHs detected above LOD in the moss samples. Empty cells indicate no PAH found in the given sample. ShX, AbX, and SvX denote sample X from Stuphallet, Austre Brøggerbre, and Storvatnet, respectively.

	Concentration (ng g^{-1})										
	NAP	FLU	PHE	ANT	FLT	PYR	BaA	CHR	BbF	BkF	BgP
Sh1	27.48		31.71		14.48	5.015					
Sh2	33.07	7.032	34.24		14.12	4.939					
Sh3	27.27	5.963	33.75		14.53						
Sh4	28.26		28.51		12.59						
Sh5	30.99	6.757	30.45		13.47	4.700					
Sh6	25.74	7.342	31.23								
Ab1		6.694									
Ab2	28.24	7.746	28.08		12.02						
Ab3	26.30		29.16		13.99						
Ab4											
Ab5											
Ab6	30.63	7.216									
Ab7	28.10	7.811	30.18								
Sv1	47.46	9.120	44.28		14.64	6.666	5 .129				
Sv2	127.0	14.01	96.97	13.14	22.88	17.11	16.50	19.50	9 .597	1 2.28	1 0.50

The total PAH concentrations (\sum PAHs) are visually presented in figure 4.1. Storvatnet ($n = 3$) had the highest total concentration (486.8 ng g^{-1}), while Austre Brøggerbre ($n = 7$) had the lowest total concentration (256.2 ng g^{-1}). The total concentration found at Stuphallet ($n = 6$) was (473.6 ng g^{-1}). NAP contributed the most to the overall concentration at all sampling sites, and PHE the second most.

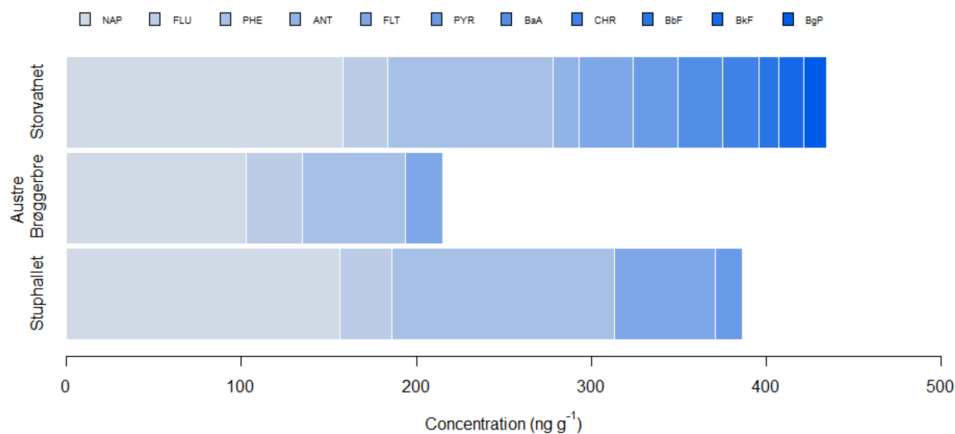


Figure 4.1: Total concentration (ng g^{-1}) of PAHs found at the different locations.

4.2 Concentrations of trace metals

4.2.1 Concentrations of trace elements in moss

Nineteen elements (V, Cr, Co, Ni, Cu, Zn, As, Se, Mo, Ag, Cd, In, Sn, Sb, W, Hg, Tl, Pb, and Bi) were chosen to focus on due to their relation to long-range atmospheric transport [30, 91, 92, 93]. The mean concentration from each sampling area (Storphallet, Austre Brøggerbre, and Storvatnet) of these elements are presented in table 4.2.

The only two elements with highest mean concentration at Austre Brøggerbre were Ni ($4.42 \mu\text{g g}^{-1} \pm 1.62$) and Zn ($61.0 \mu\text{g g}^{-1} \pm 24.9$). Both Sb and W had almost twice the concentration at Storphallet compared to the two other sample sites ($0.0477 \mu\text{g g}^{-1} \pm 0.0116$ and $0.0139 \mu\text{g g}^{-1} \pm 0.00354$, respectively). The highest concentration of the rest of the elements were found in the samples close to Storvatnet.

Table 4.2: Mean concentration with belonging standard deviation (SD) of elements in moss samples at different sampling locations.

	Concentration ($\mu\text{g g}^{-1}$)		
	Stuphallet, n = 14 Mean \pm SD	Austre Brøggerbre, n = 10 Mean \pm SD	Storvann, n = 3 Mean \pm SD
V	3.20 \pm 1.36	3.94 \pm 1.53	7.26 \pm 1.44
Cr	2.76 \pm 0.944	3.56 \pm 1.22	5.65 \pm 1.46
Co	0.428 \pm 0.183	1.33 \pm 0.455	1.55 \pm 0.385
Ni	2.11 \pm 0.832	4.42 \pm 1.62	3.98 \pm 0.827
Cu	1.67 \pm 0.563	3.05 \pm 0.707	4.06 \pm 0.509
Zn	21.5 \pm 8.75	61.0 \pm 24.9	48.9 \pm 5.07
As	0.372 \pm 0.123	0.301 \pm 0.114	0.616 \pm 0.131
Se	0.357 \pm 0.0991	0.267 \pm 0.0415	0.538 \pm 0.104
Mo	0.145 \pm 0.0366	0.119 \pm 0.0231	0.237 \pm 0.0397
Ag	0.0188 \pm 0.0128	0.0231 \pm 0.00928	0.0321 \pm 0.00615
Cd	0.430 \pm 0.187	0.437 \pm 0.238	0.457 \pm 0.0605
In	0.00276 \pm 0.00106	0.00332 \pm 0.00105	0.00727 \pm 0.00125
Sn	0.102 \pm 0.0286	0.0731 \pm 0.0111	0.141 \pm 0.193
Sb	0.0477 \pm 0.0116	0.0232 \pm 0.0118	0.0176 \pm 0.00998
W	0.0139 \pm 0.00364	0.00521 \pm 0.00359	0.00500 \pm 0.00365
Hg	0.145 \pm 0.0644	0.0612 \pm 0.0264	0.151 \pm 0.0661
Tl	0.0177 \pm 0.00738	0.0173 \pm 0.00729	0.0386 \pm 0.0111
Pb	3.10 \pm 2.45	2.17 \pm 0.685	5.60 \pm 1.54
Bi	0.0208 \pm 0.00839	0.0180 \pm 0.00567	0.0467 \pm 0.00588

Mann-Whitney U tests were performed for the sampling sites for each element to check for significant variance between locations. The p-values are listed in table 4.3, and visual presentation given in form of Box-plot can be viewed in 6.5. The sample site at Storvatnet differed significantly from the two other sampling sites for eight elements: V, Cr, As, Mo, In, Tl, Pb, Bi. W and Sb, Co, Ni, Cu, and Zn were significantly different at Stuphallet compared to Storvatnet and Austre Brøggerbre, but not between the two latter. Antimony and Hg were significantly different at Austre Brøggerbre compared to Stuphallet and Storvatnet, but not between the two latter.

Cadmium was the only element not showing significant difference between any of the sampling areas, and Se was the only elements showing significant difference between all sampling areas.

Table 4.3: p-values obtained from running Mann-Whitney U tests on moss data. Sh, Ab, and Sv denote Stuphallet, Austre Brøggerbre, and Storvatnet, respectively.

p-values obtained with Mann-Whitney U test			
	Sh vs Ab	Sh vs Sv	Ab vs Sv
V	0.172	0.00588	0.0280
Cr	0.074	0.0118	0.0280
Co	0.00000410	0.00294	0.469
Ni	0.000198	0.0118	0.937
Cu	0.0000459	0.00294	0.0769
Zn	0.00000102	0.00294	0.937
As	0.0841	0.0206	0.0280
Se	0.048	0.0206	0.00699
Mo	0.0956	0.00588	0.00699
Ag	0.108	0.0324	0.161
Cd	0.886	0.768	0.469
In	0.142	0.00962	0.0139
Sn	0.0118	0.0677	0.00699
Sb	0.000198	0.00588	0.469
W	0.000178	0.00588	0.937
Hg	0.00067	0.859	0.0490
Tl	0.884	0.0197	0.0341
Pb	0.546	0.0471	0.00699
Bi	0.508	0.00294	0.00699

4.2.2 Concentrations of trace elements in snow

To compare moss samples with snow, snow samples collected in 2017 was included. Snow samples were only collected at two of the three relevant sampling locations. The sampling locations corresponding to the moss sampling locations Austre Brøggerbre and Storvatnet are shown in 4.2 and 4.3. The mean concentration together with standard deviation of the selected elements are listed in table 4.4.



Figure 4.2: The snow sampling locations corresponding to Austre Brøggerbre (Ab) and Storvatnet (Sv). From Norwegian Polar Institute.



Figure 4.3: The sampling sites for snow collections. Ab and Sv denote Austre Brøggerbre and Storvatnet, respectively. From Norwegian Polar Institute.

The highest concentration of various elements was found at Storvatnet, except from Se and Hg, where the highest concentration was found at Austre Brøggerbre ($0.0902 \mu\text{g L}^{-1} \pm$

0.0403 and $0.00300 \mu\text{g L}^{-1} \pm 0.00141$, respectively). Snow samples were not analyzed for In and Bi.

Table 4.4: Mean concentration with belonging standard deviation (SD) of elements in snow samples at the two sampling locations.

	Concentration ($\mu\text{g L}^{-1}$)	
	Austre Brøggerbre, n = 7 Mean \pm SD	Storvatnet, n = 6 Mean \pm SD
V	0.0298 \pm 0.0364	0.923 \pm 1.15
Cr	0.0324 \pm 0.0320	0.932 \pm 1.26
Co	0.0590 \pm 0.0533	0.471 \pm 0.621
Ni	0.0774 \pm 0.0645	0.812 \pm 0.999
Cu	0.313 \pm 0.519	1.60 \pm 1.81
Zn	3.79 \pm 3.60	44.4 \pm 16.9
As	0.0311 \pm 0.0187	0.135 \pm 0.114
Se	0.0902 \pm 0.0403	0.0690 \pm 0.0114
Mo	0.00525 \pm 0.00675	0.0305 \pm 0.0228
Ag	0.00123 \pm 0.00105	0.00277 \pm 0.00157
Cd	0.00918 \pm 0.00341	0.0123 \pm 0.00347
In	N/A	N/A
Sn	0.00277 \pm 0.00317	0.0116 \pm 0.00705
Sb	0.00610 \pm 0.00476	0.0192 \pm 0.00948
W	0.000511 \pm 0.000425	0.00557 \pm 0.00648
Hg	0.00300 \pm 0.00141	0.00114 \pm 0.000284
Tl	0.00114 \pm 0.000351	0.00900 \pm 0.0106
Pb	0.0838 \pm 0.0775	0.619 \pm 0.491
Bi	N/A	N/A

The p-values obtained from running Mann-Whitney U tests are given in table 4.5. A significant difference ($p < 0.05$) between the two sample locations was found for all elements except Co, Se, Ag, and Cd.

Table 4.5: p-values obtained from running Mann-Whitney U tests on snow data.

p-values obtained with Mann-Whitney U test	
Austre Brøggerbre vs Storvatnet	
V	0.00233
Cr	0.00816
Co	0.181
Ni	0.0221
Cu	0.0140
Zn	0.00117
As	0.00816
Se	0.445
Mo	0.00816
Ag	0.0734
Cd	0.234
In	N/A
Se	0.0140
Sb	0.00466
W	0.00466
Hg	0.00466
Tl	0.0140
Pb	0.00117
Bi	N/A

Discussion

5.1 Persistent organic pollutants in moss samples

5.1.1 PCBs

GC-MS was used to analyze the moss for seven PCBs, but none were detected. PCBs have earlier been detected in vegetation from Ny-Ålesund, including moss samples [94, 95, 84], as well as *Hylocomium Splendens* has been used for studying PCBs in other areas [40, 96, 97]. Thus, there were reasons to believe that the lack of observation of PCBs in the samples may have been a result of the method of analysis. The LOD values for PCBs in the study performed by Lead et al. [40] ranged from 0.02 to 0.16 ng g⁻¹, while the LOD values obtained in this study were between 0.57 and 0.87 ng g⁻¹, indicating that the analysis has potential for improvement.

The method for determining organic compounds used in this study was originally optimized for soil samples. Organic matter (OM) content in moss is higher compared to soil samples, which may have affected the obtained results. The higher the OM content, the more challenging is the matrix. This is because of the larger amount of interfering substances and matrix constituents that are co-extracted. In a study performed by Brändli et al. [98] it was shown that pure dichloromethane as solvent in ASE for compost analysis gave the highest concentration of PAHs compared to other solvents/mixtures. This solvent was also good for PCBs in compost, however, alternatives (toluene/acetone-mixture) showed higher concentrations [98]. It is common to use a mixture of polar and nonpolar solvent when extracting PAHs/PCBs from moss [99, 100]. Thus, the extraction of PCBs in this study could potentially been more efficient.

5.1.2 PAHs

The samples were analyzed for PAHs in addition to the PCBs. Out of the 16 PAHs, eleven were detected. NAP, FLU, PHE, and FLT were found at all sampling sites. The concentration of these PAHs were similar throughout the samples taken at Stuphallet and Austre Brøggerbre, while the concentrations at Storvatnet were higher, especially in the sample denoted Sv2. The observed elevation in concentration found at Storvatnet for all PAHs detected are likely explained by the larger contribution from local sources compared to the other sampling sites. NAP, FLU, PHE, PYR are all associated with traffic pollution [101], and can be associated with the airport runway together with the vehicles used in Ny-Ålesund. Additionally, ANT, BaA, CHR, BbF, BkF, and BgP, most of which are on the heavier side of PAHs (4-6 aromatic rings), were only observed in a sample from Storvatnet. These compounds, except ANT, occur usually in particle phase [102], and are less prone to long-range atmospheric transport [101].

Wania and Mackay [4] divided POP contaminants into four categories dependent on mobility. According to this categorization, PAHs with three rings and PCBs with one to four chlorine atoms are of relatively high mobility and will deposit in polar latitudes. Four ringed PAHs and PCBs with four to eight chlorine atoms are of relatively low mobility and therefore preferably deposit in mid-latitudes. Above and below these groups, the categories “low mobility” and “high mobility” are characterized by deposition close to the source and no deposition at all, respectively [4]. The observation of NAP in samples from all sampling sites indicates that the moss does in fact take up PAHs in gaseous phase from the atmosphere, since two ringed PAHs are not likely to deposit. Furthermore, this characterization of PAHs emphasizes the possibility that the concentrations of heavier PAHs found at Storvatnet stem from local sources as these are expected to deposit close to the source. This also enables contributions of (at least) NAP, FLU, and PHE to be affected by long range atmospheric transport.

Wang et al. [29] measured concentrations of PAHs in, among other sampling media, moss from Ny-Ålesund. The mean concentrations of the relevant eleven PAHs found in the study are listed in table 5.1. By comparing the mean values from Wang et al. [29] with the individual concentrations found at the different locations in this study, it can be seen that the concentrations measured in sample Sv2 from Storvatnet are, in various extent, higher compared to the mean values. The only compound that does not show this trend is FLU, where the mean concentration from Wang et al. [29] is much higher. The concentrations found at Stuphallet and Austre Brøggerbre in this study are lower for NAP, FLU, and PHE, similar for PYR, and twice as high for FLT, compared to the mean values found by Wang et al. [29]. Since individual concentration values are compared to mean concentrations, it is expected that sampling sites farther away from local sources will show a lower concentration, while Storvatnet – which is closest to Ny-Ålesund – is expected to show increased concentration of the PAHs. Thus, the concentrations of FLT and PYR found at Stuphallet and Austre Brøggerbre, as well as the concentration of FLU found at Storvatnet, are interesting as these do not show this expected pattern. Furthermore, it should be emphasized that Wang et al. [29] also detected the five remaining PAHs (ACY, ACE, BaP, DbA, and InP) in the moss. The differences in PAH observations may be explained by the different extraction techniques used in these studies. While in this master study accelerated solvent

extraction with dichloromethane was performed, Wang et al. [29] performed three rounds of extraction with acetone/hexane in ultrasonic bath. This did potentially contribute to better extraction of the remaining PAHs.

Table 5.1: Mean concentrations (ng g^{-1}) of eleven PAHs in moss from Ny-Ålesund in a study performed by Wang et al. [29].

Mean concentration (ng g^{-1}) [29]										
NAP	FLU	PHE	ANT	FLT	PYR	BaA	CHR	BbF	BkF	BgP
41	38	72	8	7	5	3	5	6	1.3	4

In a study of PAHs in soil samples from Ny-Ålesund performed by Han et al. [103], the highest total concentration of the 16 PAHs was found at the sampling location closest to the airport. Except from this location, no explanation was found for the concentration levels. This is also the case in this master study, where the highest concentration of PAHs was observed at Storvatnet which is closest to the airport, while no clear difference was observed between Stuphallet and Austre Brøggerbre. Han et al. [103] observed that three and four ringed PAHs had the highest content in the samples, while two, five and six rings contributed less. In this master study, the contributions of three and four ringed PAHs were large as well, however, in the moss samples here, high content was also found of the two ringed PAH, Nap [103]. This is probably due to the fact that moss mainly take up PAHs in their vapor phase, while soil accumulates PAHs in particular phase from deposition [29]. Thus, higher concentration of NAP in moss compared to soil would be expected.

In the study performed by Na et al. [104], the dominating PAHs in soil samples were the same PAHs dominating in the moss samples in this master study, namely PHE, NAP, FLT, and FLU. Overall, it seems like the results obtained for PAHs in this master study agrees well with results from earlier studies from Ny-Ålesund.

5.2 Trace elements

5.2.1 Trace elements in moss

Storvatnet yielded concentrations significantly different from Stuphallet and Austre Brøggerbre for nine elements (V, Cr, As, Se, Mo, In, Tl, Pb, Bi), all in which the mean concentration was higher at Storvatnet. This is probably due to Storvatnet being closer located to settlement and runway, as several of these elements have shown to derive from anthropogenic sources [105]. A contribution from the continental crust should not be excluded as both V, Cr, As, In, and Pb have been suggested to be affected by crust particles [105].

Mean concentrations of Ni and Zn are highest at Austre Brøggerbre, but the concentrations of these elements were not significantly different here compared to Storvatnet (p -value 0.937 for both Ni and Zn). Boxplots (see figure 6.12 in 6.5) and p -values from Mann-Whitney U test show that several elements have similar mean concentrations at Austre Brøggerbre and Storvatnet (Co, Ni, Cu, Zn, Ag, Cd, Sb, and W), indicating that these sampling locations are influenced by the same pollution sources. However, other elements

show the same trend as the PAHs, where elevated concentrations were found at Storvatnet and similar concentrations were found at Stuphallet and Austre Brøggerbre. This is the case for V, Cr, As, Mo, In, Tl, Pb, and Bi.

Antimony and W were the only elements found to have significantly higher concentrations at Stuphallet compared to Austre Brøggerbre and Storvatnet. According to Blundell et al. [106], Sb, W, and As are important element additions to shear zones. Thus, this observation of higher concentrations at Stuphallet can be explained by the presence of a potential shear zone nearby. If this was the case, a correlation between these three elements would probably be expected. However, as seen from the correlation matrix in 6.7, only Sb and W seems to correlate.

The larger concentration of Sb found at Stuphallet may indicate bird influence [107], as this area is considered a bird nesting site [108]. Elevated concentrations of Sb in conjunction with bird influence may be expected to be accompanied with elevated concentrations of P, at least for soil samples [109]. The concentration of P found in this study does not seem to be higher at Stuphallet compared to the two other sampling areas (see supplementary files). However, there is a chance that the uptake of P in moss is poor, thus, an elevation of P would not be shown in the results. Furthermore, as the uptake and accumulation of compounds differ between sample media, there is a chance that P does not indicate bird influence in moss samples the way it does for soil samples.

If Stuphallet was influenced by birds, it would be expected to also observe elevated concentrations of other elements, such as Cd, as Cd is another metal indicating bird influence [110, 111]. Elevated concentrations of Cd is not found at this location, and the mean concentration of Cd is stable between the sampling locations. Cadmium is, in fact, the only element that did not show any significant difference between all three sampling sites. The distribution of Cd is stable throughout the sample locations, with an approximate mean concentration of $0.45 \mu\text{g g}^{-1}$. The same observation was made in a study performed by Aslam et al. [84] on soil and above-lying vegetation. Here, the concentrations of Cd were similar at both study locations, and it was concluded that the concentrations of Cd in soils at Svalbard show no influence from local activities [84]. As the concentration of Cd found in this master study was higher compared to the results obtained in a master study from 2021 [112], this may indicate long-range transport as a potential source of Cd to Ny-Ålesund. The variation in the Cd concentrations is large at both Stuphallet and Austre Brøggerbre, which can be seen in the box plot of Cd (figure 6.12k). This would potentially also be the case at Storvatnet if more samples were collected and analyzed, and the variation can possibly be a result of the moss samples containing various age and therefore have been exposed for atmospheric Cd over various periods.

As Stuphallet is located closer to the coast compared to the two other sampling locations, the potential influence of sea spray should be considered. Sea salt elements may reduce the uptake of other elements due to competition, and might have contributed to the lower concentrations found at Stuphallet. However, the concentration of Mg and Na are not elevated at Stuphallet compared to other sampling sites (see the supplementary files). This suggests that Stuphallet is not substantially influenced by the sea.

Although moss does not take up pollutants from the underlying soil, particulate bounded

elements in nearby soil can be windblown onto the moss. As the samples were not rinsed before further sample preparation, the effects of this have likely contributed to the overall concentration detected in the moss samples. The impact of soil components will probably correlate with the extent of vegetation at the sampling location, hence, the contribution will be largest at Storvatnet where the vegetation was sparse, and smallest at Stuphallet due to the more complete vegetation cover. It is suggested to wash moss samples before analysis in order to reduce the effect of windblown dust on the overall concentration. However, Steinnes and Jacobsen [113] observed that washing/shaking the moss samples prior to analysis did not effect the overall concentration [113].

Comparison with earlier studies

Concentrations of elements found in a selection of earlier studies are given in table 5.2.

Table 5.2: Mean concentrations ($\mu\text{g g}^{-1}$) of selected elements found in earlier studies [112, 87, 32, 34].

	Concentration ($\mu\text{g g}^{-1}$)				
	This study	Ny-Ålesund [112]	Ny-Ålesund [87]	Siberian Arctic [32]	Norwegian mainland [34]
V	4.07	4.33	N/A	4.97	1.6
Cr	3.47	3.47	2.1	N/A	1.1
Co	0.916	N/A	N/A	N/A	0.5
Ni	3.20	N/A	2.9	4.24	5.1
Cu	2.50	N/A	5.0	4.57	7.2
Zn	38.8	24.7	44	27.5	36
As	0.383	0.334	0.40	0.39	0.17
Se	0.346	N/A	N/A	<0.34	0.3
Mo	0.146	0.0847	N/A	N/A	N/A
Ag	0.0218	0.243	N/A	N/A	0.03
Cd	0.430	0.222	0.20	0.166	0.12
In	0.00366	N/A	N/A	N/A	N/A
Sn	0.0982	0.0954	N/A	N/A	N/A
Sb	0.0345	0.0561	0.13	N/A	0.08
W	0.00990	0.0123	N/A	N/A	N/A
Hg	0.113	N/A	N/A	0.051	0.08
Tl	0.0205	0.144	N/A	N/A	2.2
Pb	3.16	2.16	3.7	1.84	0.06
Bi	0.0236	0.0170	N/A	N/A	0.1

The mean concentration of most of the elements (V, Cr, Ni, Zn, As, Ag, Sn, W, Pb, Bi) was similar to the mean concentrations found in Ny-Ålesund previously. The measured concentration for Cu was $2.50 \mu\text{g g}^{-1}$ in this study, but found to be $5.0 \mu\text{g g}^{-1}$ in a study from 2020. Variation in concentrations are probably influenced by variation in sampling

location. The concentration of Cd is elevated compared to earlier, perhaps partly due to long range transport as mentioned earlier.

It is, however, important to emphasize that different species can have different capacity of accumulating elements. In the study performed by Ma et al. [87], the mean concentration was obtained by analyzing six different plant species. Thus, the levels of pollutants found may potentially differ from the levels found if solely moss was used. Schick [112] analyzed the same moss species as has been studied in this study, and it is therefore assumed, exclusively considering moss species, that the accumulation potential is not different.

Mean concentrations for most of the elements found in this study were comparable with concentrations found by Allen-Gil et al. [32] in the Siberian Arctic as well. The only substantial difference was found for Cu, Cd, Hg, and Pb, where the three latter concentrations were notably elevated. Due to their locations, Svalbard and the Siberian Arctic are not influenced by the same pollution transport pathways. In addition to receiving pollutants from Europe, Svalbard receives pollutants from America as well due to the wind trajectories. The Siberian Arctic is, on the other hand, influenced by Europe and Asia. As the pollutants from Europe have a shorter transportation path to Svalbard compared to the Siberian Arctic, this may influence the concentrations of atmospheric transported pollutants [114]. In a study of long-range transport of atmospheric Pb performed by Bazzano et al. [88] in Ny-Ålesund, it was concluded that the atmospheric Pb during summer was most affected by industrial emission from North America.

Steinnes et al. [34] have frequently conducted national moss surveys of metals in the Norwegian mainland in the time period 1977-2015 [34]. Comparing the mean concentrations found in the latest survey with the mean concentrations obtained in this study, most of the elements are either more enriched or have a similar concentration in Ny-Ålesund. Only Ni, Cu, Sb, Tl, and Bi out of the 15 elements analyzed for in both studies showed a substantial higher mean concentration in the mainland Norway. Vanadium, Cr, (Co), (As), Cd, and Pb was found in an elevated amount in Ny-Ålesund compared to the mainland. Especially the comparison of the two latter is noteworthy, as these concentrations were found to be four and five times as high in Ny-Ålesund for Cd and Pb, respectively. This may potentially be a result of long-range atmospheric transport. However, as the growth rate of *Hylocomium Splendens* is lower in the Arctic compared to areas of lower latitudes, the moss in Arctic will have longer time to accumulate elements. Therefore, similar concentrations of elements in moss from lower latitudes do not necessarily mean similar extent of surrounding pollution [41, 113].

5.2.2 Trace elements in moss samples compared to snow samples

The moss samples collected for this thesis are compared to snow sampled in proximity of Ny-Ålesund in 2017. Unfortunately, during this sampling no snow was collected from Stuphallet, and only moss sampled close to Austre Brøggerbre and Storvatnet is therefore included here. Furthermore, the snow was not analyzed for In and Bi, and these elements are consequently excluded from the following part.

The trend of most elements in moss having their highest concentration at Storvatnet is also

the case for snow samples where the highest concentration of all elements, except Se and Hg, was found at the sampling site closest to Storvatnet. No significant difference was however found for Co, Ag, and Cd. Thus, the highest concentration of V, Cr, Ni, Cu, Zn, As, Mo, Sn, Sb, W, Tl, Pb was found for snow samples at Storvatnet. Comparing this with the moss results, it can be seen that V, Cr, As, Mo, Tl, and Pb show highest concentration for both moss and snow at Storvatnet, as well as they differentiate significantly from moss and snow results from Austre Brøggerbre.

Mercury is the only element shown to have a significantly higher concentration for snow data collected at Austre Brøggerbre compared to Storvatnet. This is not the case for moss data, where the concentration of Hg at Austre Brøggerbre is significantly lower compared to Stuphallet and Storvatnet. This may be in relation with the differences in sampling location for snow and moss samples.

Comparing the concentrations of the various elements found in snow and moss samples would not provide any indicative information, as the snow only reflects pollutants deposited over one winter, while the moss in this study has been exposed for up to several years. What will provide valuable information, and therefore are being compared in this study, is the relative amount of the different elements found in the two sample media. Bar charts showing relative distribution of the selected elements in snow and moss can be seen in figure 5.1.

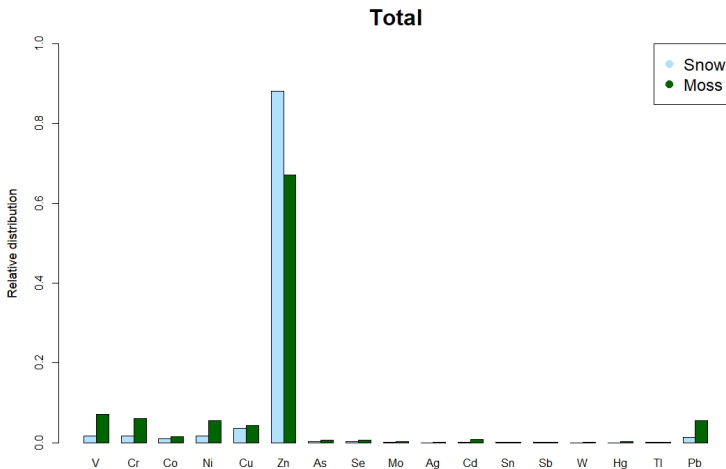


Figure 5.1: Relative distribution of the elements in snow and moss.

It is clearly observed that Zn has the largest contribution to the overall element concentration in both snow and moss (0.88 and 0.67, respectively). Zn has also the highest concentration in the studies used for comparison of moss as well (ref. table 5.2). The reason why Zn is dominating in snow and moss from Ny-Ålesund is potentially due to influence by both anthropogenic and geogenic sources as several of the rock types present in

Ny-Ålesund contains Zn [18].

As Zn is highly dominating in both snow and moss – causing the distribution of other elements to be overshadowed – four additional bar charts were made. Bar charts containing relative distribution of Ag, W, and Tl (5.2a), Mo, Sn, Sb, and Hg (5.2b), Co, As, Se, and Cd (5.2c), and V, Cr, Ni, Cu, Pb (5.2d) are given in figure 5.2. The division of elements between these charts were based on the elements' relative contribution to the overall metal concentration in order to better observe similarities and differences. Notice that the scaling along the y-axis varies, and heights of bars in different charts must be compared with care.

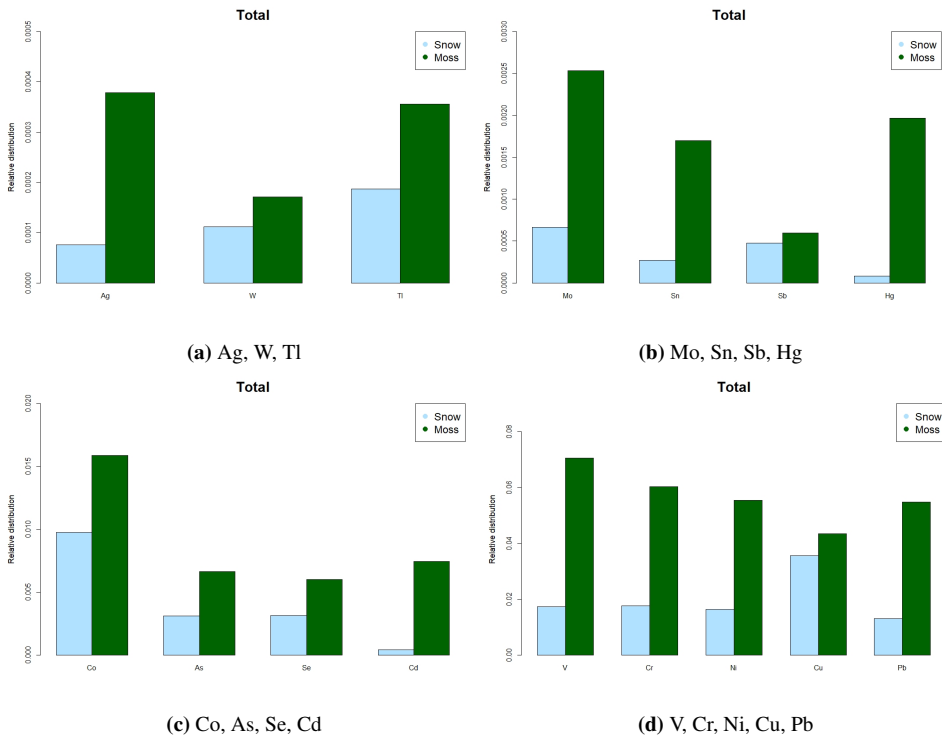


Figure 5.2: Relative distribution of elements in snow and moss. Be aware of different scaling along the y-axis.

The relative distribution of the remaining elements when Zn is excluded is larger in moss than in snow, probably due to the large contribution of Zn to the overall concentration in the snow sample. The contribution of Hg and Cd is especially elevated in moss, with a relative distribution value that is about 20 times more concentrated for moss compared to snow. Ag, and Sn, (Mo, Pb, Se, V, Cr, and Ni) contributions were also substantial higher in moss than snow. This can potentially be explained by the moss' possibility to accumulate elements over a longer period of time compared to snow, which primarily contains elements present in the atmosphere over one season. Thus, elements present

in lower concentrations in the atmosphere over the snowy season will naturally show a smaller contribution to the total concentration.

Copper, Sb and W are more or less contributing with the same amount to the overall element composition when comparing moss and snow at the two sampling areas close to Ny-Ålesund. Cobalt and Tl do also show similar contributions in moss and snow. Copper, Co, and Tl show good correlation with Sc (see 6.6), indicating a geogenic origin. Antimony and W, on the other hand, show a negative correlation with Sc, indicating anthropogenic origin. It is interesting that these two anthropogenic elements show similar contribution in moss and snow, as these were found to have their highest concentrations in moss samples from Stuphallet which was furthest away from local pollution sources. This may potentially indicate that these elements are primarily taken up from the atmosphere.

Bar charts where moss and snow sampled from Austre Brøggerbre and Storvatnet are separately compared are placed in 6.6, in figure 6.13 and figure 6.15, respectively. The bar charts of relative distributions of the different elements at Storvatnet are closely similar to the bar charts where Storvatnet and Austre Brøggerbre are presented as a whole. Austre Brøggerbre, on the other hand, shows several differences. In this case, the difference in contribution of Zn is not as large. It can be seen that, in addition to W and Cu, also Ag, Tl, Mo, Sn, and Pb have similar distribution in moss compared to snow. It is also worth noting that the relative distribution of Sb and Se are substantially larger in snow samples compared to moss samples from this area. Potential explanation of this is that the sampling location at Austre Brøggerbre is more remote compared to Storvatnet which have potential dominating point sources, and that the snow and moss samples become more similar the more remote-lying the sample location is. Thus, local sources have a lesser impact and the elemental concentration may be more indicative of the long range atmospheric transport. Another possible explanation is the better vegetation cover at Austre Brøggerbre, which reduces the potential of windblown dust. Windblown dust is not affecting the snow samples in the same way as for the moss samples, and perhaps the reduction in the contribution from soil elements would make the relative distribution of elements in snow and moss samples more similar. Both these suggested explanations would have been better investigated if snow samples were also collected at the most remote location Stuphallet, where the vegetation cover was better. However, it is important to emphasize that the sample locations for snow were not completely overlapping with the sample locations Austre Brøggerbre and Storvatnet for moss. Features with the location, such as wind direction, shelter, etc., may therefore have influenced the concentration found in snow compared to moss.

5.3 Principal component analysis

Three principal component analyses were run: one only considering moss, one containing both moss and snow, and one additional also including soil samples from an earlier master thesis [115]. Only PC1 and PC2 are discussed here, as other PCs described less than 10% of the variance. Plots with PC3 and PC4 for the two latter PCA plots can however be viewed in 6.8.

5.3.1 PCA for moss samples

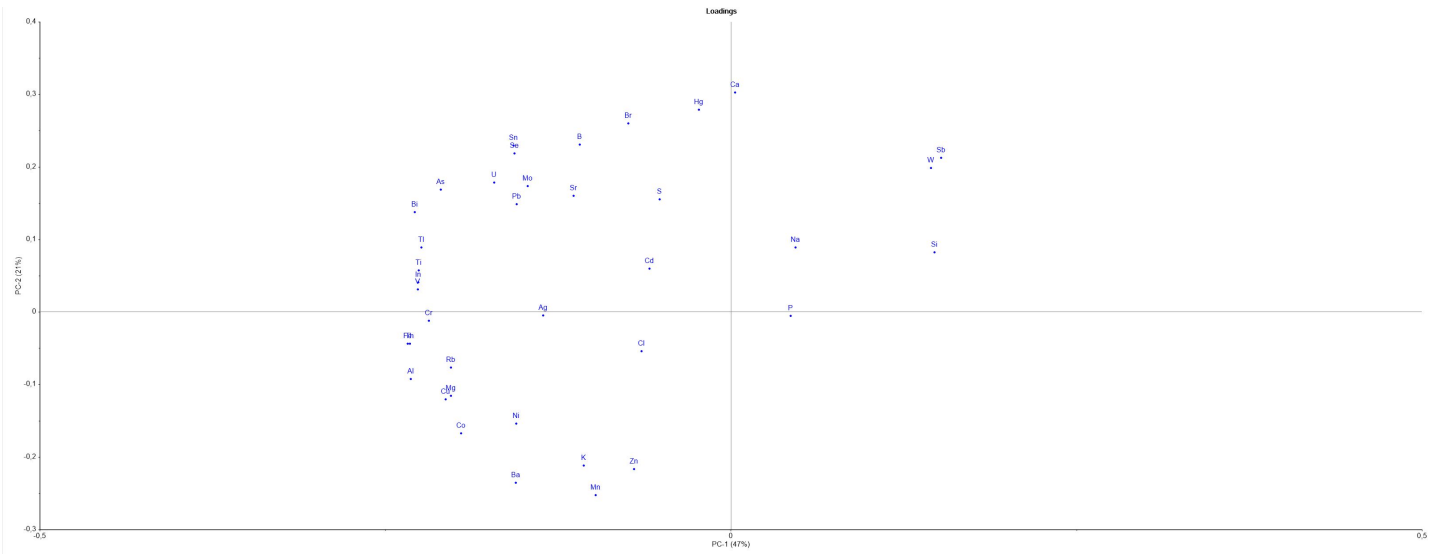


Figure 5.3: PCA loading plot for moss samples, showing first and second component.

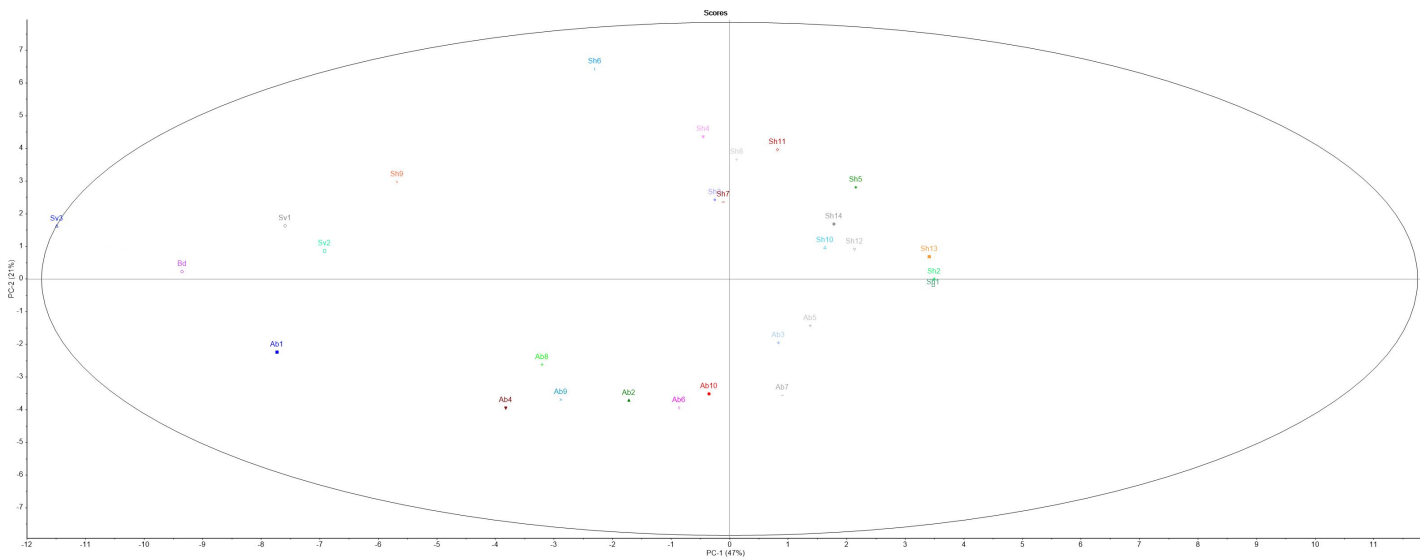


Figure 5.4: PCA score plot for moss samples, showing first and second component.

Almost 70% of the variance was explained by the two first components of the PCA including only moss samples, see figure 5.3. The first component (PC1) in the analysis covered 47% of the variance itself. From the loading plot it can be seen that Al, Fe, Th, Cr, V, In, Ti, Tl, and Bi, in particular, have high negative values in PC1. These elements correlates well with each other in the correlation matrix (correlation ranging from 0.64 to 0.98). As especially Al, Fe, and Ti are related to soil components, this indicates an influence from soil sources [87]. To investigate the potential geogenic origin, the ratio between the elements and Sc can be used [116]. From the correlation matrix given in the supplementary files, it can be observed that all these elements have a high correlation with Sc, ranging from 0.79 for Bi to 0.99 for Fe. This indicates that the elements with high negative PC1 values are of geogenic origin. In the positive direction of PC1, Si, W, and Sb are dominating. The correlation in this case range from 0.45 to 0.74. These elements are found in the opposite direction as to the soil elements, and are therefore less likely to be influenced by soil components. This is emphasized by their ratio to Sc, where the correlation range from -0.57 for W to -0.72 for Sb. Thus, it seems that these elements are primarily of anthropogenic origin. No explained correlation has been found in the literature for these three elements, but they are potentially affected by an atmospheric source.

The second component (PC2) explained 21% of the variance. Here it was observed high negative values for Zn, Mn, Ba, and K. The correlation between K and the three other elements are not very strong (0.41 to 0.58), but the correlation between Zn, Mn, and Ba range between 0.75 to 0.92. These three elements have been associated with traffic [117], which may be the case here as well. However, the reason why K is found together with these elements remains unknown. High positive values are found for Ca, Hg and Br, with correlation ranging from 0.65 between Hg and Br to 0.77 between Ca and Hg. As these were found in the opposite direction of the traffic related elements, it is assumed that the contribution from traffic is minimal for Ca, Hg, and Br. Br has been related to the marine environment, and Ca has earlier been shown to correlate with marine components [118], indicating a contribution from marine environment.

The fact that Na and Cl are observed close to origin indicates that the moss samples are not particularly influenced by sea spray. Thus, the elements found in moss samples stems primarily from other sources than the sea.

A tripartite distribution can be observed in the score plot (figure 5.4) along the first component, with most of the samples from each sampling location found together. Storvatnet is closest to the values of the soil elements, while Stuphallet is furthest away, thus indicating that Storvatnet is most influenced by soil elements and Stuphallet is least influenced by such compounds. This is as expected, since the sampling area at Storvatnet had least vegetation, and just a bit more cover was observed at Austre Brøggerbreen, thus, both areas facilitating windblow of soil particles. Stuphallet, on the other hand, had a denser vegetation cover resulting in a reduced potential for windblown dust impact.

Overlapping the score and loading plot, it can be noticed that Stuphallet correlates with Sb, W, Si on PC1 and Ca, Hg, and Br along PC2. (The samples from Stuphallet is less impacted by traffic, which is expected as this is the most remote sampling location in this study.) Austre Brøggerbreen is located on the opposite side of PC2 compared to Stuphallet,

thus, are not correlating with Hg, Ca, Sb, and W. Instead, Austre Brøggerbre correlates with K, Zn, and Mn, indicating an influence of traffic.

5.3.2 PCA for moss and snow samples

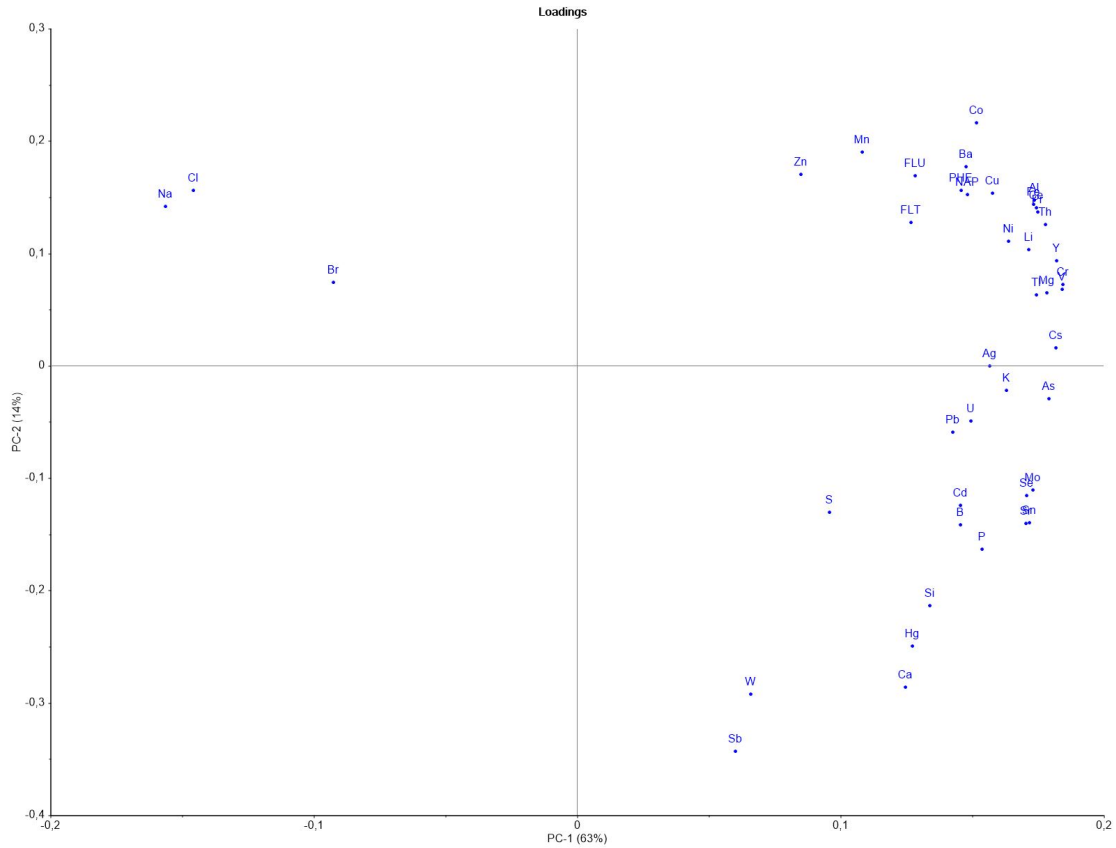


Figure 5.5: PCA loading plot for moss and snow samples, showing first and second component.

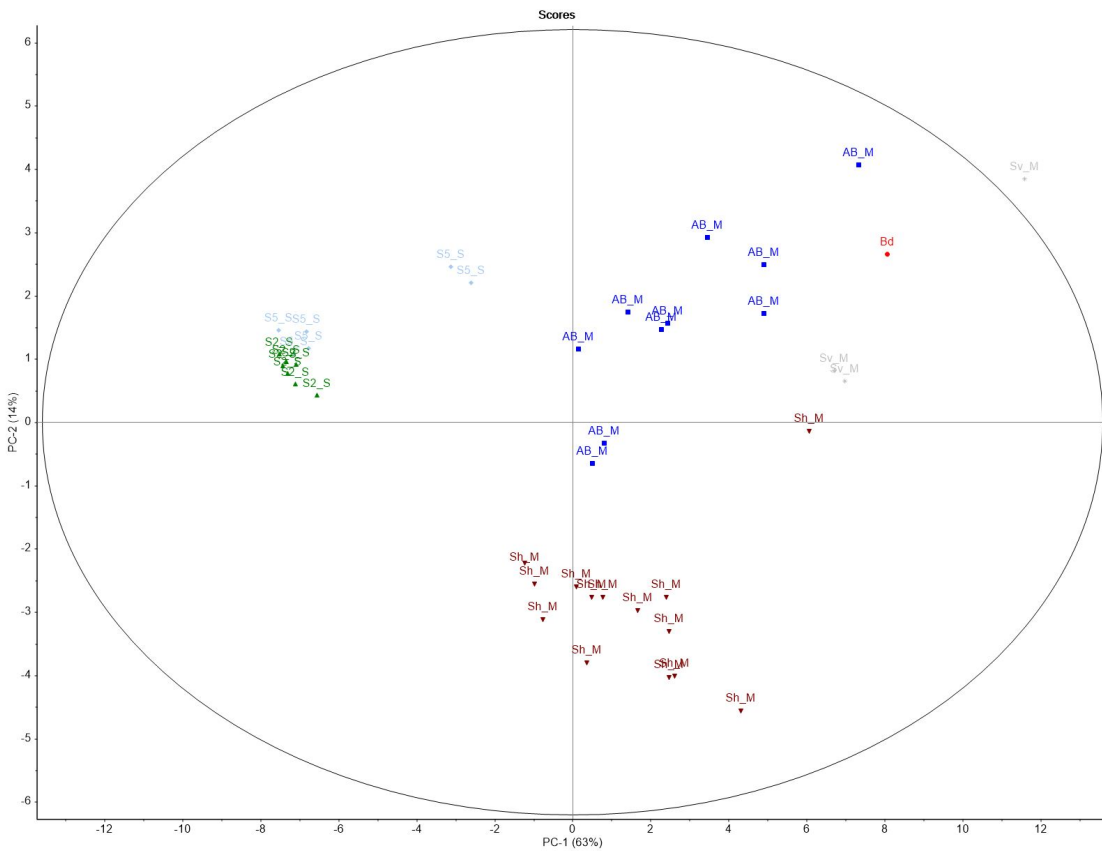


Figure 5.6: PCA score plot for moss and snow samples, showing first and second component.

In the PCA plot comprising both moss and snow samples (figure 5.5 and 5.6), the four “most found” PAHs (NAP, PHE, FLU, FLT) were also included. In this case, almost 80% of the variance was explained by the two first components, with PC1 being responsible for 63%. Along the first component a clear division is observed between the sea spray correlating elements Na, Cl, and Br in the negative direction – indicating a sea component/factor – and all other elements/compounds in the positive direction. The highest positive values are found for Al, Fe, Ce, Pr, Th, Li, Y, Cr, V, Mg, Tl, Cs, As, Mo, Se, Sr, and Sn. As these are found on the opposite side of the sea elements, this indicates that the largest influence on these elements stems from another source than the sea. Both aerial and soil sources can be potential impacts. Soil sources are perhaps of extra importance for the elements found in the upper right, as these show good correlation with Sc. The correlation with Sc decreases for elements with high value for PC1 from upper right to lower right, emphasizing that aerial sources are also likely to contribute to the overall concentration.

High positive values along PC2 are observed for Co, Mn, Zn, Ba, PAHs, Cu, Al, Fe, Ce, Pr, Cl, and Na. This can potentially be explained by combustion, for instance from coal or oil. In the negative direction, high values are found for Sb, W, Ca, and Hg, connecting positive PC1 and PC2 elements from the moss PCA plot (figure 5.3). As both Sb and Hg are two elements highly affected by atmospheric transport [118, 92], this can indicate an aerial source of these elements. Additionally, both Sb, W, Ca, and Hg showed a negative (or very weak positive) correlation with most of the other metals that are suggested to be influenced by local sources.

The snow samples are separated from the moss samples in the score plot. Snow samples are found in the second quadrant (upper left), while moss samples are more or less found in the first and fourth quadrant, namely with positive values for PC1. This is of interest, as it indicates that snow samples correlate with sea elements, while moss samples do not show this correlation. Thus, snow samples seem to be more affected by sea spray compared to moss samples. Aerosols formed by sea spray can be transported by wind and deposit on the snow pack [119].

Although the moss samples differentiate from the snow samples, the moss alone is also divided in two, showing similar patterns as in the first discussed PCA plot. Stuphallet is yet again shown to correlate with Sb, W, Ca, and Hg, possibly related to more of an atmospheric component. Samples from Austre Brøggerbre and Storvatnet are mostly found in the first quadrant, correlating with elements potentially related to combustion and soil sources. What the first discussed PCA plot does not show, is that PAHs are found together with these elements, which may indicate that the PAHs found in the samples are more related to local sources in preference to long-range atmospheric transport.

By PC2 in the score plot it is observed that snow samples correlate more with moss samples from Austre Brøggerbre and Storvatnet rather than Stuphallet. This is expected as these samples are taken in the same area. However, as Stuphallet is suggested to be more influenced by long-range atmospheric elements, this observation also indicates that snow samples are more affected by local sources rather than long-range atmospheric transport. If the snow samples were mainly influenced by long-range atmospheric transport, they would probably correlate more with the moss samples from Stuphallet.

PCA plot including soil samples

A PCA plot with the snow and moss samples together with soil samples from an earlier master thesis [115] can be viewed in 6.8. This plot was created in order to better see in which extend the effect of windblown soil particles had on the samples discussed in this thesis. Here, more than 80% of the variance is explained by the first two components. A clear threefold division between snow, moss and soil is observed in the score plot (figure 6.18), where the two separate clusters containing snow and moss samples are found in the negative direction of PC1 – on each their own side of PC2 – while soil samples are found in positive PC1 direction. From PC1 in the loading plot, it can be observed that snow correlates most with Na, moss most with Sb, and soil with the rest of the elements. This indicate that snow is influenced by a marine component as previously stated, but also that moss is well influenced by potential long range atmospheric transport due to its correlation with Sb rather than the other elements. Also, as moss cluster and snow cluster are found on the negative side of PC1, while the soil samples are found on the opposite side of PC1, snow and moss sample media are more similar to each other than to soil.

5.4 Validation of the method

As the snow analysis was not performed in conjunction with this study, the sampling and analysis method used for snow will not be further discussed here.

Several measures were taken in order to minimize the potential for contamination of the samples throughout the fieldwork and subsequent sample handling. During fieldwork, nitrile gloves were used while sampling. To avoid contamination from storage containers, the samples were stored in aluminum boxes and paper bags for organic and inorganic analyses, respectively. During sample pretreatment, equipment was frequently washed. The containers with belonging balls were washed with soap and water between every new sample, in order to avoid cross-contamination between samples. The outside of the instrument was also wiped over with a wet paper tissue. Nitrile gloves were used in addition.

To avoid cross contamination during ASE running, cells and other equipment (such as sample beaker, stirring rod, and sample spatula) was cleaned with water and soap, MiliQ water and acetone, and put to dry between every sample. The instrument was also rinsed three times between each sample type, letting dichloromethane flush through the system.

By including a concentration blank consisting only solvent (ethyl acetate) while concentrating with the TurboVap, potential cross-contamination could be observed. The concentration blanks were subsequently treated and analyzed in the same manner as every other sample. Reagent blanks – amber vials containing solvent (ethyl acetate) – were frequently run in the GC-MS sequence to provide an overview of potential cross-contamination occurring in the injection system or column. Neither Concentration blanks nor reagent blanks was found to be contaminated from the GC-MS results, thus, cross-contamination in these parts of the sample treatment/analyses was neglected.

5.5 Limitations regarding study design

Accompanying limitations in time, economics, and equipment, the study design was not optimal. As the accuracy of pollution characterization studies increases with number of sampling sites [52], the research done in this thesis could with advantage included more sampling sites. However, this was difficult due to time constraints, and the restricted occurrence of *Hylocomium Splendens* in the study area. Extended study area would have been possible with access to means of transportation.

According to Fernández et al. [52], it is preferred with 30 or more samples in order for the statistical certainty to be ensured. In this study, the amount of samples ranged from 3-14 and 2-10 for inorganic and organic analysis, respectively. This is far below the recommended amount of 30 samples. Especially the results obtained at Storvatnet should be carefully interpreted, as the moss sample amounts are only two and three. Since the sparse vegetation cover caused this limitation, alternatives like moss bags or sampling of other species could be considered. As different moss species have different capacity / accumulation properties, mixing moss species in the same study should be performed with awareness.

To get a more accurate comparison of snow and moss samples, it would be preferable to perform the snow and moss sampling the same year. Additionally, the moss and snow sampling should have a better overlap, ensuring the sampling areas to primarily be influenced by the same pollution sources.

Comparing the concentrations found in moss from the different locations does neither give accurate information because of the variation in age. Age determination was not performed, and the moss samples between different sampling sites consisted of moss of different size. The older the moss, the more pollutants are potentially accumulated due to longer time of exposure. Thus, older moss will probably contain elevated concentrations of pollutants compared to younger moss in the same area.

Conclusion

The aim of this study was to investigate the extent of pollutants found in moss sampled from different locations in proximity of Ny-Ålesund, Svalbard, and to compare the pollutants found in moss samples with pollutants found in snow samples. The moss sampled in this study was analyzed for a selection of the persistent organic pollutants PCBs and PAHs, in addition to (trace) metals.

No PCBs were found in the analyzed samples, which is not in concordance with earlier studies of moss in Ny-Ålesund. The method of analysis is probably the reason for this observation, and the potential for PCBs to be present in the moss should not be ruled out. The results obtained for PAHs, however, correlated well with earlier studies. Eleven PAHs were detected, all in which elevated concentrations were found at the sampling location closest to potential local pollution sources (Storvatnet). Four PAHs were found at all sampling locations. The concentration of these were similar between the two other sampling locations (Stuphallet and Austre Brøggerbre), indicating the possibility of LRAT. However, PCA plots suggested the contribution to be more influenced by local sources.

Elevated concentrations found at Storvatnet compared to the two other sampling locations were also the case for nine trace elements. (The results indicate that Austre Brøggerbre is influenced by the same sources as Storvatnet, but to a lesser extent.) Antimony and W were the only elements that had significantly higher concentrations in another sampling site than Storvatnet, and these elevated concentrations were found at Stuphallet. From the PCA plots, Sb and W seemed to stem from an anthropogenic atmospheric input. The concentration of Cd was stable throughout the sampling locations, and showed no significant difference. This has also been observed earlier, and indicate LRAT potential.

The relative distributions of the elements in snow and moss were used for comparing the two sample media. Zn had by far the largest contribution to the overall metal concentration in both moss and snow, possibly due to the contribution from both anthropogenic and geogenic sources. The contribution of Hg and Cd to the overall concentration was

much higher in moss compared to snow, likely because of moss' ability to accumulate over several years, while the contribution of Cu, Sb, and W was similar in the sample media.

This study emphasizes the choice of sufficient sampling sites when studying long-range atmospheric transport. The results obtained in this study suggest the potential for moss and snow samples to correlate with each other if suited sampling sites are selected. It is recommended that, in addition to choosing sampling sites in a remote area, snow samples should be collected in a sufficient distance from the sea, and moss samples should be collected in areas of dense vegetation cover.

Bibliography

- [1] Jacobson, M. Z.; Jacobson, M. Z. *Atmospheric pollution: history, science, and regulation*; Cambridge University Press, 2002.
- [2] Burkow, I. C.; Kallenborn, R. Sources and transport of persistent pollutants to the Arctic. *Toxicology letters* **2000**, *112*, 87–92.
- [3] Harmens, H.; Foan, L.; Simon, V.; Mills, G. Terrestrial mosses as biomonitors of atmospheric POPs pollution: a review. *Environmental Pollution* **2013**, *173*, 245–254.
- [4] Wania, F.; Mackay, D. Peer reviewed: tracking the distribution of persistent organic pollutants. *Environmental science & technology* **1996**, *30*, 390A–396A.
- [5] AMAP, AMAP Assessment 2002: Heavy Metals in the Arctic. **2005**,
- [6] Schroeder, W. H.; Munthe, J. Atmospheric mercury—An overview. *Atmospheric Environment* **1998**, *32*, 809–822.
- [7] Mahapatra, B.; Dhal, N. K.; Dash, A. K.; Panda, B. P.; Panigrahi, K. C. S.; Pradhan, A. Perspective of mitigating atmospheric heavy metal pollution: using mosses as biomonitoring and indicator organism. *Environmental Science and Pollution Research* **2019**, *26*, 29620–29638.
- [8] Salo, H.; Berisha, A.-K.; Mäkinen, J. Seasonal comparison of moss bag technique against vertical snow samples for monitoring atmospheric pollution. *Journal of Environmental Sciences* **2016**, *41*, 128–137.
- [9] Nemirovskaya, I. A.; Shevchenko, V. P. Organic Compounds and Suspended Particulate Matter in Snow of High Latitude Areas (Arctic and Antarctic). *Atmosphere* **2020**, *11*, 928.
- [10] Blagnytė, R.; Paliulis, D. Research into heavy metals pollution of atmosphere applying moss as bioindicator: a literature review. *Environmental Research, Engineering and Management* **2010**, *54*, 26–33.

-
- [11] Wania, F. Assessing the potential of persistent organic chemicals for long-range transport and accumulation in polar regions. *Environmental science & technology* **2003**, *37*, 1344–1351.
- [12] Wania, F.; Mackay, D. Global fractionation and cold condensation of low volatility organochlorine compounds in polar regions. *Ambio* **1993**, 10–18.
- [13] Gouin, T.; Mackay, D.; Jones, K. C.; Harner, T.; Meijer, S. N. Evidence for the “grasshopper” effect and fractionation during long-range atmospheric transport of organic contaminants. *Environmental pollution* **2004**, *128*, 139–148.
- [14] Bhardwaj, L.; Chauhan, A.; Ranjan, A.; Jindal, T. Persistent Organic Pollutants in Biotic and Abiotic Components of Antarctic Pristine Environment. *Earth Systems and Environment* **2018**, *2*, 35–54.
- [15] Catalan, J. *Tracking Long-Range Atmospheric Transport of Trace Metals, Polycyclic Aromatic Hydrocarbons, and Organohalogen Compounds Using Lake Sediments of Mountain Regions*; Springer Netherlands, 2015; pp 263–322.
- [16] Hassaniien, M. A. *Atmospheric Heavy Metals Pollution: Exposure and Prevention Policies in Mediterranean Basin*; Springer Netherlands, 2011; pp 287–307.
- [17] Chaligava, O.; Shetekauri, S.; Badawy, W. M.; Frontasyeva, M. V.; Zinicovscaia, I.; Shetekauri, T.; Kvlividze, A.; Vergel, K.; Yushin, N. Characterization of Trace Elements in Atmospheric Deposition Studied by Moss Biomonitoring in Georgia. *Archives of Environmental Contamination and Toxicology* **2021**, *80*, 350–367.
- [18] Alloway, B. J. *Heavy metals in soils*; Springer, 2013; Chapter 2, pp 11–50.
- [19] Hicks, W. T. Evaluation of vapor-pressure data for mercury, lithium, sodium, and potassium. *The Journal of Chemical Physics* **1963**, *38*, 1873–1880.
- [20] Clarkson, T. W. The Toxicology of Mercury. *Critical Reviews in Clinical Laboratory Sciences* **1997**, *34*, 369–403.
- [21] Douglas, T. A.; Loseto, L. L.; Macdonald, R. W.; Outridge, P.; Dommergue, A.; Poulain, A.; Amyot, M.; Barkay, T.; Berg, T.; Chételat, J. The fate of mercury in Arctic terrestrial and aquatic ecosystems, a review. *Environmental Chemistry* **2012**, *9*, 321–355.
- [22] Obrist, D.; Kirk, J. L.; Zhang, L.; Sunderland, E. M.; Jiskra, M.; Selin, N. E. A review of global environmental mercury processes in response to human and natural perturbations: Changes of emissions, climate, and land use. *Ambio* **2018**, *47*, 116–140.
- [23] Jones, K. C.; De Voogt, P. Persistent organic pollutants (POPs): state of the science. *Environmental pollution* **1999**, *100*, 209–221.
- [24] Borja, J.; Taleon, D. M.; Aurensenia, J.; Gallardo, S. Polychlorinated biphenyls and their biodegradation. *Process Biochemistry* **2005**, *40*, 1999–2013.

-
- [25] Organization, W. H. *Polychlorinated biphenyls and terphenyls*; World Health Organization, 1993.
- [26] Li, N.; Wania, F.; Lei, Y. D.; Daly, G. L. A comprehensive and critical compilation, evaluation, and selection of physical–chemical property data for selected polychlorinated biphenyls. *Journal of physical and chemical reference data* **2003**, *32*, 1545–1590.
- [27] Abdel-Shafy, H. I.; Mansour, M. S. M. A review on polycyclic aromatic hydrocarbons: Source, environmental impact, effect on human health and remediation. *Egyptian Journal of Petroleum* **2016**, *25*, 107–123.
- [28] Kim, K.-H.; Jahan, S. A.; Kabir, E.; Brown, R. J. C. A review of airborne polycyclic aromatic hydrocarbons (PAHs) and their human health effects. *Environment International* **2013**, *60*, 71–80.
- [29] Wang, Z.; Ma, X.; Na, G.; Lin, Z.; Ding, Q.; Yao, Z. Correlations between physicochemical properties of PAHs and their distribution in soil, moss and reindeer dung at Ny-Ålesund of the Arctic. *Environmental Pollution* **2009**, *157*, 3132–3136.
- [30] Berg, T.; Pedersen, U.; Steinnes, E. Environmental indicators for long-range atmospheric transported heavy metals based on national moss surveys. *Environmental Monitoring and Assessment* **1996**, *43*, 11–17.
- [31] Zinicovscaia, I.; Hramco, C.; Dului, O. G.; Vergel, K.; Culicov, O. A.; Frontasyeva, M. V.; Duca, G. Air Pollution Study in the Republic of Moldova Using Moss Biomonitoring Technique. *Bulletin of Environmental Contamination and Toxicology* **2017**, *98*, 262–269.
- [32] Allen-Gil, S. M.; Ford, J.; Lasorsa, B. K.; Monetti, M.; Vlasova, T.; Landers, D. H. Heavy metal contamination in the Taimyr Peninsula, Siberian Arctic. *Science of the total environment* **2003**, *301*, 119–138.
- [33] Martinez-Swatson, K.; Mihály, E.; Lange, C.; Ernst, M.; Dela Cruz, M.; Price, M. J.; Mikkelsen, T. N.; Christensen, J. H.; Lundholm, N.; Rønsted, N. Biomonitoring of polycyclic aromatic hydrocarbon deposition in Greenland using historical moss herbarium specimens shows a decrease in pollution during the 20th century. *Frontiers in plant science* **2020**, *11*, 1085.
- [34] Steinnes, E.; Uggerud, H. T.; Pfaffhuber, K. A.; Berg, T. Atmospheric deposition of heavy metals in Norway. National moss survey 2015. *NILU rapport* **2017**,
- [35] Onianwa, P. C. Monitoring Atmospheric Metal Pollution: A Review of the Use of Mosses as Indicators. *Environmental Monitoring and Assessment* **2001**, *71*, 13–50.
- [36] Tyler, G. Bryophytes and heavy metals: a literature review. *Botanical journal of the Linnean Society* **1990**, *104*, 231–253.
- [37] Vázquez, M. D.; López, J.; Carballeira, A. Uptake of Heavy Metals to the Extracellular and Intracellular Compartments in Three Species of Aquatic Bryophyte. *Ecotoxicology and Environmental Safety* **1999**, *44*, 12–24.
-

-
- [38] Soudzilovskaia, N. A.; Cornelissen, J. H. C.; Doring, H. J.; Van Logtestijn, R. S. P.; Lang, S. I.; Aerts, R. Similar cation exchange capacities among bryophyte species refute a presumed mechanism of peatland acidification. *Ecology* **2010**, *91*, 2716–2726.
- [39] Chakraborty, S.; Paratkar, G. T. Biomonitoring of trace element air pollution using mosses. *Aerosol and air quality research* **2006**, *6*, 247–258.
- [40] Lead, W. A.; Steinnes, E.; Jones, K. C. Atmospheric deposition of PCBs to moss (*Hylocomium splendens*) in Norway between 1977 and 1990. *Environmental science & technology* **1996**, *30*, 524–530.
- [41] Berg, T.; Røyset, O.; Steinnes, E. Moss (*Hylocomium splendens*) used as biomonitor of atmospheric trace element deposition: estimation of uptake efficiencies. *Atmospheric Environment* **1995**, *29*, 353–360.
- [42] Tamm, C. O. *Growth, yield and nutrition in carpets of a forest moss (Hylocomium splendens)*; 1953.
- [43] Wiersma, G. B.; Harmon, M. E.; Baker, G. A.; Greene, S. E. Elemental composition of Hoh Rainforest Olympic National Park Washington, USA. *Chemosphere* **1987**, *16*, 2631–2645.
- [44] Shevchenko, V. P.; Vorobyev, S. N.; Krickov, I. V.; Boev, A. G.; Lim, A. G.; Novigatsky, A. N.; Starodymova, D. P.; Pokrovsky, O. S. Insoluble Particles in the Snowpack of the Ob River Basin (Western Siberia) a 2800 km Submeridional Profile. *Atmosphere* **2020**, *11*, 1184.
- [45] Nawrot, A. P.; Migala, K.; Luks, B.; Pakszys, P.; Glowacki, P. Chemistry of snow cover and acidic snowfall during a season with a high level of air pollution on the Hans Glacier, Spitsbergen. *Polar Science* **2016**, *10*, 249–261.
- [46] Sakai, H.; Sasaki, T.; Saito, K. Heavy metal concentrations in urban snow as an indicator of air pollution. *Science of the total environment* **1988**, *77*, 163–174.
- [47] Dinu, M.; Moiseenko, T.; Baranov, D. Snowpack as Indicators of Atmospheric Pollution: The Valday Upland. *Atmosphere* **2020**, *11*, 462.
- [48] Lebedev, A. T.; Mazur, D. M.; Polyakova, O. V.; Hänninen, O. *Snow Samples as Markers of Air Pollution in Mass Spectrometry Analysis*; Springer Netherlands, 2015; Chapter 31, pp 515–541.
- [49] Nazarenko, Y.; Ariya, P. A. Interaction of Air Pollution with Snow and Seasonality Effects. *Atmosphere* **2021**, *12*, 490.
- [50] Jackson, T. A. Long-range atmospheric transport of mercury to ecosystems, and the importance of anthropogenic emissions A critical review and evaluation of the published evidence. *Environmental Reviews* **1997**, *5*, 99–120.
- [51] Manual, Heavy metals, nitrogen and POPs in European mosses: 2020 survey. 2015.

-
- [52] Fernández, J. A.; Boquete, M. T.; Carballeira, A.; Aboal, J. R. A critical review of protocols for moss biomonitoring of atmospheric deposition: Sampling and sample preparation. *Science of The Total Environment* **2015**, *517*, 132–150.
- [53] Lambie, K. J.; Hill, S. J. Microwave digestion procedures for environmental matrices. *The Analyst* **1998**, *123*, 103–133.
- [54] Davidson, C. M. *Methods for the Determination of Heavy Metals and Metalloids in Soils*; Springer Netherlands, 2013; Chapter 4, pp 97–140.
- [55] Richter, B. E.; Jones, B. A.; Ezzell, J. L.; Porter, N. L.; Avdalovic, N.; Pohl, C. Accelerated Solvent Extraction: A Technique for Sample Preparation. *Analytical Chemistry* **1996**, *68*, 1033–1039.
- [56] Giergielewicz-Możajska, H.; Dąbrowski, Ł.; Namieśnik, J. Accelerated Solvent Extraction (ASE) in the Analysis of Environmental Solid Samples — Some Aspects of Theory and Practice. *Critical Reviews in Analytical Chemistry* **2001**, *31*, 149–165.
- [57] Helaleh, M. I. H.; Al-Omair, A.; Ahmed, N.; Gevao, B. Quantitative determination of organochlorine pesticides in sewage sludges using Soxhlet, Soxtec and pressurized liquid extractions and ion trap mass–mass spectrometric detection. *Analytical and Bioanalytical Chemistry* **2005**, *382*, 1127–1134.
- [58] Hubert, A.; Wenzel, K.-D.; Engewald, W.; Schüürmann, G. Accelerated solvent extraction—more efficient extraction of POPs and PAHs from real contaminated plant and soil samples. *Reviews in Analytical Chemistry* **2001**, *20*, 101–144.
- [59] Björklund, E.; Nilsson, T.; Bøwadt, S. Pressurised liquid extraction of persistent organic pollutants in environmental analysis. *TrAC Trends in Analytical Chemistry* **2000**, *19*, 434–445.
- [60] Konieczka, P.; Wolska, L.; Namieśnik, J. Quality problems in determination of organic compounds in environmental samples, such as PAHs and PCBs. *TrAC Trends in Analytical Chemistry* **2010**, *29*, 706–717.
- [61] Wilschefski, S.; Baxter, M. Inductively Coupled Plasma Mass Spectrometry: Introduction to Analytical Aspects. *Clinical Biochemist Reviews* **2019**, *40*, 115–133.
- [62] Thomas, R. *Practical guide to ICP-MS: a tutorial for beginners*; CRC press, 2008.
- [63] Miller, D. D.; Rutzke, M. A. *Food analysis*; Springer, 2010; pp 421–442.
- [64] Ammann, A. A. Inductively coupled plasma mass spectrometry (ICP MS): a versatile tool. *Journal of Mass Spectrometry* **2007**, *42*, 419–427.
- [65] Stauffer, E.; Dolan, J. A.; Newman, R. *Fire debris analysis*; Academic Press, 2007.
- [66] Sparkman, O. D.; Penton, Z. E.; Kitson, F. G. *Quantitation with GC/MS*; Elsevier, 2011; Chapter 6, pp 207–218.
-

-
- [67] Weging, S. Study of trace elements, natural organic matter and selected environmental toxicants in soil at Mítrahelvøya, to establish bias correction for studies of long-range atmospheric transported pollutants in Ny-Ålesund. Master's thesis, NTNU, 2021.
- [68] Sutherland, K. Gas chromatography/mass spectrometry techniques for the characterisation of organic materials in works of art. *Physical Sciences Reviews* **2019**, *4*.
- [69] Popek, E. P. *Sampling and analysis of environmental chemical pollutants: a complete guide*; Elsevier, 2017.
- [70] Batley, G. E. Quality Assurance in Environmental Monitoring. *Marine Pollution Bulletin* **1999**, *39*, 23–31.
- [71] Vidal, J. L. M.; Frenich, A. G.; González, F. J. E. Quality Control Criteria for Analysis of Organic Traces in Water. *The Scientific World JOURNAL* **2002**, *2*, 1040–1043.
- [72] Macdougall, D.; Crummett, W. B.; et al., Guidelines for data acquisition and data quality evaluation in environmental chemistry. *Analytical Chemistry* **1980**, *52*, 2242–2249.
- [73] Ulberth, F. Certified reference materials for inorganic and organic contaminants in environmental matrices. *Analytical and Bioanalytical Chemistry* **2006**, *386*, 1121–1136.
- [74] Shrivastava, A.; Gupta, V. B. Methods for the determination of limit of detection and limit of quantitation of the analytical methods. *Chron. Young Sci* **2011**, *2*, 21–25.
- [75] Al-Rashdan, A.; Helaleh, M. I. H.; Nisar, A.; Ibtisam, A.; Al-Ballam, Z. Determination of the Levels of Polycyclic Aromatic Hydrocarbons in Toasted Bread Using Gas Chromatography Mass Spectrometry. *International Journal of Analytical Chemistry* **2010**, *2010*, 1–8.
- [76] Thompson, M.; Ellison, S. L.; Fajgelj, A.; Willetts, P.; Wood, R. Harmonized guidelines for the use of recovery information in analytical measurement. *Pure and applied chemistry* **1999**, *71*, 337–348.
- [77] Lundanes, E.; Reubsæet, L.; Greibrokk, T. *Chromatography: basic principles, sample preparations and related methods*; John Wiley & Sons, 2013.
- [78] Asimakopoulos, A. G.; Wang, L.; Thomaidis, N. S.; Kannan, K. A multi-class bioanalytical methodology for the determination of bisphenol A diglycidyl ethers, p-hydroxybenzoic acid esters, benzophenone-type ultraviolet filters, triclosan, and triclocarban in human urine by liquid chromatography–tandem mass spectrometry. *Journal of Chromatography A* **2014**, *1324*, 141–148.
- [79] McNally, M. E.; Usher, K.; Hansen, S. W.; Amoo, J. S.; Bernstein, A. P. Precision of internal standard and external standard methods in high performance liquid chromatography. **2015**,

-
- [80] Smith, L. I. A tutorial on principal components analysis. **2002**,
- [81] Nachar, N. The Mann-Whitney U: A test for assessing whether two independent samples come from the same distribution. *Tutorials in quantitative Methods for Psychology* **2008**, *4*, 13–20.
- [82] Lever, J.; Krzywinski, M.; Altman, N. Points of significance: Principal component analysis. *Nature methods* **2017**, *14*, 641–643.
- [83] Esbensen, K. H.; Guyot, D.; Westad, F.; Houmoller, L. P. *Multivariate data analysis: in practice: an introduction to multivariate data analysis and experimental design*; Multivariate Data Analysis, 2002.
- [84] Aslam, S. N.; Huber, C.; Asimakopoulos, A. G.; Steinnes, E.; Mikkelsen, O. Trace elements and polychlorinated biphenyls (PCBs) in terrestrial compartments of Svalbard, Norwegian Arctic. *Science of the Total Environment* **2019**, *685*, 1127–1138.
- [85] Brekke, B. *Ny-Ålesund: international research at 79° N*; Norsk Polarinstitut: Oslo, 1996; p 19 s. ill., "Published by Norsk Polarinstitut in cooperation with Kings Bay Kull Comp." 2. rev. ed.
- [86] Granberg, M. E.; Ask, A.; Gabrielsen, G. W. *Local contamination in Svalbard: overview and suggestions for remediation actions*; Norsk Polarinstitut, 2017.
- [87] Ma, H.; Shi, G.; Cheng, Y. Accumulation Characteristics of Metals and Metalloids in Plants Collected from Ny-Ålesund, Arctic. *Atmosphere* **2020**, *11*, 1129.
- [88] Bazzano, A.; Cappelletti, D.; Udisti, R.; Grotti, M. Long-range transport of atmospheric lead reaching Ny-Ålesund: Inter-annual and seasonal variations of potential source areas. *Atmospheric environment* **2016**, *139*, 11–19.
- [89] Pacyna, J. M.; Ottar, B.; Tomza, U.; Maenhaut, W. Long-range transport of trace elements to Ny Ålesund, Spitsbergen. *Atmospheric Environment (1967)* **1985**, *19*, 857–865.
- [90] Retsch GmbH, Operating Instructions for Oscillating Mill MM400. Retsch.
- [91] Schaug, J.; Rambæk, J. P.; Steinnes, E.; Henry, R. C. Multivariate analysis of trace element data from moss samples used to monitor atmospheric deposition. *Atmospheric Environment. Part A. General Topics* **1990**, *24*, 2625–2631.
- [92] Steinnes, E.; Friedland, A. J. Metal contamination of natural surface soils from long-range atmospheric transport: existing and missing knowledge. *Environmental Reviews* **2006**, *14*, 169–186.
- [93] Steinnes, E.; Berg, T.; Uggerud, H. T. Three decades of atmospheric metal deposition in Norway as evident from analysis of moss samples. *Science of the Total Environment* **2011**, *412*, 351–358.
-

-
- [94] Zhu, C.; Li, Y.; Wang, P.; Chen, Z.; Ren, D.; Ssebugere, P.; Zhang, Q.; Jiang, G. Polychlorinated biphenyls (PCBs) and polybrominated biphenyl ethers (PBDEs) in environmental samples from Ny-Ålesund and London Island, Svalbard, the Arctic. *Chemosphere* **2015**, *126*, 40–46.
- [95] Zhang, P.; Ge, L.; Gao, H.; Yao, T.; Fang, X.; Zhou, C.; Na, G. Distribution and transfer pattern of polychlorinated biphenyls (PCBs) among the selected environmental media of Ny-Ålesund, the Arctic: as a case study. *Marine pollution bulletin* **2014**, *89*, 267–275.
- [96] Knulst, J. C.; Westling, H. O.; Brorström-Lundén, E. Airborne organic micropollutant concentrations in mosses and humus as indicators for local versus long-range sources. *Environmental monitoring and assessment* **1995**, *36*, 75–91.
- [97] Danielsson, H.; Hansson, K.; Potter, A.; Friedrichsen, J.; Brorström-Lundén, E. Persistent organic pollutants in Swedish mosses. 2016.
- [98] Brändli, R. C.; Bucheli, T. D.; Kupper, T.; Stadelmann, F. X.; Tarradellas, J. Optimised accelerated solvent extraction of PCBs and PAHs from compost. *International Journal of Environmental Analytical Chemistry* **2006**, *86*, 505–525.
- [99] Foan, L.; Simon, V. Optimization of pressurized liquid extraction using a multivariate chemometric approach and comparison of solid-phase extraction cleanup steps for the determination of polycyclic aromatic hydrocarbons in mosses. *Journal of Chromatography A* **2012**, *1256*, 22–31.
- [100] Carlberg, G. E.; Ofstad, E. B.; Drangsholt, H.; Steinnes, E. Atmospheric deposition of organic micropollutants in Norway studied by means of moss and lichen analysis. *Chemosphere* **1983**, *12*, 341–356.
- [101] Halse, A. K.; Uggerud, H. T.; Schlabach, M.; Steinnes, E. PAH measurements in air and moss around selected industrial sites in Norway 2015. *NILU rapport* **2017**,
- [102] Ravindra, K.; Sokhi, R.; Vangrieken, R. Atmospheric polycyclic aromatic hydrocarbons: Source attribution, emission factors and regulation. *Atmospheric Environment* **2008**, *42*, 2895–2921.
- [103] Han, B.; Gao, W.; Li, Q.; Liu, A.; Gong, J.; Zheng, Y.; Wang, N.; Zheng, L. Residues of persistent toxic substances in surface soils of Ny-Ålesund in the arctic: Occurrence, source, and ecological risk assessment. *Chemosphere* **2022**, 135092.
- [104] Na, G.; Liang, Y.; Li, R.; Gao, H.; Jin, S. Flux of Polynuclear Aromatic Compounds (PAHs) from the Atmosphere and from Reindeer/Bird Feces to Arctic Soils in Ny-Ålesund (Svalbard). *Archives of Environmental Contamination and Toxicology* **2021**, *81*, 166–181.
- [105] Conca, E.; Abollino, O.; Giacomino, A.; Buoso, S.; Traversi, R.; Becagli, S.; Grotti, M.; Malandrino, M. Source identification and temporal evolution of trace elements in PM10 collected near to Ny-Ålesund (Norwegian Arctic). *Atmospheric Environment* **2019**, *203*, 153–165.
-

-
- [106] Blundell, C. C.; Armit, R.; Ailleres, L.; Micklethwaite, S.; Martin, A.; Betts, P. Interpreting geology from geophysics in poly-deformed and mineralised terranes; the Otago Schist and the Hyde-Macraes Shear Zone. *New Zealand Journal of Geology and Geophysics* **2019**, *62*, 550–572.
- [107] Brimble, S. K.; Blais, J. M.; Kimpe, L. E.; Mallory, M. L.; Keatley, B. E.; Douglas, M. S.; Smol, J. P. Bioenrichment of trace elements in a series of ponds near a northern fulmar (*Fulmarus glacialis*) colony at Cape Vera, Devon Island. *Canadian Journal of Fisheries and Aquatic Sciences* **2009**, *66*, 949–958.
- [108] Pim, W. v. d. K.; van Leeuwen, J. Interplay between peat formation and animal behaviour in the Spitsbergen archipelago, recorded in peat sections. *Permanence in Diversity: Netherlands Ecological Research on Edgeøya, Spitsbergen* **2004**, *1*, 72.
- [109] Ziółek, M.; Melke, J. The impact of seabirds on the content of various forms of phosphorus in organic soils of the Bellsund coast, western Spitsbergen. *Polar Research* **2014**, *33*, 19986.
- [110] Brimble, S. K.; Foster, K. L.; Mallory, M. L.; Macdonald, R. W.; Smol, J. P.; Blais, J. M. High arctic ponds receiving biotransported nutrients from a nearby seabird colony are also subject to potentially toxic loadings of arsenic, cadmium, and zinc. *Environmental Toxicology and Chemistry: An International Journal* **2009**, *28*, 2426–2433.
- [111] Ziółek, M.; Bartmiński, P.; Stach, A. The influence of seabirds on the concentration of selected heavy metals in organic soil on the Bellsund coast, western Spitsbergen. *Arctic, Antarctic, and Alpine Research* **2017**, *49*, 507–520.
- [112] Schick, A. Using *Hylocomium splendens* as a Bioindicator for the Long Range Transport of Pollutants to Arctic. Master's Thesis, NTNU, 2021.
- [113] Steinnes, E.; Jacobsen, L. B. *The use of mosses as monitors of trace element deposition from the atmosphere in Arctic regions: a feasibility study from Svalbard*; 1994.
- [114] Kirk, J.; Gleason, A. *Environmental Contaminants*; Springer, 2015; pp 223–262.
- [115] Damhaug, M. E. F. Studie av kvikksølv, svovel og naturlig organisk materiale i jord i Ny-Ålesund, Svalbard. Thesis, 2014.
- [116] Vergel, K.; Zinicovscaia, I.; Yushin, N.; Chaligava, O.; Nekhoroshkov, P.; Grozdov, D. Moss Biomonitoring of Atmospheric Pollution with Trace Elements in the Moscow Region, Russia. *Toxics* **2022**, *10*, 66.
- [117] Ugolini, F.; Tognetti, R.; Raschi, A.; Bacci, L. *Quercus ilex* L. as bioaccumulator for heavy metals in urban areas: effectiveness of leaf washing with distilled water and considerations on the trees distance from traffic. *Urban forestry & urban greening* **2013**, *12*, 576–584.
-

-
- [118] Berg, T.; Røyset, O.; Steinnes, E.; Vadset, M. Atmospheric trace element deposition: principal component analysis of ICP-MS data from moss samples. *Environmental Pollution* **1995**, *88*, 67–77.
- [119] Domine, F.; Sparapani, R.; Ianniello, A.; Beine, H. J. The origin of sea salt in snow on Arctic sea ice and in coastal regions. *Atmospheric Chemistry and Physics* **2004**, *4*, 2259–2271.

Appendix

6.1 Chemicals and materials

Table 6.1: Overview of chemicals and materials used during fieldwork, sample preparation, and sample analysis.

Chemical	Specification	Supplier
Nitric acid	Suprapur 50 % v/v	
“Dutch seven” PCBs, multicomponent stock solution	PCB-28, -52, -101, -118, -138, -153, -180, each of 100 micro g mL ⁻¹ in isooctane	Chiron AS
16 U.S. EPA priority PAHs	NAP, ACY, ACE, FLU, PHE, ANT, FLT, PYR, BaA, CHR, BbF, BkF, BaP, DBA, BgP, IND, each of 100 micro g mL ⁻¹ in toluene	Chiron AS
3'-F-PCB-28 (internal standard)	10 mikro g mL ⁻¹ in isooctane	Chiron AS
5'-F-PCB-118 (internal standard)	10 mikro g mL ⁻¹ in isooctane	Chiron AS
F-PAHs (internal standard)	1-Fluornaphthalene, 4-Fluorobiphenyl, 3-Fluorophenanthrene, 1-Fluoropyrene, 3-Fluorochrysene, each of 200 mikro g mL ⁻¹ in toluene	Chiron As
Acetone	Technical grade	VWR
Dichloromethane	GC - capillary grade	VWR
Copper powder	<425 micro m, 99.5% trace metal basis	Aldrich
Aluminum oxide	Activated, basic, Brockmann I	Sigma-Aldrich
Diatomaceous earth		Sigma-Aldrich
Ottawa sand	General purpose grade	Fisher Scientific
Reference material, moss	Intercalibration standard, <i>Pleurozium schreberi</i>	Finnish forest research institute Muhos research station
Material	Specification	Supplier
Nitrile gloves		VWR
Baking bag	Paper bag for storing samples meant for inorganic analysis	Norwegian Paper
Aluminum box	Aluminum boxes for storing samples meant for organic analysis	

Table 6.1: Continued.

Kitchen foil	Aluminium foil for sample handling	Snappies
Amber vials		
Screw cap for amber vials	Open top, polypropylene, silicone, PTFE	Duran Wheaton Kimble
Pasteur pipettes	Disposable glass, 230 mm	VWR
Syringe	10 mL	Fisher Scientific
Nylon syringe filter		
Sterican cannula	”Ø” 0.90 x 70 mm	Braun
Centrifuge tube	15 mL, metal free	VWR
Centrifuge tube	50 mL	VWR
ASE Extraction Filters	Cellulose, for 1, 5, 10, 22 mL ASE cell	Thermo Scientific
Laboratory film		Parafilm

6.2 Sample locations

Table 6.2: The coordinates of the different moss sampling locations. All samples at Stuphallet and Austre Brøggerbre shared the same coordinates (within a radius of 50 meters).

Location	Coordinates
Stuphallet	78.95982 °N 11.63026 °E
Austre Brøggerbre	78.91413 °N 11.85103 °E
Storvatnet 1	78.92342 °N 11.87169 °E
Storvatnet 2	78.92322 °N 11.87577 °E
Storvatnet 3	78.92226 °N 11.87764 °E

Table 6.3: Coordinates for snow sampling locations.

Location	Coordinates	Location	Coordinates
	78.9042 °N 11.8417 °E		78.91806 °N 11.85944 °E
	78.9075 °N 11.8428 °E		78.91861 °N 11.84917 °E
	78.9095 °N 11.8415 °E		78.91944 °N 11.83694 °E
Austre Brøggerbre n = 7	78.9111 °N 11.84 °E	Storvatnet n = 6	78.92028 °N 11.82667 °E
	78.9139 °N 11.839 °E		78.92222 °N 11.81139 °E
	78.915 °N 11.8397 °E		78.92444 °N 11.79833 °E
	78.9181 °N 11.8403 °E		

6.3 Calibration curves for PAHs

Calibration curves for the detected PAHs are made by plotting relative response (equation 2.5) along the y-axis and the concentration of analyte (A) over the concentration of internal standard in the standard solutions along the x-axis.

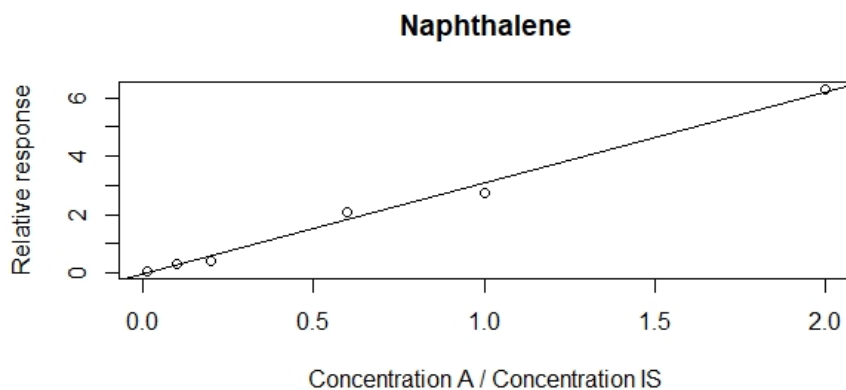


Figure 6.1: Calibration curve for NAP ($y = 3.11651x - 0.03976$). $R^2 = 0.9925$. A and IS denotes analyte and internal standard.

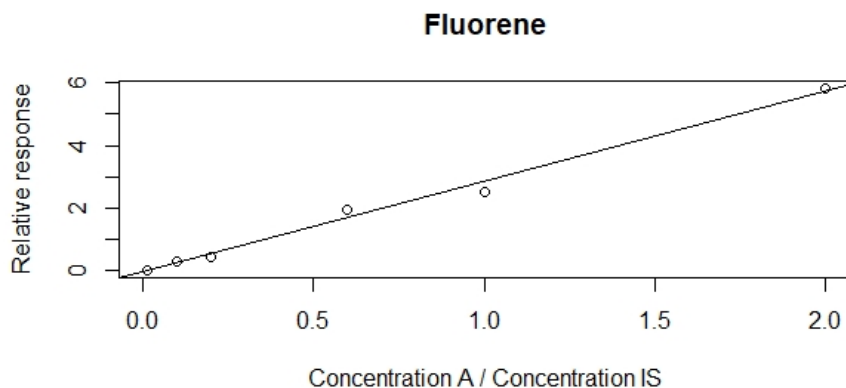


Figure 6.2: Calibration curve for fluorene ($y = 2.88704x - 0.04359$). $R^2 = 0.9916$. A and IS denotes analyte and internal standard.

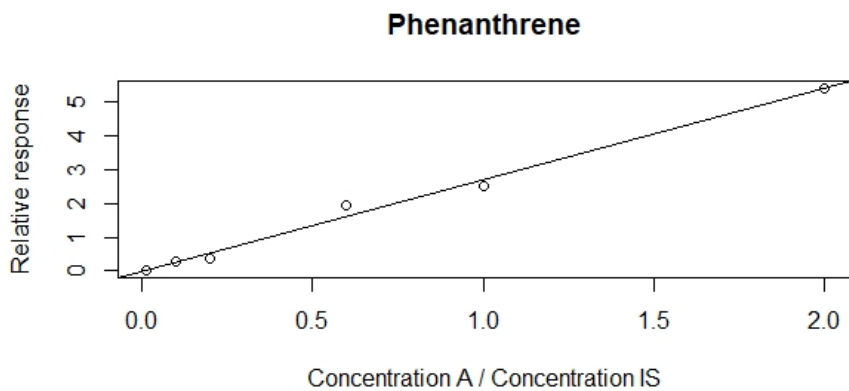


Figure 6.3: Calibration curve for phenanthrene ($y = 2.69667x - 0.003417$). $R^2 = 0.9917$. A and IS denotes analyte and internal standard.

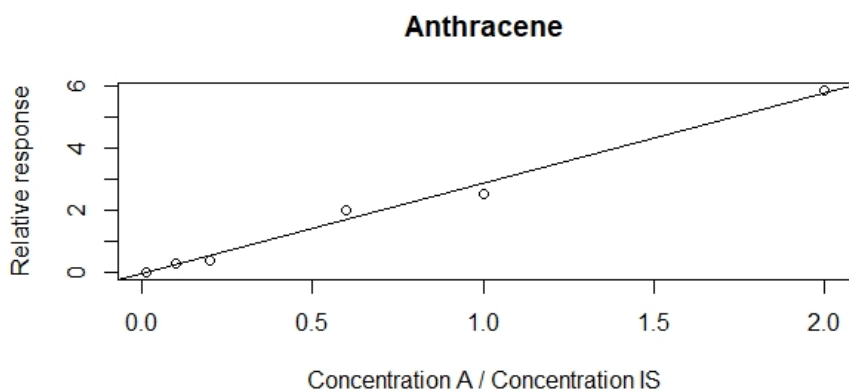


Figure 6.4: Calibration curve for anthracene ($y = 2.91045x - 0.04151$). $R^2 = 0.9907$. A and IS denotes analyte and internal standard.

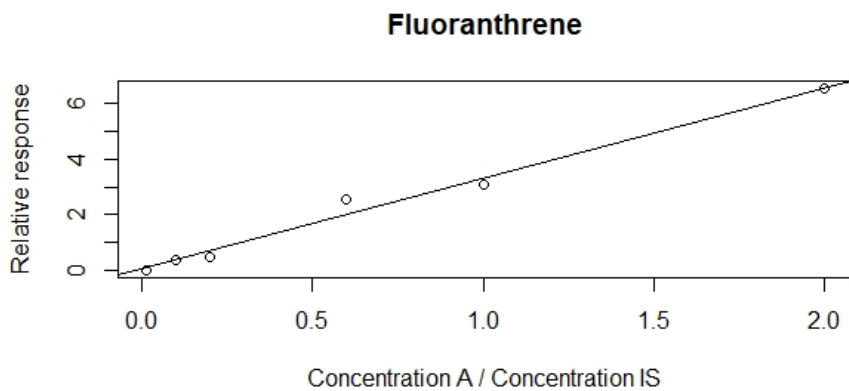


Figure 6.5: Calibration curve for fluoranthrene ($y = 3.25723x + 0.04738$). $R^2 = 0.987$. A and IS denotes analyte and internal standard.

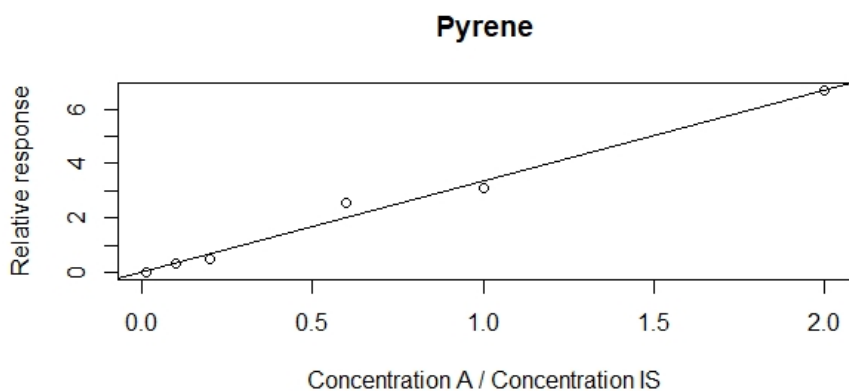


Figure 6.6: Calibration curve for pyrene ($y = 3.32711x + 0.03761$). $R^2 = 0.9884$. A and IS denotes analyte and internal standard.

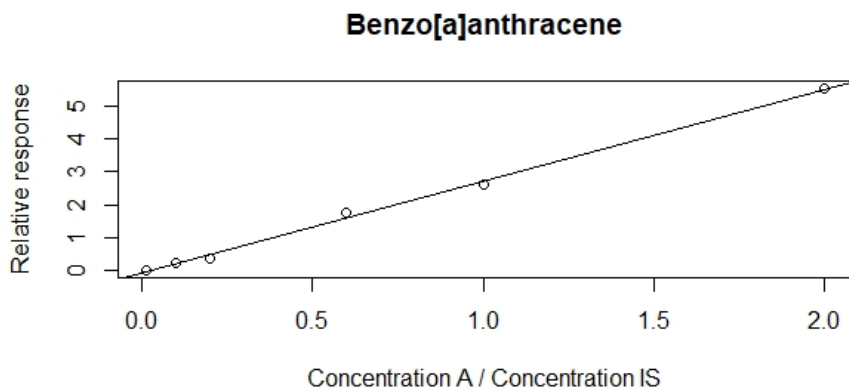


Figure 6.7: Calibration curve for benzo[a]anthracene ($y = 2.78433x - 0.06606$). $R^2 = 0.998$. A and IS denotes analyte and internal standard.

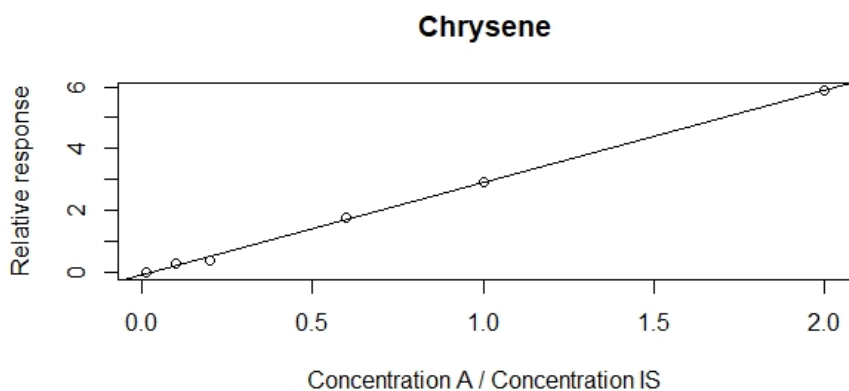


Figure 6.8: Calibration curve for chrysene ($y = 2.97159x - 0.05429$). $R^2 = 0.9989$. A and IS denotes analyte and internal standard.

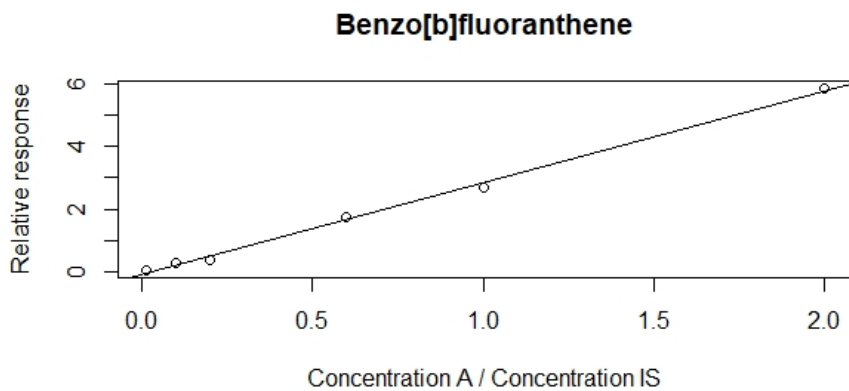


Figure 6.9: Calibration curve for benzo[b]fluoranthene ($y = 2.92946x - 0.07639$). $R^2 = 0.9969$. A and IS denotes analyte and internal standard.

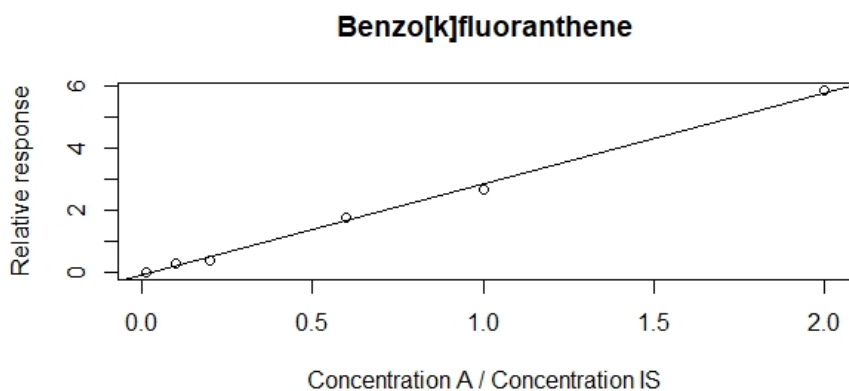


Figure 6.10: Calibration curve for benzo[k]fluoranthene ($y = 2.93792x - 0.08755$). $R^2 = 0.9972$. A and IS denotes analyte and internal standard.

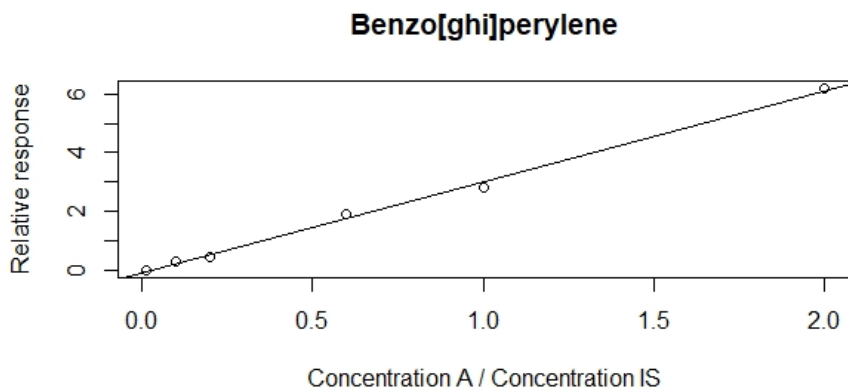


Figure 6.11: Calibration curve for benzo[ghi]perylene ($y = 3.09396x - 0.07591$). $R^2 = 0.9971$. A and IS denotes analyte and internal standard.

6.4 PAH concentrations

6.4.1 PAH concentrations corrected for recoveries

Table 6.4: PAH concentrations (ng g⁻¹) corrected for absolute (Abs) and relative (Rel) recoveries.

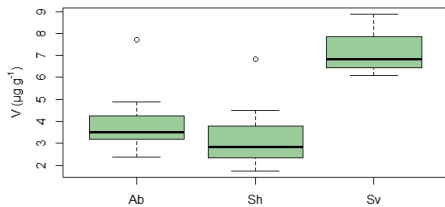
	NAP		FLU		PHE		ANT		FLT		PYR		BaA		CHR		BbF		BkF		BgP		
	Abs	Rel	Abs	Rel	Abs	Rel	Abs	Rel	Abs	Rel	Abs	Rel	Abs	Rel	Abs	Rel	Abs	Rel	Abs	Rel	Abs	Rel	
Sh1	24.88	11.92			21.24	13.38			11.99	8.695	5.381	4.256											
Sh2	29.94	14.35	7.716	5.455	22.94	14.45			11.69	8.478	5.300	4.192											
Sh3	24.69	11.83	6.543	4.626	22.61	14.25			12.03	8.725													
Sh4	25.58	12.26			19.10	12.03			10.43	7.560													
Sh5	28.06	13.44	7.414	5.242	20.40	12.85			11.15	8.088	5.043	3.989											
Sh6	23.30	11.17	8.056	5.695	20.92	13.18																	
Ab1			7.345	5.193																			
Ab2	25.57	12.25	8.499	6.009	18.81	11.85			9.954	7.217													
Ab3	23.81	11.41			19.53	12.31			11.58	8.400													
Ab4																							
Ab5																							
Ab6	27.73	13.29	7.917	5.598																			
Ab7	25.44	12.19	8.570	6.059	20.22	12.74																	
Sv1	42.97	20.59	10.01	7.075	29.66	18.69			12.12	8.791	7.153	5.658	6 .045	4 .882									
Sv2	114.97	55.10	15.37	10.868	64.95	40.93	14.77	11.88	18.95	13.74	18.36	14.52	19.45	15.71	21.15	17.09	1 1.38	9 .298	1 4.35	1 1.61	1 2.75	1 0.42	

6.4.2 LOD and LOQ for POPs

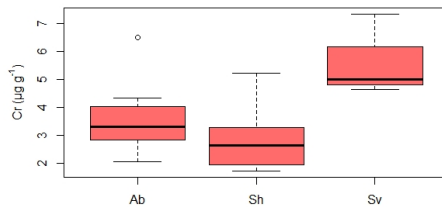
Table 6.5: Calculated limits of detection (LOD) and limits of quantification (LOQ) for POPs.

	LOD		LOQ	
	Instrument (ng mL ⁻¹)	Sample (ng g ⁻¹)	Instrument (ng mL ⁻¹)	Sample (ng g ⁻¹)
NAP	0.93	1.86	3.1	6.2
ACY	0.54	1.08	1.79	3.58
ACE	0.66	1.32	2.18	4.36
FLU	1.11	2.22	3.71	7.42
PHE	0.78	1.56	2.59	5.18
ANT	0.92	1.84	3.07	6.14
FLT	0.61	1.22	2.04	4.08
PYR	0.72	1.44	2.4	4.8
BaA	1.5	3	5	10
CHR	1.31	2.62	4.36	8.72
BbF	1.91	3.82	6.36	12.72
BkF	1.91	3.82	6.38	12.76
BaP	2.55	5.1	8.5	17
IND	2.58	5.16	8.61	17.22
DBA	3.76	7.52	12.53	25.06
BgP	4.09	8.18	13.62	27.24
PCB-28	0.85	1.7	2.83	5.66
PCB-52	0.78	1.56	2.62	5.24
PCB-101	0.6	1.2	2.02	4.04
PCB-118	0.82	1.64	2.75	5.5
PCB-138	0.57	1.14	1.92	3.84
PCB-153	0.67	1.34	2.24	4.48
PCB-180	0.87	1.74	2.91	5.82

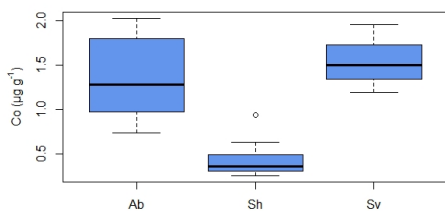
6.5 Box plots



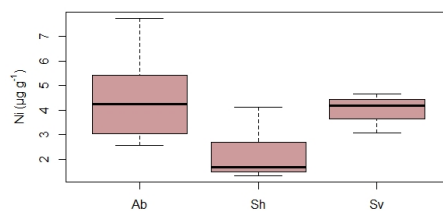
(a) V



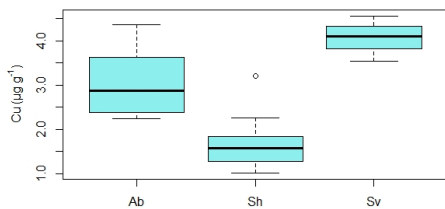
(b) Cr



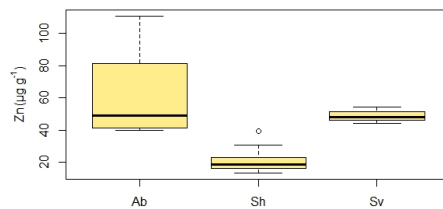
(c) Co



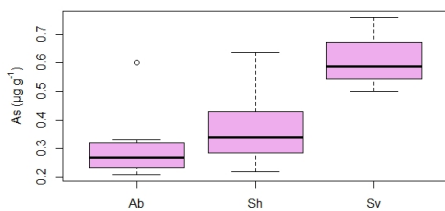
(d) Ni



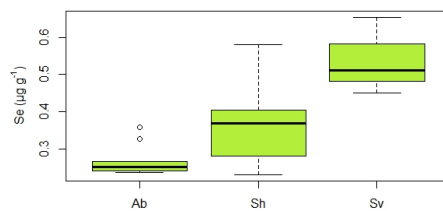
(e) Cu



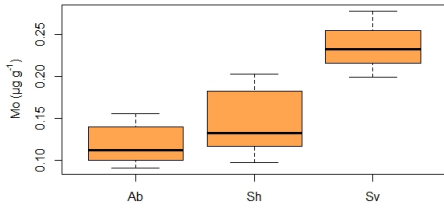
(f) Zn



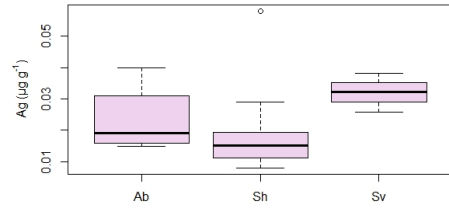
(g) As



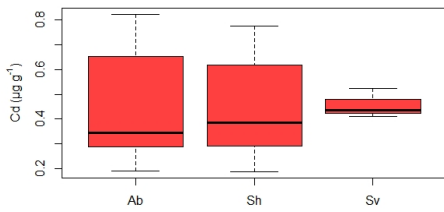
(h) Se



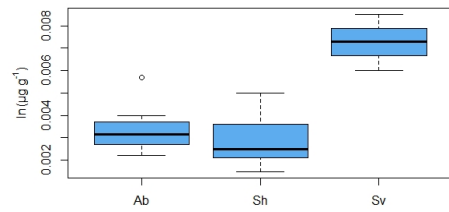
(i) Mo



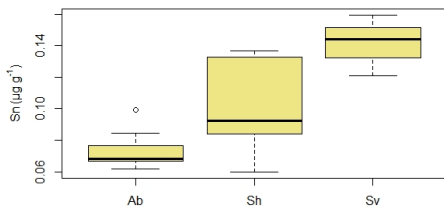
(j) Ag



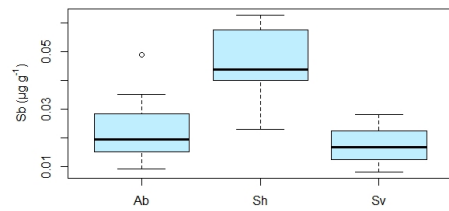
(k) Cd



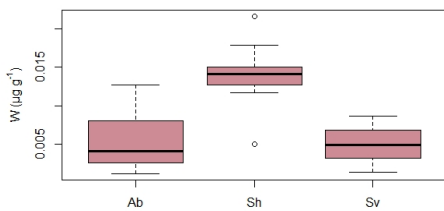
(l) In



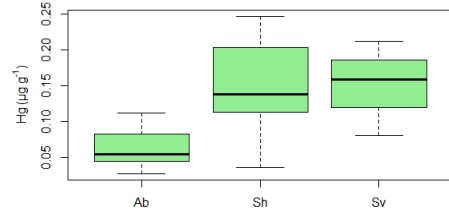
(m) Sn



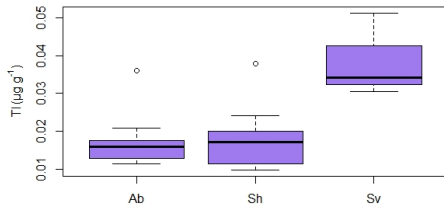
(n) Sb



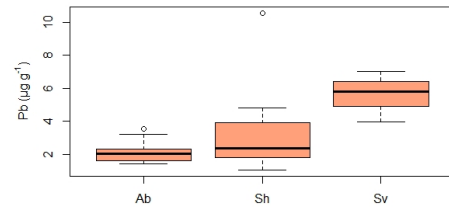
(o) W



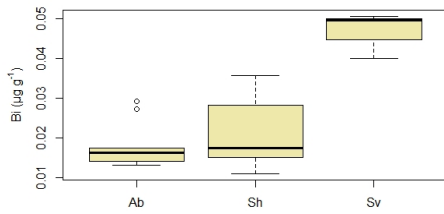
(p) Hg



(q) Tl



(r) Pb



(s) Bi

Figure 6.12: Boxplots for the selected elements in moss sampled at Austre Brøggerbre (Ab), Stuphallet (Sh), and Storvatnet (Sv).

6.6 Bar charts

Austre Brøggerbre

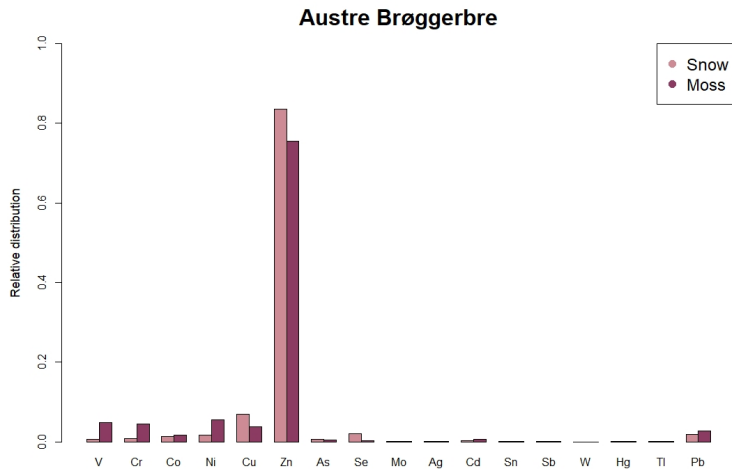


Figure 6.13: Relative distribution of elements in snow and moss samples from Austre Brøggerbre.

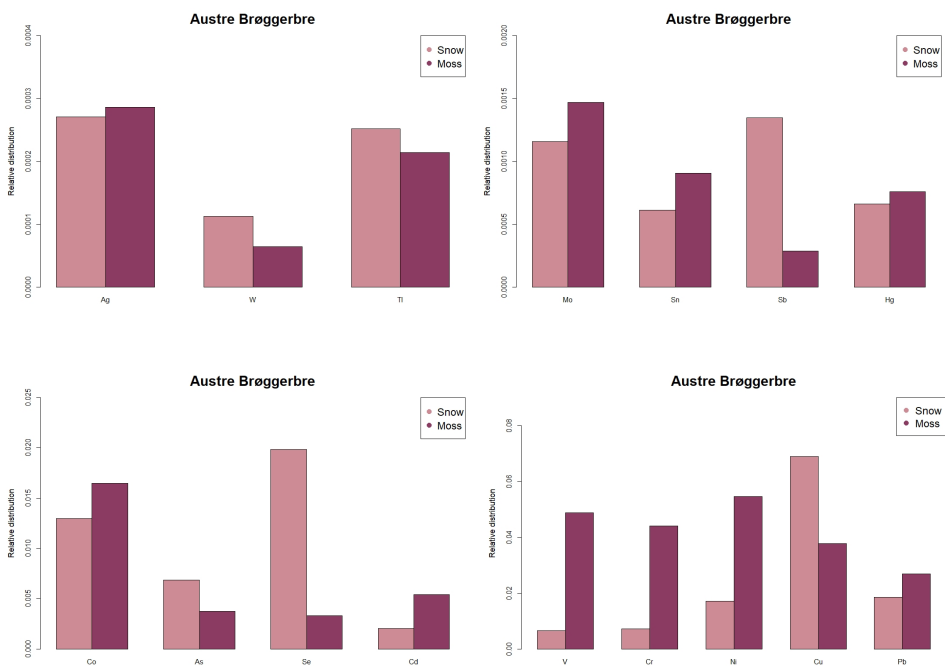


Figure 6.14: Relative distribution of elements in snow and moss from Austre Brøggerbre. Be aware of different scaling along the y-axis.

Storvatnet

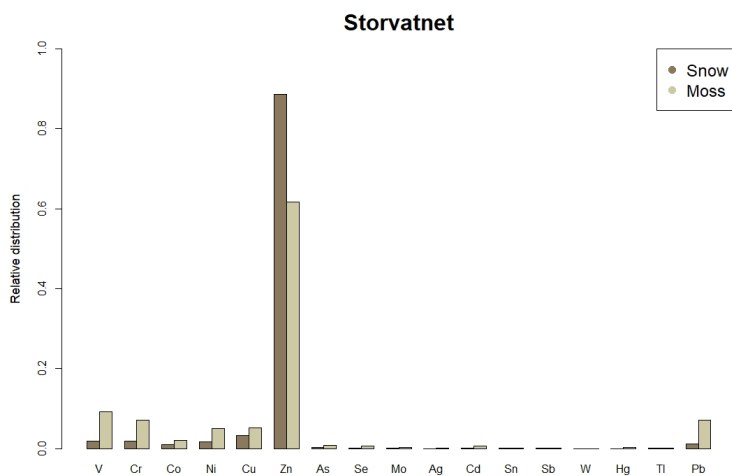


Figure 6.15: Relative distribution of elements in snow and moss samples from Storvatnet.

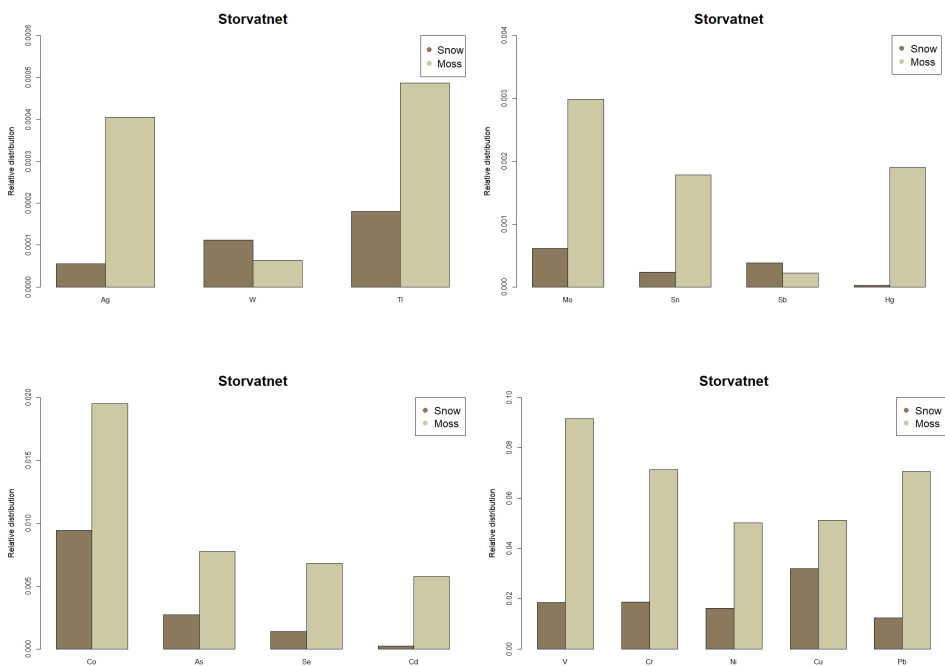


Figure 6.16: Relative distribution of elements in snow and moss from Storvatnet. Be aware of different scaling along the y-axis.

6.7 Correlation matrix

	V	Cr	Co	Ni	Cu	Zn	As	Se	Mo	Ag	Cd	In	Sn	Sb	W	Hg	Tl	Pb	Bi
V	1	0.964660	0.712860	0.760004	0.712860	0.760004	0.712860	0.760004	0.712860	0.760004	0.712860	0.760004	0.712860	0.760004	0.712860	0.760004	0.712860	0.760004	0.712860
Cr	0.964660	1	0.760004	0.712860	0.760004	0.712860	0.760004	0.712860	0.760004	0.712860	0.760004	0.712860	0.760004	0.712860	0.760004	0.712860	0.760004	0.712860	0.760004
Co	0.712860	0.760004	1	0.92273	0.92273	0.92273	0.92273	0.92273	0.92273	0.92273	0.92273	0.92273	0.92273	0.92273	0.92273	0.92273	0.92273	0.92273	0.92273
Ni	0.760004	0.712860	0.92273	1	0.842072	0.842072	0.842072	0.842072	0.842072	0.842072	0.842072	0.842072	0.842072	0.842072	0.842072	0.842072	0.842072	0.842072	0.842072
Cu	0.760004	0.712860	0.92273	0.842072	1	0.743136	0.743136	0.743136	0.743136	0.743136	0.743136	0.743136	0.743136	0.743136	0.743136	0.743136	0.743136	0.743136	0.743136
Zn	0.712860	0.760004	0.92273	0.842072	0.743136	1	0.70552	0.70552	0.70552	0.70552	0.70552	0.70552	0.70552	0.70552	0.70552	0.70552	0.70552	0.70552	0.70552
As	0.760004	0.712860	0.92273	0.842072	0.743136	0.70552	1	0.859386	0.859386	0.859386	0.859386	0.859386	0.859386	0.859386	0.859386	0.859386	0.859386	0.859386	0.859386
Se	0.712860	0.760004	0.92273	0.842072	0.743136	0.70552	0.859386	1	0.695543	0.695543	0.695543	0.695543	0.695543	0.695543	0.695543	0.695543	0.695543	0.695543	0.695543
Mo	0.760004	0.712860	0.92273	0.842072	0.743136	0.70552	0.859386	0.695543	1	0.210829	0.210829	0.210829	0.210829	0.210829	0.210829	0.210829	0.210829	0.210829	0.210829
Ag	0.712860	0.760004	0.92273	0.842072	0.743136	0.70552	0.859386	0.695543	0.210829	1	0.429704	0.429704	0.429704	0.429704	0.429704	0.429704	0.429704	0.429704	0.429704
Cd	0.760004	0.712860	0.92273	0.842072	0.743136	0.70552	0.859386	0.695543	0.429704	0.429704	1	0.284287	0.284287	0.284287	0.284287	0.284287	0.284287	0.284287	0.284287
In	0.712860	0.760004	0.92273	0.842072	0.743136	0.70552	0.859386	0.695543	0.429704	0.429704	0.284287	1	0.573150	0.573150	0.573150	0.573150	0.573150	0.573150	0.573150
Sn	0.760004	0.712860	0.92273	0.842072	0.743136	0.70552	0.859386	0.695543	0.429704	0.429704	0.284287	0.573150	1	0.70675	0.70675	0.70675	0.70675	0.70675	0.70675
Sb	0.712860	0.760004	0.92273	0.842072	0.743136	0.70552	0.859386	0.695543	0.429704	0.429704	0.284287	0.573150	0.70675	1	0.019041	0.019041	0.019041	0.019041	0.019041
W	0.760004	0.712860	0.92273	0.842072	0.743136	0.70552	0.859386	0.695543	0.429704	0.429704	0.284287	0.573150	0.70675	0.019041	1	0.157926	0.157926	0.157926	0.157926
Hg	0.712860	0.760004	0.92273	0.842072	0.743136	0.70552	0.859386	0.695543	0.429704	0.429704	0.284287	0.573150	0.70675	0.019041	0.157926	1	0.73826	0.73826	0.73826
Tl	0.760004	0.712860	0.92273	0.842072	0.743136	0.70552	0.859386	0.695543	0.429704	0.429704	0.284287	0.573150	0.70675	0.019041	0.157926	0.73826	1	0.545288	0.545288
Pb	0.712860	0.760004	0.92273	0.842072	0.743136	0.70552	0.859386	0.695543	0.429704	0.429704	0.284287	0.573150	0.70675	0.019041	0.157926	0.73826	0.545288	1	0.30390
Bi	0.760004	0.712860	0.92273	0.842072	0.743136	0.70552	0.859386	0.695543	0.429704	0.429704	0.284287	0.573150	0.70675	0.019041	0.157926	0.73826	0.545288	0.30390	1

6.7.1 Correlation with Sc

Table 6.6: The elements' correlation with Sc. The 19 elements this study focuses on are marked with yellow.

	Sc		Sc		Sc		Sc
Li	0,857	Fe	0,994	Pd	0,937	Dy	0,978
Be	0,911	Co	0,819	Ag	0,460	Ho	0,977
B	0,263	Ni	0,622	Cd	0,042	Er	0,975
Na	-0,193	Cu	0,856	In	0,933	Tm	0,974
Mg	0,895	Zn	0,293	Sn	0,472	Yb	0,972
Al	0,968	Ga	0,989	Sb	-0,720	Lu	0,963
Si	-0,707	As	0,778	Cs	0,845	Hf	0,640
P	-0,202	Se	0,522	Ba	0,654	Ta	0,314
S	0,100	Br	0,180	La	0,959	W	-0,571
Cl	0,184	Rb	0,913	Ce	0,970	Pt	-0,218
K	0,542	Sr	0,373	Pr	0,964	Hg	-0,040
Ca	-0,242	Y	0,962	Nd	0,965	Tl	0,890
Ti	0,903	Zr	0,764	Sm	0,972	Pb	0,454
V	0,958	Nb	-0,672	Eu	0,958	Bi	0,786
Cr	0,948	Mo	0,483	Gd	0,972	Th	0,991
Mn	0,340	Ru	-0,908	Tb	0,974	U	0,577

6.8 Additional PCA plots

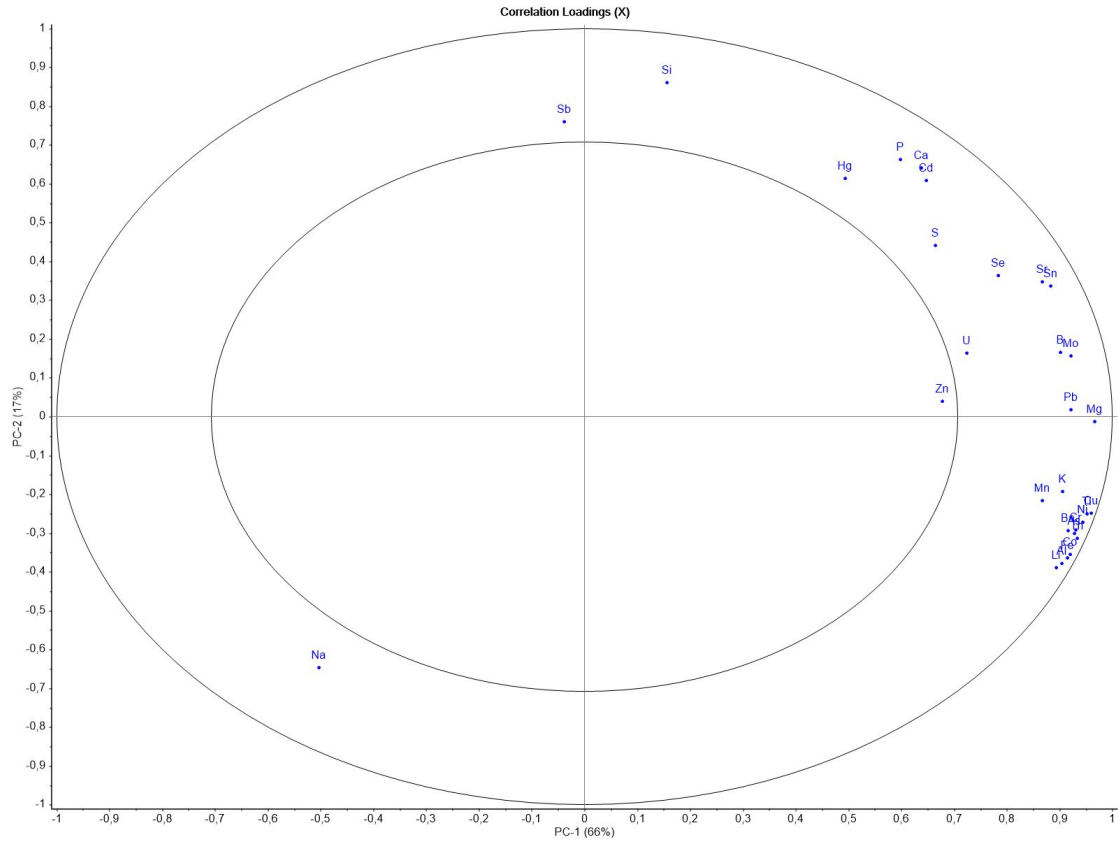


Figure 6.17: PCA loading plot for moss, snow, and soil samples, showing first and second component.

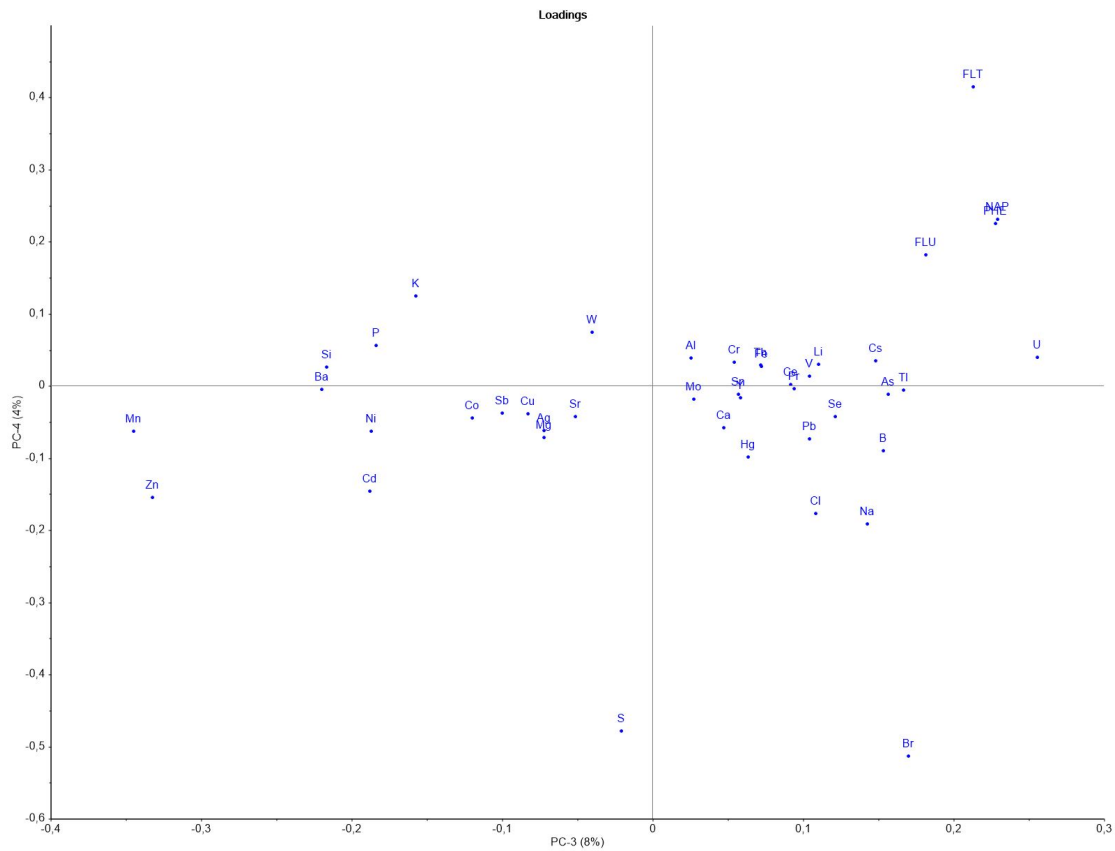


Figure 6.19: PCA loading plot for moss and snow samples, showing third and fourth component.

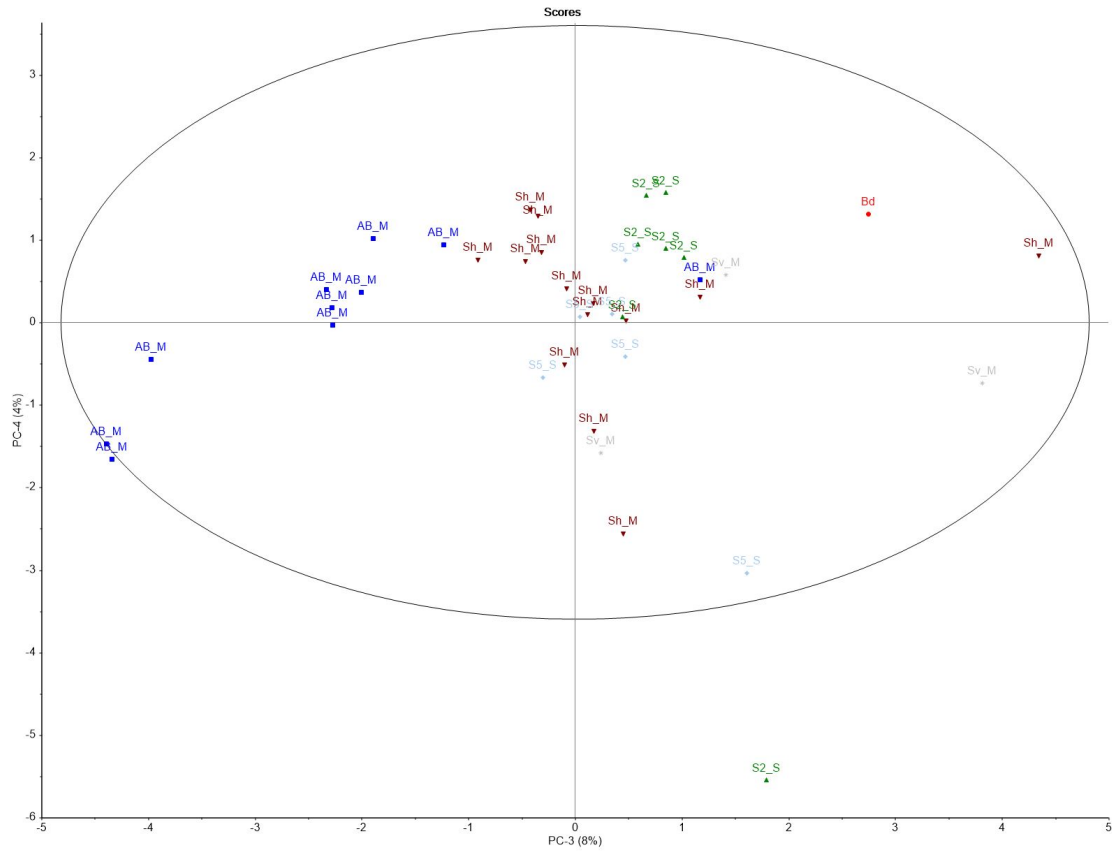


Figure 6.20: PCA score plot for moss and snow samples, showing third and fourth component.

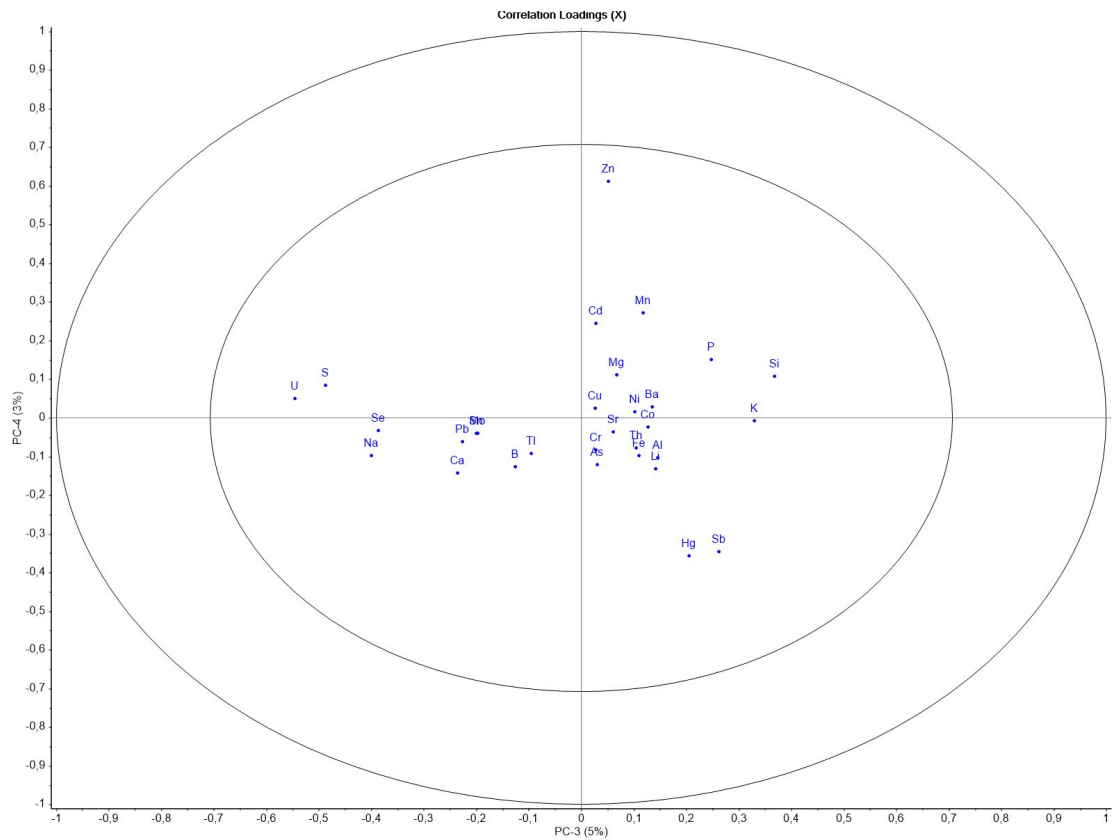


Figure 6.21: PCA loading plot for moss and snow samples, showing third and fourth component.

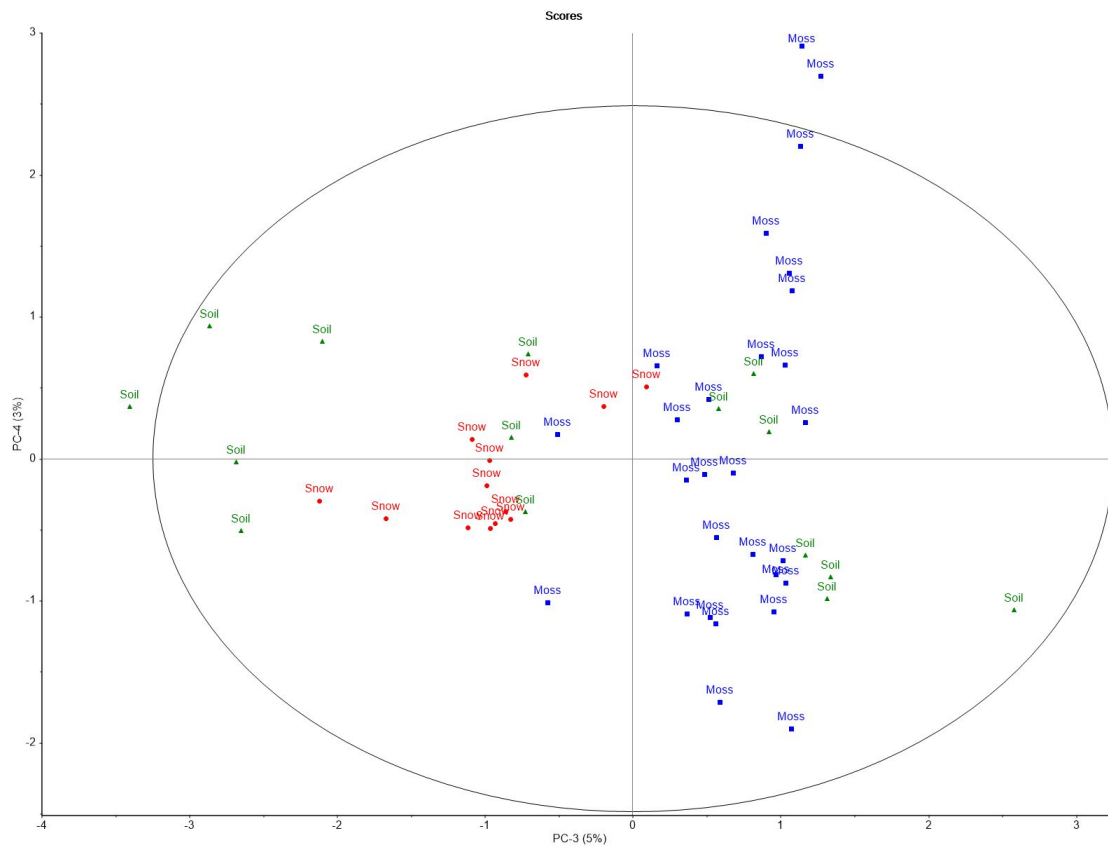


Figure 6.22: PCA score plot for moss and snow samples, showing third and fourth component.

